Investigating structure and function of the dopaminergic midbrain: with a special focus on the human VTA

Trutti, A.C.

Appendices

Appendix A

Supplementary materials to chapter 4

A1. Supplementary tables

Table A.1. Look-up table.

ID	Label	ID	Label	ID	Label
1	VCcm-l	38	Sdm-r	75	OFCv-l
2	VCcm-r	39	ICC-l	76	OFCv-r
3	VCl-l	40	ICC-r	77	OFCvm-l
4	VCl-r	41	PCC-l	78	OFCvm-r
5	VCs-l	42	PCC-r	79	PFCvm-l
6	VCs-r	43	MCC-l	80	PFCvm-r
7	Cu-l	44	MCC-r	81	Insula-l
8	Cu-r	45	ACC-l	82	Insula-r
9	VCrm-l	46	ACC-r	83	Str-l
10	VCrm-r	47	Mv-l	84	Str-r
11	ITCm-l	48	Mv-r	85	STN-l
12	ITCm-r	49	Mdl-l	86	STN-r
13	ITCr-l	50	Mdl-r	87	GPi-l
14	ITCr-r	51	Mdm-l	88	GPi-r
15	MTCc-l	52	Mdm-r	89	GPe-l
16	MTCc-r	53	PMrv-l	90	GPe-r
17	STCc-l	54	PMrv-r	91	Tha-l
18	STCc-r	55	PMdl-l	92	Tha-r
19	STCr-l	56	PMdl-r	93	Amg-l
20	STCr-r	57	PMdm-l	94	Amg-r
21	MTCr-l	58	PMdm-r	95	VTA-l
22	MTCr-r	59	PFcdl-l	96	VTA-r
23	IPCv-l	60	PFcdl-r	97	SN-l
24	IPCv-r	61	PFcdm-l	98	SN-r
25	IPCd-l	62	PFcdm-r	99	RN-l
26	IPCd-r	63	PFrvl-l	100	RN-r
27	SPC-l	64	PFrvl-r	101	PAG-l
28	SPC-r	65	Pfrdli-l	102	PAG-r
29	SPCm-l	66	Pfrdli-r	103	PPN-l
30	SPCm-r	67	Pfrdls-l	104	PPN-r
31	PCm-l	68	Pfrdls-r	105	Cl-l
32	PCm-r	69	PFrd-l	106	Cl-r
33	Sv-l	70	PFrd-r	107	LV-l
34	Sv-r	71	PFrm-l	108	LV-r
35	Sdl-l	72	PFrm-r	109	3V
36	Sdl-r	73	OFCvl-l	110	4V
37	Sdm-l	74	OFCvl-r		

Table A.2. Descriptive statistics of fibre densities associated with the tracts connecting to the cortical lobes and subcortex for the left and right VTA and SN, respectively.

Area	Hemisphere	*Mean*				*SD*			
		left		right		left		right	
		VTA	SN	VTA	SN	VTA	SN	VTA	SN
Visual cortex	l	0.033	0.174	0.012	0.013	0.014	0.065	0.007	0.006
	r	0.010	0.016	0.035	0.165	0.006	0.008	0.017	0.058
Temporal cortex	l	0.146	0.885	0.076	0.097	0.066	0.315	0.038	0.063
	r	0.033	0.050	0.098	0.638	0.019	0.029	0.028	0.158
Parietal cortex	l	0.115	0.460	0.053	0.067	0.045	0.150	0.024	0.030
	r	0.033	0.065	0.121	0.440	0.016	0.031	0.052	0.148
Cingular cortex	l	0.148	0.648	0.042	0.057	0.067	0.268	0.023	0.034
	r	0.036	0.062	0.202	0.796	0.023	0.032	0.082	0.256
Motor cortex	l	0.142	0.551	0.061	0.079	0.061	0.234	0.037	0.050
	r	0.034	0.058	0.150	0.546	0.027	0.040	0.068	0.222
Prefrontal cortex	l	0.091	0.273	0.039	0.041	0.039	0.099	0.022	0.028
	r	0.025	0.036	0.093	0.287	0.014	0.016	0.034	0.109
Orbitofrontal cortex	l	0.155	0.438	0.118	0.135	0.058	0.174	0.047	0.056
	r	0.075	0.122	0.128	0.274	0.029	0.051	0.050	0.108
Insular cortex	l	0.061	0.257	0.020	0.017	0.028	0.094	0.013	0.010
	r	0.009	0.013	0.053	0.216	0.006	0.011	0.033	0.087
Subcortex	l	1.635	3.105	1.399	1.264	0.400	0.614	0.417	0.360
	r	1.027	1.118	1.729	3.042	0.332	0.330	0.443	0.514

Table A.3. Descriptive statistics of the node tracts' fibre densities.

Area	Hemisphere	*Mean*				*SD*			
		left		right		left		right	
		VTA	SN	VTA	SN	VTA	SN	VTA	SN
VCcm	l	0.031	0.182	0.011	0.012	0.013	0.072	0.005	0.005
	r	0.005	0.006	0.124	0.023	0.005	0.004	0.048	0.011
VCl	l	0.016	0.080	0.004	0.005	0.012	0.074	0.006	0.003
	r	0.001	0.001	0.050	0.009	0.001	0.001	0.033	0.007
VCs	l	0.018	0.098	0.002	0.003	0.014	0.066	0.002	0.003
	r	0.002	0.002	0.093	0.019	0.002	0.004	0.068	0.019
Cu	l	0.024	0.130	0.010	0.007	0.014	0.065	0.008	0.006
	r	0.008	0.015	0.170	0.036	0.007	0.011	0.081	0.028
VCrm	l	0.075	0.380	0.040	0.034	0.037	0.160	0.023	0.021
	r	0.034	0.056	0.385	0.088	0.023	0.034	0.166	0.046
ITCm	l	0.584	3.886	0.458	0.336	0.297	1.553	0.315	0.177
	r	0.121	0.188	2.571	0.322	0.077	0.129	0.762	0.098
ITCr	l	0.127	0.659	0.073	0.063	0.071	0.281	0.053	0.037
	r	0.041	0.061	0.537	0.103	0.029	0.037	0.218	0.045
MTCc	l	0.009	0.052	0.001	0.002	0.008	0.036	0.001	0.002
	r	0.002	0.001	0.076	0.016	0.002	0.002	0.059	0.014
STCc	l	0.036	0.178	0.016	0.010	0.023	0.084	0.015	0.007
	r	0.007	0.015	0.197	0.045	0.006	0.011	0.117	0.035

Area	Hemisphere	*Mean*				*SD*			
		left		**right**		**left**		**right**	
		VTA	**SN**	**VTA**	**SN**	**VTA**	**SN**	**VTA**	**SN**
STCr	l	0.051	0.215	0.012	0.017	0.030	0.129	0.010	0.010
	r	0.012	0.012	0.186	0.043	0.006	0.007	0.067	0.018
MTCr	l	0.069	0.318	0.021	0.027	0.036	0.154	0.015	0.014
	r	0.018	0.021	0.260	0.061	0.009	0.012	0.108	0.033
IPCv	l	0.353	1.369	0.190	0.197	0.131	0.514	0.090	0.092
	r	0.116	0.192	0.816	0.260	0.069	0.088	0.224	0.101
IPCd	l	0.058	0.255	0.023	0.019	0.041	0.147	0.023	0.013
	r	0.012	0.017	0.289	0.068	0.010	0.017	0.200	0.051
SPC	l	0.042	0.179	0.008	0.009	0.047	0.143	0.009	0.011
	r	0.003	0.004	0.129	0.029	0.003	0.006	0.153	0.037
SPCm	l	0.101	0.417	0.033	0.034	0.072	0.287	0.024	0.030
	r	0.019	0.026	0.522	0.123	0.021	0.028	0.429	0.098
PCm	l	0.147	0.595	0.031	0.030	0.115	0.295	0.028	0.027
	r	0.022	0.026	0.765	0.190	0.016	0.028	0.340	0.112
Sv	l	0.102	0.421	0.104	0.044	0.057	0.211	0.077	0.029
	r	0.032	0.116	0.460	0.133	0.025	0.127	0.232	0.093
Sdl	l	0.084	0.283	0.138	0.082	0.058	0.272	0.135	0.086
	r	0.051	0.131	0.348	0.121	0.033	0.081	0.364	0.102
Sdm	l	0.035	0.160	0.009	0.009	0.023	0.094	0.011	0.008
	r	0.005	0.007	0.191	0.045	0.006	0.006	0.112	0.035
ICC	l	0.129	0.589	0.034	0.032	0.086	0.376	0.018	0.023
	r	0.018	0.024	0.599	0.135	0.014	0.017	0.351	0.091
PCC	l	0.285	1.201	0.147	0.093	0.142	0.532	0.109	0.055
	r	0.091	0.164	1.587	0.424	0.061	0.093	0.570	0.169
MCC	l	0.041	0.187	0.007	0.010	0.027	0.113	0.008	0.011
	r	0.011	0.013	0.373	0.090	0.012	0.011	0.197	0.061
ACC	l	0.137	0.616	0.041	0.033	0.075	0.309	0.031	0.024
	r	0.023	0.046	0.627	0.158	0.016	0.029	0.325	0.105
Mv	l	0.366	1.552	0.214	0.140	0.195	0.848	0.155	0.090
	r	0.071	0.142	1.294	0.329	0.055	0.098	0.607	0.166
Mdl	l	0.097	0.403	0.023	0.027	0.054	0.203	0.019	0.018
	r	0.019	0.019	0.497	0.136	0.014	0.014	0.227	0.084
Mdm	l	0.086	0.327	0.032	0.033	0.050	0.174	0.022	0.022
	r	0.025	0.043	0.404	0.113	0.023	0.043	0.227	0.079
PMrv	l	0.156	0.579	0.116	0.085	0.081	0.304	0.088	0.061
	r	0.046	0.086	0.555	0.154	0.045	0.078	0.328	0.091
PMdl	l	0.062	0.206	0.021	0.022	0.049	0.140	0.020	0.022
	r	0.019	0.023	0.247	0.074	0.019	0.017	0.170	0.050
PMdm	l	0.082	0.239	0.068	0.057	0.042	0.127	0.058	0.045
	r	0.028	0.037	0.280	0.091	0.021	0.025	0.171	0.047
PFcdl	l	0.108	0.306	0.163	0.109	0.070	0.250	0.152	0.093
	r	0.070	0.140	0.405	0.146	0.055	0.085	0.351	0.101
PFcdm	l	0.126	0.407	0.020	0.035	0.076	0.206	0.018	0.026
	r	0.015	0.011	0.374	0.116	0.015	0.010	0.222	0.083
PFrvl	l	0.119	0.355	0.017	0.028	0.083	0.229	0.016	0.023
	r	0.017	0.015	0.386	0.118	0.011	0.009	0.242	0.067
Pfrdli	l	0.090	0.262	0.021	0.029	0.062	0.175	0.020	0.024
	r	0.017	0.017	0.300	0.093	0.013	0.012	0.290	0.069

Table A.3. Descriptive statistics of the node tracts' fibre densities.

Area	Hemisphere	*Mean*				*SD*			
		left		**right**		**left**		**right**	
		VTA	**SN**	**VTA**	**SN**	**VTA**	**SN**	**VTA**	**SN**
VCcm	l	0.031	0.182	0.011	0.012	0.013	0.072	0.005	0.005
	r	0.005	0.006	0.124	0.023	0.005	0.004	0.048	0.011
VCl	l	0.016	0.080	0.004	0.005	0.012	0.074	0.006	0.003
	r	0.001	0.001	0.050	0.009	0.001	0.001	0.033	0.007
VCs	l	0.018	0.098	0.002	0.003	0.014	0.066	0.002	0.003
	r	0.002	0.002	0.093	0.019	0.002	0.004	0.068	0.019
Cu	l	0.024	0.130	0.010	0.007	0.014	0.065	0.008	0.006
	r	0.008	0.015	0.170	0.036	0.007	0.011	0.081	0.028
VCrm	l	0.075	0.380	0.040	0.034	0.037	0.160	0.023	0.021
	r	0.034	0.056	0.385	0.088	0.023	0.034	0.166	0.046
ITCm	l	0.584	3.886	0.458	0.336	0.297	1.553	0.315	0.177
	r	0.121	0.188	2.571	0.322	0.077	0.129	0.762	0.098
ITCr	l	0.127	0.659	0.073	0.063	0.071	0.281	0.053	0.037
	r	0.041	0.061	0.537	0.103	0.029	0.037	0.218	0.045
MTCc	l	0.009	0.052	0.001	0.002	0.008	0.036	0.001	0.002
	r	0.002	0.001	0.076	0.016	0.002	0.002	0.059	0.014
STCc	l	0.036	0.178	0.016	0.010	0.023	0.084	0.015	0.007
	r	0.007	0.015	0.197	0.045	0.006	0.011	0.117	0.035
STCr	l	0.051	0.215	0.012	0.017	0.030	0.129	0.010	0.010
	r	0.012	0.012	0.186	0.043	0.006	0.007	0.067	0.018
MTCr	l	0.069	0.318	0.021	0.027	0.036	0.154	0.015	0.014
	r	0.018	0.021	0.260	0.061	0.009	0.012	0.108	0.033
IPCv	l	0.353	1.369	0.190	0.197	0.131	0.514	0.090	0.092
	r	0.116	0.192	0.816	0.260	0.069	0.088	0.224	0.101
IPCd	l	0.058	0.255	0.023	0.019	0.041	0.147	0.023	0.013
	r	0.012	0.017	0.289	0.068	0.010	0.017	0.200	0.051
SPC	l	0.042	0.179	0.008	0.009	0.047	0.143	0.009	0.011
	r	0.003	0.004	0.129	0.029	0.003	0.006	0.153	0.037
SPCm	l	0.101	0.417	0.033	0.034	0.072	0.287	0.024	0.030
	r	0.019	0.026	0.522	0.123	0.021	0.028	0.429	0.098
PCm	l	0.147	0.595	0.031	0.030	0.115	0.295	0.028	0.027
	r	0.022	0.026	0.765	0.190	0.016	0.028	0.340	0.112
Sv	l	0.102	0.421	0.104	0.044	0.057	0.211	0.077	0.029
	r	0.032	0.116	0.460	0.133	0.025	0.127	0.232	0.093
Sdl	l	0.084	0.283	0.138	0.082	0.058	0.272	0.135	0.086
	r	0.051	0.131	0.348	0.121	0.033	0.081	0.364	0.102
Sdm	l	0.035	0.160	0.009	0.009	0.023	0.094	0.011	0.008
	r	0.005	0.007	0.191	0.045	0.006	0.006	0.112	0.035
ICC	l	0.129	0.589	0.034	0.032	0.086	0.376	0.018	0.023
	r	0.018	0.024	0.599	0.135	0.014	0.017	0.351	0.091
PCC	l	0.285	1.201	0.147	0.093	0.142	0.532	0.109	0.055
	r	0.091	0.164	1.587	0.424	0.061	0.093	0.570	0.169
MCC	l	0.041	0.187	0.007	0.010	0.027	0.113	0.008	0.011
	r	0.011	0.013	0.373	0.090	0.012	0.011	0.197	0.061
ACC	l	0.137	0.616	0.041	0.033	0.075	0.309	0.031	0.024
	r	0.023	0.046	0.627	0.158	0.016	0.029	0.325	0.105
Mv	l	0.366	1.552	0.214	0.140	0.195	0.848	0.155	0.090
	r	0.071	0.142	1.294	0.329	0.055	0.098	0.607	0.166
Mdl	l	0.097	0.403	0.023	0.027	0.054	0.203	0.019	0.018
	r	0.019	0.019	0.497	0.136	0.014	0.014	0.227	0.084

Area	Hemisphere	*Mean*				*SD*			
		left		**right**		**left**		**right**	
		VTA	**SN**	**VTA**	**SN**	**VTA**	**SN**	**VTA**	**SN**
Mdm	l	0.086	0.327	0.032	0.033	0.050	0.174	0.022	0.022
	r	0.025	0.043	0.404	0.113	0.023	0.043	0.227	0.079
PMrv	l	0.156	0.579	0.116	0.085	0.081	0.304	0.088	0.061
	r	0.046	0.086	0.555	0.154	0.045	0.078	0.328	0.091
PMdl	l	0.062	0.206	0.021	0.022	0.049	0.140	0.020	0.022
	r	0.019	0.023	0.247	0.074	0.019	0.017	0.170	0.050
PMdm	l	0.082	0.239	0.068	0.057	0.042	0.127	0.058	0.045
	r	0.028	0.037	0.280	0.091	0.021	0.025	0.171	0.047
PFcdl	l	0.108	0.306	0.163	0.109	0.070	0.250	0.152	0.093
	r	0.070	0.140	0.405	0.146	0.055	0.085	0.351	0.101
PFcdm	l	0.126	0.407	0.020	0.035	0.076	0.206	0.018	0.026
	r	0.015	0.011	0.374	0.116	0.015	0.010	0.222	0.083
PFrvl	l	0.119	0.355	0.017	0.028	0.083	0.229	0.016	0.023
	r	0.017	0.015	0.386	0.118	0.011	0.009	0.242	0.067
Pfrdli	l	0.090	0.262	0.021	0.029	0.062	0.175	0.020	0.024
	r	0.017	0.017	0.300	0.093	0.013	0.012	0.290	0.069
Pfrdls	l	0.070	0.203	0.015	0.019	0.055	0.168	0.013	0.015
	r	0.011	0.009	0.164	0.055	0.006	0.006	0.107	0.030
PFrd	l	0.045	0.118	0.034	0.031	0.028	0.092	0.035	0.025
	r	0.029	0.036	0.123	0.057	0.025	0.029	0.083	0.037
PFrm	l	0.081	0.260	0.014	0.023	0.048	0.125	0.011	0.018
	r	0.017	0.021	0.259	0.066	0.013	0.014	0.170	0.040
OFCvl	l	0.057	0.212	0.022	0.024	0.037	0.139	0.016	0.013
	r	0.034	0.048	0.208	0.076	0.018	0.032	0.125	0.043
OFCv	l	0.110	0.349	0.077	0.073	0.054	0.180	0.043	0.035
	r	0.022	0.028	0.141	0.051	0.014	0.020	0.094	0.031
OFCvm	l	0.149	0.407	0.154	0.120	0.061	0.189	0.072	0.051
	r	0.100	0.175	0.336	0.161	0.039	0.079	0.130	0.065
PFCvm	l	0.303	0.786	0.288	0.254	0.125	0.309	0.124	0.119
	r	0.146	0.237	0.413	0.223	0.066	0.099	0.176	0.114
Insular	l	0.061	0.257	0.017	0.020	0.028	0.093	0.009	0.013
	r	0.009	0.013	0.216	0.053	0.006	0.011	0.086	0.033
Str	l	0.718	2.464	0.202	0.254	0.236	0.627	0.083	0.093
	r	0.214	0.242	2.525	0.842	0.079	0.082	0.585	0.281
STN	l	1.398	3.000	0.444	0.697	0.587	0.978	0.230	0.332
	r	0.712	0.538	3.214	1.693	0.558	0.348	1.268	0.897
GPi	l	1.607	5.174	0.528	0.700	0.462	1.396	0.227	0.257
	r	0.629	0.645	5.751	2.080	0.262	0.288	1.283	0.682
GPe	l	0.866	3.040	0.274	0.325	0.238	0.651	0.108	0.110
	r	0.263	0.288	3.096	0.986	0.101	0.113	0.641	0.279
Tha	l	0.921	2.333	0.321	0.414	0.241	0.517	0.119	0.103
	r	0.346	0.356	1.968	1.032	0.117	0.109	0.377	0.307
Amg	l	0.950	6.526	0.467	0.467	0.462	2.715	0.310	0.244
	r	0.399	0.503	7.303	1.038	0.240	0.285	2.659	0.432
VTA	l	0.000	5.901	3.418	3.110	0.000	2.000	1.544	1.216
	r	3.110	4.292	6.652	0.000	1.216	1.745	2.176	0.000
SN	l	5.901	0.000	4.334	4.292	2.000	0.000	1.653	1.745
	r	3.418	4.334	0.000	6.652	1.544	1.653	0.000	2.176
RN	l	1.683	1.792	0.409	0.828	0.607	0.548	0.174	0.318
	r	0.766	0.459	1.586	1.992	0.291	0.161	0.580	0.842
PAG	l	2.000	2.786	1.162	1.712	0.763	1.036	0.497	0.808
	r	1.587	1.425	2.338	2.634	0.667	0.595	0.937	1.165

Area	Hemisphere	*Mean*				*SD*			
		left		**right**		**left**		**right**	
		VTA	**SN**	**VTA**	**SN**	**VTA**	**SN**	**VTA**	**SN**
PPN	l	2.645	3.781	1.157	2.107	0.842	0.958	0.500	0.789
	r	1.718	1.157	3.391	2.947	0.948	0.653	1.026	1.122
Cl	l	0.104	0.374	0.027	0.036	0.052	0.144	0.024	0.021
	r	0.022	0.025	0.339	0.109	0.016	0.018	0.115	0.055

Table A.4. Summary of results from one-sample *t*-tests on the difference of SN-VTA fibre densities to cortical lobes and the subcortex.

Difference	Lobe	Hemisphere	*t*	*p*	
left SN – left VTA	Visual cortex	l	16.372	0.0	***
		r	6.848	0.0	***
	Temporal cortex	l	17.221	0.0	***
		r	4.898	0.0002	***
	Parietal cortex	l	18.382	0.0	***
		r	7.450	0.0	***
	Cingular cortex	l	15.203	0.0	***
		r	6.059	0.0	***
	Motor cortex	l	14.850	0.0	***
		r	6.499	0.0	***
	Prefrontal cortex	l	16.210	0.0	***
		r	5.968	0.0	***
	Orbitofrontal cortex	l	12.278	0.0	***
		r	8.843	0.0	***
	Insular cortex	l	17.244	0.0	***
		r	3.356	0.031	*
	Subcortex	l	21.190	0.0	***
		r	2.146	0.709	
right SN – right VTA	Visual cortex	l	1.755	1.0	
		r	17.366	0.0	***
	Temporal cortex	l	2.536	0.28	
		r	23.842	0.0	***
	Parietal cortex	l	2.932	0.1	
		r	18.544	0.0	***
	Cingular cortex	l	3.369	0.029	*
		r	19.197	0.0	***
	Motor cortex	l	3.403	0.027	*
		r	15.239	0.0	***
	Prefrontal cortex	l	0.450	1.0	
		r	15.057	0.0	***
	Orbitofrontal cortex	l	1.888	1.0	
		r	11.152	0.0	***
	Insular cortex	l	-1.485	1.0	
		r	17.079	0.0	***
	Subcortex	l	-1.943	1.0	
		r	21.286	0.0	***

Note. *p*-values represent Bonferroni-corrected *p*-values.
* = $p < .05$; ** = $p < 0.01$; *** = $p < 0.001$.

Table A.5. Summary of results from one-sample t-tests on the difference between left SN and left VTA fibre densities for each cortical and subcortical node.

Node	Hem	*t*	*p*		Node	Hem	*t*	*p*	
VCcm	l	21.680	0.0	***	PMdl	l	14.093	0.0	***
	r	2.193	1.0			r	2.928	0.474	
VCl	l	9.515	0.0	***	PMdm	l	15.417	0.0	***
	r	-0.110	1.0			r	5.929	0.0	***
VCs	l	13.511	0.0	***	PFcdl	l	10.072	0.0	***
	r	0.757	1.0			r	11.161	0.0	***
Cu	l	18.571	0.0	***	PFcdm	l	18.399	0.0	***
	r	6.054	0.0	***		r	-4.241	0.006	**
VCrm	l	21.038	0.0	***	PFrvl	l	13.795	0.0	***
	r	10.140	0.0	***		r	-2.143	1.0	
ITCm	l	22.309	0.0	***	Pfrdli	l	12.881	0.0	***
	r	6.444	0.0	***		r	0.151	1.0	
ITCr	l	20.057	0.0	***	Pfrdls	l	9.861	0.0	***
	r	6.798	0.0	***		r	-3.815	0.027	*
MTCc	l	13.634	0.0	***	PFrd	l	9.902	0.0	***
	r	-1.529	1.0			r	4.057	0.012	*
STCc	l	19.604	0.0	***	PFrm	l	18.235	0.0	***
	r	7.092	0.0	***		r	3.350	0.130	
STCr	l	14.577	0.0	***	OFCvl	l	12.953	0.0	***
	r	0.464	1.0			r	5.643	0.0	***
MTCr	l	17.683	0.0	***	OFCv	l	14.674	0.0	***
	r	2.983	0.403			r	4.178	0.007	**
IPCv	l	20.969	0.0	***	OFCvm	l	15.059	0.0	***
	r	7.841	0.0	***		r	12.164	0.0	***
IPCd	l	15.369	0.0	***	PFCvm	l	17.794	0.0	***
	r	3.140	0.251			r	14.107	0.0	***
SPC	l	12.539	0.0	***	Insular	l	24.522	0.0	***
	r	2.779	0.729			r	4.772	0.001	***
SPCm	l	13.001	0.0	***	Str	l	32.148	0.0	***
	r	3.661	0.046	*		r	3.373	0.120	
PCm	l	20.172	0.0	***	STN	l	19.004	0.0	***
	r	1.381	1.0			r	-4.802	0.001	***
Sv	l	18.391	0.0	***	GPi	l	27.294	0.0	***
	r	7.257	0.0	***		r	0.591	1.0	
Sdl	l	8.276	0.0	***	GPe	l	34.467	0.0	***
	r	12.176	0.0	***		r	2.540	1.0	
Sdm	l	15.734	0.0	***	Tha	l	30.443	0.0	***
	r	3.009	0.373			r	0.886	1.0	
ICC	l	14.467	0.0	***	Amg	l	20.681	0.0	***
	r	3.482	0.084			r	4.868	0.001	***
PCC	l	20.204	0.0	***	VTA	l			
	r	8.850	0.0	***		r	9.383	0.0	***
MCC	l	15.210	0.0	***	SN	l			
	r	1.328	1.0			r	6.390	0.0	***
ACC	l	18.353	0.0	***	RN	l	2.117	1.0	
	r	8.961	0.0	***		r	-12.430	0.0	***
Mv	l	16.604	0.0	***	PAG	l	9.473	0.0	***
	r	9.813	0.0	***		r	-3.495	0.081	
Mdl	l	18.208	0.0	***	PPN	l	16.945	0.0	***
	r	0.329	1.0			r	-11.620	0.0	***
Mdm	l	17.419	0.0	***	Cl	l	23.839	0.0	***
	r	5.799	0.0	***		r	1.736	1.0	
PMrv	l	17.084	0.0	***					
	r	8.817	0.0	***					

Note. p-values represent Bonferroni-corrected p-values. * = $p < .05$; ** = $p < 0.01$; *** = $p < 0.001$.

Table A.6. Summary of results from one-sample *t*-tests on the difference between right SN and right VTA fibre densities for each cortical and subcortical node.

Node	Hem	*t*	*p*		Node	Hem	*t*	*p*	
VCcm	l	-1.140	1.0		PMdl	l	-0.642	1.0	
	r	22.078	0.0	***		r	12.522	0.0	***
VCl	l	-1.028	1.0		PMdm	l	2.437	1.0	
	r	14.194	0.0	***		r	13.062	0.0	***
VCs	l	-3.220	0.1956		PFcdl	l	6.032	0.0	***
	r	13.425	0.0	***		r	9.356	0.0	***
Cu	l	4.097	0.01	*	PFcdm	l	-7.115	0.0	***
	r	19.830	0.0	***		r	15.639	0.0	***
VCrm	l	3.602	0.0566		PFrvl	l	-5.991	0.0	***
	r	20.046	0.0	***		r	13.171	0.0	***
ITCm	l	4.260	0.0055	**	Pfrdli	l	-4.018	0.0133	*
	r	29.275	0.0	***		r	8.637	0.0	***
ITCr	l	2.193	1.0		Pfrdls	l	-3.838	0.0251	*
	r	21.364	0.0	***		r	12.679	0.0	***
MTCc	l	-5.368	0.0001	***	PFrd	l	1.541	1.0	
	r	11.922	0.0	***		r	10.903	0.0	***
STCc	l	3.638	0.05		PFrm	l	-5.534	0.0	***
	r	15.667	0.0	***		r	13.386	0.0	***
STCr	l	-5.487	0.0	***	OFCvl	l	-1.618	1.0	
	r	23.492	0.0	***		r	12.545	0.0	***
MTCr	l	-3.468	0.0882		OFCv	l	0.969	1.0	
	r	20.511	0.0	***		r	12.181	0.0	***
IPCv	l	-0.636	1.0		OFCvm	l	4.560	0.0018	**
	r	26.805	0.0	***		r	14.643	0.0	***
IPCd	l	2.233	1.0		PFCvm	l	2.438	1.0	
	r	13.402	0.0	***		r	16.124	0.0	***
SPC	l	-0.562	1.0		Insular	l	-2.112	1.0	
	r	8.036	0.0	***		r	24.287	0.0	***
SPCm	l	-0.352	1.0		Str	l	-5.383	0.0001	***
	r	11.022	0.0	***		r	36.257	0.0	***
PCm	l	0.335	1.0		STN	l	-9.483	0.0	***
	r	21.268	0.0	***		r	17.351	0.0	***
Sv	l	8.904	0.0	***	GPi	l	-6.704	0.0	***
	r	19.127	0.0	***		r	33.570	0.0	***
Sdl	l	7.115	0.0	***	GPe	l	-4.038	0.0123	*
	r	7.951	0.0	***		r	40.058	0.0	***
Sdm	l	-0.578	1.0		Tha	l	-6.598	0.0	***
	r	16.738	0.0	***		r	26.634	0.0	***
ICC	l	0.668	1.0		Amg	l	-0.028	1.0	
	r	15.694	0.0	***		r	23.115	0.0	***
PCC	l	5.664	0.0	***	VTA	l	2.268	1.0	
	r	24.036	0.0	***		r			
MCC	l	-3.219	0.1963		SN	l	0.230	1.0	
	r	18.431	0.0	***		r			
ACC	l	2.648	1.0		RN	l	-13.999	0.0	***
	r	18.314	0.0	***		r	-5.115	0.0002	***
Mv	l	6.404	0.0	***	PAG	l	-7.191	0.0	***
	r	19.242	0.0	***		r	-2.960	0.4308	
Mdl	l	-2.343	1.0		PPN	l	-13.961	0.0	***
	r	19.783	0.0	***		r	4.084	0.0105	*
Mdm	l	-0.743	1.0		Cl	l	-3.032	0.3481	
	r	16.395	0.0	***		r	27.653	0.0	***
PMrv	l	5.199	0.0001	***					
	r	15.052	0.0	***					

Note. p-values represent Bonferroni-corrected *p*-values. * = $p < .05$; ** = $p < 0.01$; *** = $p < 0.001$.

Table A.7. Descriptive statistics of the lobe tracts' fibre densities associated with the connectome of the SN, collapsed across hemispheres.

	Ipsilateral			Contralateral	
Lobe	***Mean***	***SD***	**Lobe**	***Mean***	***SD***
Visual	0.169	0.061	Visual	0.015	0.007
Insular	0.236	0.092	Insular	0.015	0.010
PFC	0.280	0.103	PFC	0.038	0.023
Cingular	0.356	0.166	Cingular	0.060	0.033
Parietal	0.450	0.149	Parietal	0.066	0.030
Motor	0.549	0.227	Motor	0.069	0.046
Temporal	0.722	0.271	Temporal	0.073	0.054
OFC	0.761	0.277	OFC	0.129	0.054
Subcortex	3.074	0.564	Subcortex	1.191	0.351

Table A.8. Descriptive statistics of the lobe tracts' fibre densities associated with the connectome of the VTA, collapsed across hemispheres.

	Ipsilateral			Contralateral	
Lobe	***Mean***	***SD***	**Lobe**	***Mean***	***SD***
Visual	0.034	0.015	Visual	0.011	0.007
Insular	0.057	0.031	Insular	0.015	0.011
PFC	0.092	0.036	PFC	0.032	0.019
Cingular	0.118	0.048	Cingular	0.039	0.023
Parietal	0.122	0.055	Parietal	0.043	0.023
Motor	0.141	0.056	Motor	0.048	0.035
Temporal	0.146	0.064	Temporal	0.055	0.036
OFC	0.175	0.079	OFC	0.097	0.045
Subcortex	1.682	0.422	Subcortex	1.213	0.418

Table A.9. Descriptive statistics of the node tracts' fibre densities associated with the connectomes of the SN.

Ipsilateral			Contralateral		
Node	***Mean***	***SD***	**Node**	***Mean***	***SD***
Amg	6.915	2.708	SN	4.334	1.648
VTA	6.277	2.118	VTA	3.855	1.701
GPi	5.462	1.368	PAG	1.294	0.563
PPN	3.586	1.009	PPN	1.157	0.580
ITCm	3.228	1.386	GPi	0.587	0.265
STN	3.107	1.135	STN	0.491	0.298
GPe	3.068	0.645	Amg	0.485	0.298
PAG	2.562	1.010	RN	0.434	0.169
Str	2.495	0.606	Tha	0.339	0.115
Tha	2.151	0.487	ITCm	0.323	0.276
RN	1.689	0.572	GPe	0.281	0.111
Mv	1.423	0.747	PFCvm	0.262	0.115
PCC	1.394	0.583	Str	0.222	0.085
IPCv	1.093	0.483	IPCv	0.191	0.088
PCm	0.680	0.329	Mv	0.178	0.134
ACC	0.622	0.316	OFCvm	0.164	0.076
PFCvm	0.599	0.312	PCC	0.156	0.101
ITCr	0.598	0.258	PFcdl	0.152	0.123
ICC	0.594	0.363	Sdl	0.135	0.111
PMrv	0.567	0.316	Sv	0.110	0.105
SPCm	0.469	0.368	PMrv	0.101	0.084
Mdl	0.450	0.220	ITCr	0.067	0.046
Sv	0.440	0.222	OFCv	0.053	0.042
PFcdm	0.391	0.214	PMdm	0.052	0.047
VCrm	0.383	0.163	VCrm	0.048	0.030
OFCvm	0.372	0.165	ACC	0.044	0.030
PFrvl	0.371	0.236	Mdm	0.037	0.035
Mdm	0.365	0.205	PFrd	0.035	0.032
Cl	0.356	0.131	OFCvl	0.035	0.028
PFcdl	0.355	0.308	SPCm	0.030	0.026
Sdl	0.316	0.322	ICC	0.029	0.018
MTCr	0.289	0.135	PCm	0.028	0.028
Pfrdli	0.281	0.240	Cl	0.026	0.021
MCC	0.280	0.185	PMdl	0.022	0.018
IPCd	0.272	0.176	Mdl	0.021	0.016
PMdm	0.259	0.152	MTCr	0.021	0.013
PFrm	0.259	0.149	IPCd	0.020	0.020
OFCv	0.245	0.177	Pfrdli	0.019	0.017
Insula	0.236	0.092	PFrm	0.018	0.013
PMdl	0.227	0.157	PFrvl	0.016	0.013
OFCvl	0.210	0.132	PFcdm	0.016	0.015
STCr	0.200	0.103	Insula	0.015	0.010
STCc	0.187	0.102	STCc	0.015	0.013
Pfrdls	0.184	0.142	Cu	0.012	0.010
Sdm	0.175	0.104	Pfrdls	0.012	0.011
SPC	0.154	0.150	STCr	0.012	0.009
VCcm	0.153	0.068	MCC	0.010	0.010
Cu	0.150	0.076	VCcm	0.009	0.005
PFrd	0.121	0.087	Sdm	0.008	0.009
VCs	0.095	0.067	SPC	0.006	0.008
VCl	0.065	0.059	VCl	0.003	0.004
MTCc	0.064	0.050	VCs	0.002	0.003
SN	-	-	MTCc	0.001	0.001

Table A.10. Descriptive statistics of the node tracts' fibre densities associated with the connectomes of the VTA.

	Ipsilateral			Contralateral	
Node	***Mean***	***SD***	**Node**	***Mean***	***SD***
SN	6.277	2.118	SN	3.855	1.701
PPN	2.796	1.001	VTA	3.110	1.213
PAG	2.317	1.032	PPN	1.913	0.891
GPi	1.843	0.627	PAG	1.650	0.742
RN	1.837	0.748	RN	0.797	0.306
STN	1.545	0.770	STN	0.704	0.458
Amg	0.994	0.448	GPi	0.664	0.261
Tha	0.977	0.280	Amg	0.433	0.244
GPe	0.926	0.266	Tha	0.380	0.115
Str	0.780	0.266	GPe	0.294	0.110
ITCm	0.453	0.257	Str	0.234	0.088
PCC	0.355	0.171	ITCm	0.228	0.174
Mv	0.347	0.181	PFCvm	0.200	0.110
IPCv	0.307	0.126	IPCv	0.157	0.091
PFCvm	0.263	0.126	OFCvm	0.110	0.046
PCm	0.169	0.115	Mv	0.105	0.082
OFCvm	0.155	0.063	PCC	0.092	0.058
PMrv	0.155	0.086	PFcdl	0.089	0.079
ACC	0.147	0.092	Sdl	0.067	0.067
ICC	0.132	0.088	PMrv	0.065	0.057
PFcdl	0.127	0.089	ITCr	0.052	0.035
PFcdm	0.121	0.079	OFCv	0.047	0.037
PFrvl	0.118	0.075	PMdm	0.042	0.038
Sv	0.118	0.078	Sv	0.038	0.027
Mdl	0.117	0.073	VCrm	0.034	0.022
ITCr	0.115	0.060	PFrd	0.030	0.025
SPCm	0.112	0.087	Cl	0.029	0.020
Cl	0.106	0.053	OFCvl	0.029	0.016
Sdl	0.103	0.085	Mdm	0.029	0.023
Mdm	0.100	0.067	ACC	0.028	0.021
Pfrdli	0.092	0.065	SPCm	0.026	0.027
PMdm	0.087	0.045	PCm	0.026	0.022
VCrm	0.081	0.042	ICC	0.025	0.020
OFCv	0.081	0.053	PFcdm	0.025	0.024
PFrm	0.074	0.045	Pfrdli	0.023	0.020
PMdl	0.068	0.050	Mdl	0.023	0.017
OFCvl	0.066	0.041	PFrvl	0.022	0.019
MCC	0.066	0.053	MTCr	0.022	0.013
MTCr	0.065	0.035	PMdl	0.021	0.020
IPCd	0.063	0.046	PFrm	0.020	0.016
Pfrdls	0.062	0.045	IPCd	0.015	0.012
Insula	0.057	0.031	Pfrdls	0.015	0.012
PFrd	0.051	0.034	Insula	0.015	0.011
STCr	0.047	0.025	STCr	0.014	0.009
STCc	0.040	0.030	MCC	0.011	0.012
Sdm	0.040	0.030	STCc	0.009	0.006
SPC	0.036	0.043	VCcm	0.008	0.006
Cu	0.030	0.023	Cu	0.008	0.007
VCcm	0.027	0.013	Sdm	0.007	0.007
VCs	0.018	0.016	SPC	0.006	0.009
MTCc	0.012	0.012	VCl	0.003	0.003
VCl	0.012	0.010	VCs	0.002	0.003
VTA	-	-	MTCc	0.002	0.002

Table A.11. Bayesian Pearson Correlations Between Age and SN's Node Tracts' Fibre Densities.

		Left		Right	
Node	**Hem**	**Pearson's *r***	**BF_{10}**	**Pearson's *r***	**BF_{10}**
VCcm	l	-0.184	0.381	-0.177	0.361
	r	-0.036	0.189	-0.182	0.374
VCl	l	0.074	0.206	0.04	0.19
	r	0.11	0.238	-0.019	0.185
VCs	l	-0.167	0.333	0.007	0.184
	r	0.173	0.35	-0.038	0.189
Cu	l	-0.381	5.008	-0.292	1.197
	r	0.245	0.679	-0.31	1.542
VCrm	l	-0.397	6.881	**-0.437 ***	15.853
	r	**-0.437 ***	15.911	**-0.468 ****	33.322
ITCm	l	-0.134	0.269	0.088	0.217
	r	-0.035	0.188	-0.042	0.191
ITCr	l	-0.408	8.506	-0.249	0.707
	r	-0.279	1.011	-0.308	1.504
MTCc	l	0.025	0.186	0.16	0.318
	r	0.189	0.395	0.101	0.228
STCc	l	0.107	0.234	0.257	0.776
	r	0.14	0.279	0.298	1.303
STCr	l	0.048	0.193	0.019	0.185
	r	0.114	0.243	0.183	0.376
MTCr	l	-0.099	0.226	-0.195	0.417
	r	-0.157	0.312	-0.044	0.191
IPCv	l	-0.023	0.186	-0.155	0.307
	r	-0.062	0.199	0.021	0.186
IPCd	l	0.04	0.19	0.302	1.383
	r	**0.438 ***	16.339	0.319	1.778
SPC	l	-0.116	0.245	0.145	0.288
	r	0.186	0.386	0.19	0.4
SPCm	l	0.012	0.184	0.124	0.255
	r	0.199	0.43	0.263	0.832
PCm	l	-0.182	0.373	0.13	0.263
	r	0.14	0.28	0.053	0.195
Sv	l	0.005	0.184	0.072	0.205
	r	0.03	0.187	-0.077	0.209
Sdl	l	**0.423 ***	11.621	0.355	3.159
	r	0.204	0.449	**0.417 ***	10.361
Sdm	l	0.048	0.193	0.366	3.796
	r	0.039	0.19	0.109	0.236
ICC	l	-0.139	0.278	0.056	0.197
	r	0.2	0.434	0.155	0.306
PCC	l	0.005	0.184	0.046	0.192
	r	0.089	0.218	-0.002	0.184
MCC	l	-0.076	0.207	0.316	1.682
	r	0.08	0.211	-0.027	0.187
ACC	l	-0.112	0.24	0.135	0.27
	r	0.119	0.249	0.109	0.236
Mv	l	0.084	0.213	0.103	0.23
	r	0.061	0.199	0.122	0.253
Mdl	l	-0.289	1.153	0.241	0.647
	r	0.131	0.265	-0.127	0.259
Mdm	l	-0.19	0.398	-0.052	0.195
	r	0.243	0.662	0.188	0.392
PMrv	l	-0.057	0.197	-0.07	0.204
	r	0.117	0.246	0.218	0.515

		Left		Right	
Node	**Hem**	**Pearson's *r***	**BF_{10}**	**Pearson's *r***	**BF_{10}**
PMdl	l	-0.144	0.286	-0.085	0.214
	r	0.054	0.195	-0.00036	0.184
PMdm	l	-0.246	0.684	-0.209	0.472
	r	-0.017	0.185	-0.1	0.227
PFcdl	l	0.361	3.488	0.388	5.777
	r	0.027	0.187	0.374	4.414
PFcdm	l	-0.329	2.052	0.067	0.202
	r	-0.063	0.2	-0.263	0.83
PFrvl	l	-0.17	0.342	-0.138	0.276
	r	-0.028	0.187	-0.217	0.506
Pfrdli	l	-0.159	0.314	-0.032	0.188
	r	-0.197	0.423	-0.265	0.858
Pfrdls	l	-0.371	4.202	-0.203	0.448
	r	-0.144	0.287	-0.27	0.903
PFrd	l	-0.104	0.231	-0.073	0.206
	r	-0.051	0.194	0.083	0.212
PFrm	l	-0.385	5.417	0.032	0.188
	r	-0.215	0.499	-0.353	3.033
OFCvl	l	-0.31	1.55	-0.253	0.745
	r	0.081	0.211	-0.154	0.305
OFCv	l	-0.228	0.568	-0.204	0.452
	r	-0.206	0.46	-0.376	4.589
OFCvm	l	-0.163	0.325	-0.244	0.669
	r	-0.073	0.206	-0.092	0.22
PFCvm	l	0.252	0.73	0.227	0.563
	r	0.009	0.184	0.27	0.907
Insular	l	-0.392	6.198	0.024	0.186
	r	0.046	0.192	-0.258	0.788
Str	l	0.058	0.197	0.218	0.515
	r	0.368	3.947	-0.034	0.188
STN	l	0.359	3.374	0.187	0.39
	r	**0.466 ****	32.056	**0.501 ****	81.573
GPi	l	0.35	2.872	0.13	0.263
	r	**0.417 ***	10.214	**0.435 ***	15.369
GPe	l	0.179	0.365	0.038	0.189
	r	**0.423 ***	11.627	0.332	2.161
Tha	l	0.137	0.274	0.19	0.399
	r	0.289	1.159	-0.105	0.232
Amg	l	-0.016	0.185	-0.088	0.217
	r	0.05	0.194	0.249	0.712
VTA	l	0.242	0.658	0.163	0.324
	r	0.404	7.901	0.132	0.267
SN	l	-	-	0.247	0.691
	r	0.247	0.691	-	-
RN	l	0.117	0.245	0.17	0.34
	r	0.136	0.273	0.028	0.187
PAG	l	-0.337	2.339	-0.024	0.186
	r	-0.252	0.732	-0.395	6.53
PPN	l	-0.081	0.211	0.092	0.22
	r	-0.037	0.189	-0.129	0.263
Cl	l	-0.22	0.525	0.002	0.184
	r	0.08	0.21	-0.337	2.335

Note. Presence of Bayesian evidence in favour of a correlation between variables is flagged.
* $BF_{10} > 10$, ** $BF_{10} > 30$, *** $BF_{10} > 100$.

Table A.12. Bayesian Pearson Correlations Between Age and VTA's Node Tracts' Fibre Densities.

		Left		Right	
Node	**Hem**	**Pearson's *r***	**BF_{10}**	**Pearson's *r***	**BF_{10}**
VCcm	l	**-0.436 ***	15.513	-0.352	2.974
	r	-0.174	0.351	**-0.468 ****	33.771
VCl	l	-0.067	0.202	-0.169	0.338
	r	-0.196	0.418	-0.239	0.633
VCs	l	-0.22	0.526	-0.185	0.384
	r	-0.222	0.533	-0.055	0.196
Cu	l	**-0.427***	12.791	**-0.433 ****	14.702
	r	0.135	0.271	-0.285	1.096
VCrm	l	**-0.639 *****	11518.14	**-0.676 *****	69686.12
	r	**-0.478 ****	43.591	**-0.614 *****	3868.014
ITCm	l	-0.317	1.727	-0.298	1.308
	r	-0.236	0.616	-0.32	1.801
ITCr	l	-0.389	5.817	-0.376	4.577
	r	-0.35	2.873	-0.396	6.712
MTCc	l	-0.07	0.204	-0.048	0.193
	r	0.019	0.185	-0.046	0.192
STCc	l	-0.057	0.197	-0.133	0.267
	r	0.131	0.264	0.051	0.194
STCr	l	-0.036	0.189	-0.243	0.665
	r	-0.041	0.19	0.041	0.19
MTCr	l	-0.149	0.295	-0.192	0.405
	r	-0.217	0.508	0.043	0.191
IPCv	l	-0.11	0.238	-0.318	1.748
	r	0.211	0.479	-0.108	0.235
IPCd	l	-0.108	0.236	-0.061	0.199
	r	0.272	0.934	0.188	0.392
SPC	l	-0.189	0.395	-0.205	0.454
	r	0.085	0.214	0.119	0.248
SPCm	l	-0.117	0.246	-0.197	0.422
	r	0.245	0.678	0.14	0.279
PCm	l	-0.284	1.084	-0.286	1.113
	r	0.007	0.184	-0.008	0.184
Sv	l	-0.114	0.243	-0.263	0.832
	r	-0.013	0.184	-0.146	0.289
Sdl	l	0.312	1.601	0.194	0.413
	r	0.19	0.398	0.319	1.769
Sdm	l	-0.042	0.191	0.059	0.198
	r	0.094	0.221	-0.02	0.185
ICC	l	-0.279	1.01	-0.361	3.48
	r	0.064	0.2	0.075	0.207
PCC	l	-0.272	0.928	-0.249	0.707
	r	-0.054	0.195	-0.104	0.231
MCC	l	-0.192	0.407	-0.075	0.207
	r	0.022	0.186	-0.108	0.236
ACC	l	-0.245	0.681	-0.228	0.566
	r	0.122	0.252	0.044	0.192
Mv	l	-0.143	0.285	-0.158	0.314
	r	0.023	0.186	0.083	0.213
Mdl	l	-0.316	1.681	-0.202	0.444
	r	0.057	0.197	0.019	0.185
Mdm	l	-0.253	0.745	-0.27	0.91
	r	0.11	0.237	0.181	0.37
PMrv	l	-0.167	0.334	-0.276	0.973
	r	0.094	0.221	0.281	1.04

		Left		Right	
Node	**Hem**	**Pearson's *r***	**BF_{10}**	**Pearson's *r***	**BF_{10}**
PMdl	l	-0.158	0.313	-0.165	0.329
	r	-0.017	0.185	-0.005	0.184
PMdm	l	-0.277	0.986	-0.36	3.409
	r	-0.045	0.192	-0.026	0.186
PFcdl	l	0.337	2.336	0.163	0.325
	r	0.022	0.186	0.242	0.659
PFcdm	l	-0.35	2.91	-0.165	0.328
	r	-0.207	0.463	-0.105	0.232
PFrvl	l	-0.222	0.535	-0.358	3.294
	r	-0.236	0.613	-0.107	0.235
Pfrdli	l	-0.238	0.632	-0.276	0.971
	r	-0.263	0.835	-0.237	0.621
Pfrdls	l	-0.38	4.945	-0.342	2.55
	r	-0.2	0.434	-0.18	0.367
PFrd	l	-0.194	0.413	-0.178	0.361
	r	-0.047	0.193	0.029	0.187
PFrm	l	-0.305	1.442	-0.314	1.648
	r	-0.222	0.534	-0.196	0.419
OFCvl	l	-0.28	1.023	-0.254	0.749
	r	-0.003	0.184	-0.048	0.193
OFCv	l	-0.148	0.294	-0.063	0.2
	r	-0.23	0.578	-0.31	1.548
OFCvm	l	-0.102	0.229	-0.154	0.306
	r	-0.056	0.196	-0.062	0.2
PFCvm	l	0.302	1.39	0.255	0.759
	r	0.111	0.238	0.268	0.884
Insular	l	-0.362	3.536	-0.306	1.457
	r	-0.103	0.23	-0.168	0.336
Str	l	-0.142	0.283	-0.012	0.184
	r	0.043	0.191	0.024	0.186
STN	l	0.293	1.217	0.358	3.29
	r	0.342	2.528	0.323	1.867
GPi	l	0.155	0.308	0.191	0.403
	r	0.234	0.603	0.331	2.117
GPe	l	-0.072	0.205	-0.061	0.199
	r	0.168	0.335	0.216	0.501
Tha	l	-0.132	0.267	-0.112	0.239
	r	-0.015	0.185	-0.176	0.357
Amg	l	-0.215	0.499	-0.125	0.257
	r	0.023	0.186	0.208	0.467
VTA	l	-	-	0.156	0.309
	r	0.156	0.309	-	-
SN	l	0.242	0.658	0.404	7.901
	r	0.163	0.324	0.132	0.267
RN	l	0.011	0.184	0.196	0.422
	r	0.005	0.184	-0.245	0.676
PAG	l	**-0.465 ****	31.182	-0.328	2.04
	r	**-0.504 ****	89.529	**-0.586 *****	1296.52
PPN	l	-0.1	0.228	-0.012	0.184
	r	-0.14	0.28	-0.2	0.435
Cl	l	-0.379	4.805	**-0.436 ***	15.568
	r	-0.079	0.21	-0.335	2.277

Note. Presence of Bayesian evidence in favour of a correlation between variables is flagged.
* BF_{10} > 10, ** BF_{10} > 30, *** BF_{10} > 100

Appendix B

Supplementary materials to chapter 6

B1. Supplementary analyses: Cluster-based ROI analyses

B1.1. Regions-of-interest

Consistent with Nir-Cohen et al. (2020), the frontoparietal network (FPN) masks were defined based on cortical maps of Brodman areas (BA), yet they were investigated individually in this study. Cortical region parcellations were obtained from the Brodmann area segmentations by Pijnenburg et al. (2021). Accordingly, the BA 8, BA 9, and BA 46 masks represent the dorsolateral PFC, the BA 24 and BA 32 masks represent the medial PFC, and the BA 7 and BA 40 masks represent the posterior parietal cortex (PPC). Moreover, we included individual subcortical masks derived from the MASSP automated parcellation algorithm (Bazin et al., 2020) to increase delineation accuracy on a participant level, specifically the thalamus, external and internal segments of the pallidum (GPe and GPi, respectively), subthalamic nucleus (STN), substantia nigra (SN), and ventral tegmental area (VTA). To ensure that the cluster-based ROI analyses were comparable to Nir-Cohen et al. (2020), the striatum parcellation was not taken from the MASSP atlas, instead we picked the striatal masks of the caudate nucleus (Ca) and putamen (Pu) from the probabilistic atlas of Pauli, Nili, and Tyszka (2018). For a second cluster-based ROI analysis, selected midbrain (VTAnc, PBP, SNc) masks from the atlas by Pauli et al. (2018) were selected.

B1.2. fMRI statistical analysis

To assess the replicability of Nir-Cohen et al.'s (2020) findings with our data, this study extended their fMRI data analysis procedure. In addition to a whole-brain analysis, a cluster-based ROI analysis was carried out to explore the presence of significant clusters within each ROI, akin to Nir-Cohen et al. (2020). Here, the z-maps produced from the whole-brain GLM were utilized to retrieve the z-values for

every voxel inside each ROI on a group level. In an initial step, for every probabilistic map outlining the ROIs, a thresholding was applied to select only those voxels with probability greater than 30 percent of belonging to the respective region. In a second step, the thresholded masks were binarized. Subsequently, for all ROIs, a voxel-based false discovery rate (FDR) threshold of $p < 0.05$ (Yekutieli & Benjamini, 1999) was applied within each ROI in order to investigate the involvement of the FPN and subcortical regions in working memory updating processes. In short, the cluster-based ROI analysis examined each ROI for clusters of activation based on the whole-brain GLMs after correcting for multiple comparisons across the ROI's voxels.

B2. Supplementary results: Cluster-based ROI analyses

Our cluster-based ROI analyses indicated that specific Brodmann areas associated with the FPN, and subcortical ROIs differently contribute to each experimental contrast. The key findings are outlined below for each experimental contrast, but for a detailed breakdown of the contribution of each ROI area, please refer to Figure B.1, Table B.1 – B.2.

Gate opening

The dlPFC was broadly engaged during gate opening trials as suggested by cluster-based ROI analyses, along with only the involvement of the left mPFC. In the subcortex, a cluster of activity was found in the left thalamus (Table B.1). The opposing results to ROI-wise GLM analysis (Table 6.3) could be explained by the different cluster-based ROI analysis approaches and suggest that the left thalamus showed higher peaks in activation while other thalamic subnuclei perhaps show a negative change in signal, thus cancelling out the positive signal change picked up by the cluster-based ROI analyses.

Gate closing

Cluster-based ROI analyses indicated small, lateralized engagement of the dlPFC limited to the left Brodmann area 46, and broad activation of the PPC. Intriguingly, the cluster-based ROI analyses did not indicate activity in any subcortical ROI (Table B.1).

Substitution

The entire FPN is associated with the process of substitution as suggested by cluster-based ROI analyses (Table B.1). The dlPFC is bilaterally activated during substitution trials, and also the mPFC is associated with substitution, but only one

cluster, the right Brodmann area 32. Cluster-based ROI analyses also indicate activity in PPC regions, including a particularly large cluster in the left Brodmann area 7. The results from cluster-based ROI analysis confirmed the involvement of subcortical nuclei in the substitution process, yet with varying contributions. Bilateral activity in the thalamus, caudate, and putamen was observed, along with bilateral activity in fact the SN and VTA. Specifically, large clusters were found in the left thalamus and right caudate, and bilateral clusters in the SNc mask by Pauli et al. (2018) were revealed (Table B.2)

Updating mode

Cluster-based ROI analyses suggest involvement of the entire FPN during updating mode. Precisely, there is evidence for bilateral dlPFC and PPC activity in updating mode trials (Table B.1), there was also a small cluster in Brodmann area 32 of the left mPFC. Furthermore, results indicated basal ganglia activation, in particular relatively large clusters of activation in the bilateral caudate and putamen was found, along with a small cluster in left GPe in updating mode contrast.

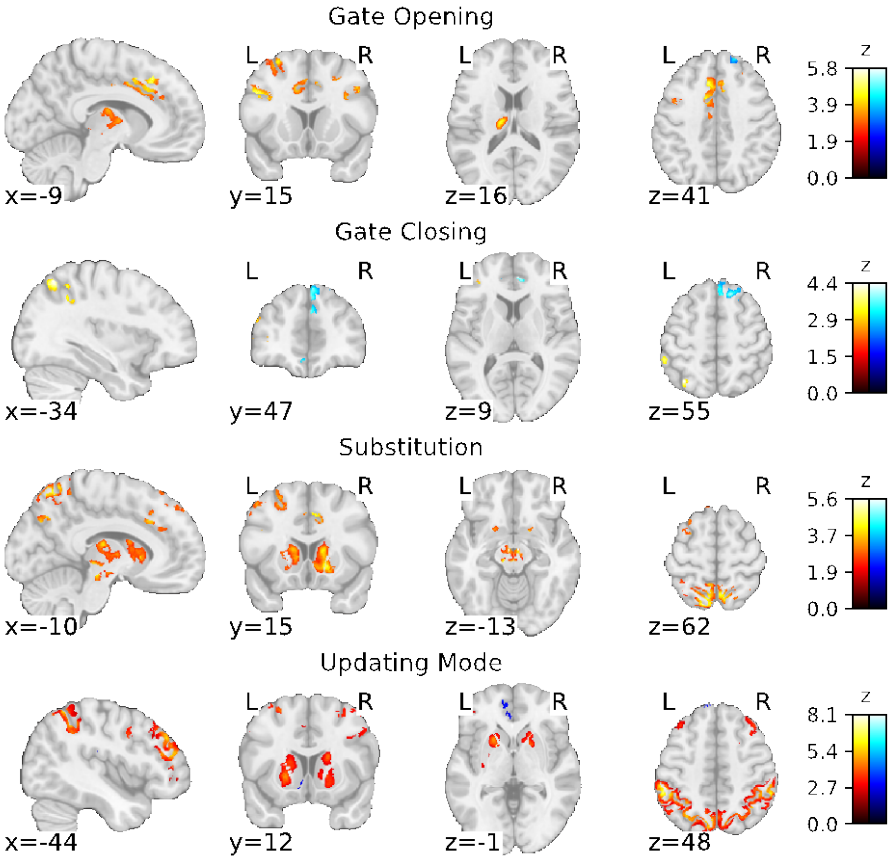

Figure B.1. Results of the voxel-wise cluster-based ROI analysis using ROI-wide FDR correction ($q<0.05$) are illustrated. Each row shows the BOLD signal change within the ROIs for one of the four working memory process contrasts, respectively.

Table B.1. List of peak activation in MNI coordinates from the cluster-based ROI analysis.

					MNI			
		ROI	**hem**	**voxels**	**x**	**y**	**z**	***Z***
Gate opening								
	dlPFC	BA8	l	401	-7.0	26.0	46.0	5.733
		BA8	r	205	9.0	25.0	45.0	4.667
		BA9	l	239	-46.0	15.0	32.0	5.122
		BA9	r	179	34.0	9.0	29.0	5.129
		BA46	l	94	-51.0	22.0	27.0	4.746
	mPFC	BA24	l	123	-9.0	4.0	40.0	4.154
		BA32	l	219	-9.0	11.0	45.0	4.667
	Subcortex	Tha	l	401	-14.0	-17.0	16.0	4.613
Gate Closing								
	dlPFC	BA46	l	57	-50.0	42.0	9.0	4.091
	PPC	BA7	l	306	-34.0	-63.0	55.0	4.392
		BA40	l	89	-45.0	-47.0	39.0	4.111
Substitution								
	dlPFC	BA8	l	258	-7.0	25.0	35.0	4.704
		BA8	r	7	4.0	15.0	42.0	4.473
		BA9	l	159	-22.0	56.0	33.0	4.763
	mPFC	BA32	r	119	9.0	13.0	40.0	4.533
	PPC	BA7	l	1839	-14.0	-70.0	62.0	5.256
		BA7	r	293	5.0	-61.0	63.0	4.675
		BA40	l	335	-63.0	-52.0	30.0	4.822
	Subcortex	Tha	l	1151	-25.0	-26.0	-8.0	5.129
		Tha	r	448	6.0	-23.0	2.0	4.963
		Ca	l	701	-14.0	11.0	10.0	4.875
		Ca	r	1021	15.0	16.0	-5.0	4.710
		Pu	l	402	-20.0	5.0	0.0	5.530
		Pu	r	296	16.0	15.0	-5.0	4.791
		GPe	l	204	-20.0	5.0	0.0	5.530
		SN	l	46	-11.0	-24.0	-13.0	4.236
		SN	r	19	11.0	-16.0	-10.0	3.962
		VTA	l	129	-2.0	-22.0	-19.0	4.911
		VTA	r	145	2.0	-22.0	-19.0	4.349
Updating mode								
	dlPFC	BA8	l	143	-26.0	5.0	60.0	5.423
		BA8	r	30	24.0	19.0	65.0	4.008
		BA9	l	832	-44.0	38.0	33.0	5.816
		BA9	r	491	32.0	38.0	26.0	4.509
		BA46	l	686	-45.0	42.0	17.0	5.695
		BA46	r	525	46.0	37.0	14.0	4.238
	mPFC	BA32	l	20	-4.0	10.0	45.0	3.367
	PPC	BA7	l	2520	-7.0	-77.0	52.0	6.111
		BA7	r	248	38.0	-40.0	42.0	5.465
		BA40	l	2140	-56.0	-41.0	55.0	8.084
		BA40	r	1870	49.0	-41.0	56.0	6.155
	Subcortex	Ca	l	474	-15.0	9.0	10.0	4.369
		Ca	r	559	17.0	13.0	16.0	4.384
		Pu	l	445	-21.0	15.0	-2.0	4.983
		Pu	r	326	18.0	9.0	-8.0	4.268
		GPe	l	13	-17.0	9.0	-1.0	3.864

Table B.2. List of peak activation in MNI Coordinates from the cluster-based ROI analysis using the dopaminergic nuclei' masks from Pauli et al. (2018), after FDR correction (q <0.05). The data suggests no activation in the VTA nucleus and parabrachial pigmented (PBP) nucleus, after FDR correction was applied.

				MNI			
	ROI	**hem**	**voxels**	**x**	**y**	**z**	***Z***
Substitution							
	SNc	l	16	-10.0	-25.0	-13.0	4.489
		r	56	10.0	-17.0	-10.0	4.178

Table B.3. Significance testing of mean RT effects using a general linear mixed model with a Gaussian link function.

Effect	**df**	***F***	***p***
Trial type	1, 36.20	73.520	< .001
Switch type	1, 44.45	32.521	< .001
Response type	1, 33.82	263.189	< .001
Trial type x Switch type	1, 56.82	19.802	< .001
Trial type x Response type	1, 33.59	29.062	< .001
Switch type x Response type	1, 166.02	6.005	0.015
Trial type x Switch type x Response type	1, 33.17	3.836	0.059

Note. Type III Sum of Squares
Trial type = reference/comparison, match = same/different, switch = repeat/switch

Table B.4. Significance testing of accuracy effects using a generalized linear mixed model with a probit link function.

Effect	**df**	***F***	***p***
Trial type	1	0.167	0.683
Switch type	1	5.666	0.017
Response type	1	0.306	0.580
Trial type x Switch type	1	9.996	0.002
Trial type x Response type	1	42.588	< .001
Switch type x Response type	1	0.086	0.770
Trial type x Switch type x Response type	1	0.007	0.934

Note. Type III Sum of Squares Trial type = reference/comparison, match = same/different, switch = repeat/switch

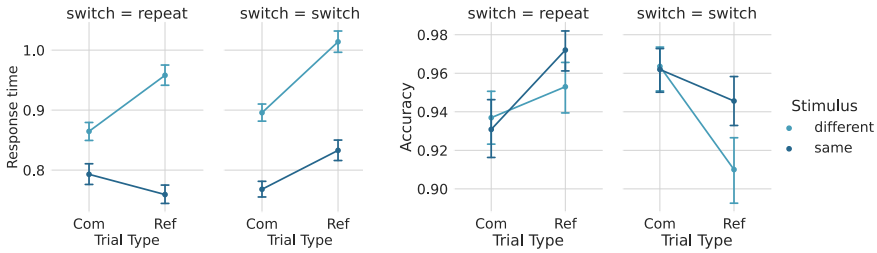

Figure B.2. The graph outlines the non-significant three-way interactions of the factors Trial-type (comparison, reference), Gate-Switch (repeat, switch), and Stimulus/Match (same, different) for both reaction time (RT; top) and accuracy (bottom), respectively. The results indicate that the difference in RT between same and different trials is more pronounced in reference trials compared to comparison trials, suggesting that additional time is required for substitution of the WM item in the reference condition. However, in contrast to previous studies, a larger gate switching cost, representing the difference between switch and repeat conditions, is only found in reference trials (gate opening) and not in comparison trials (gate closing). The error bars in the figures represent bootstrapped 95% confidence intervals.

Appendix C

Supplementary materials to chapter 7

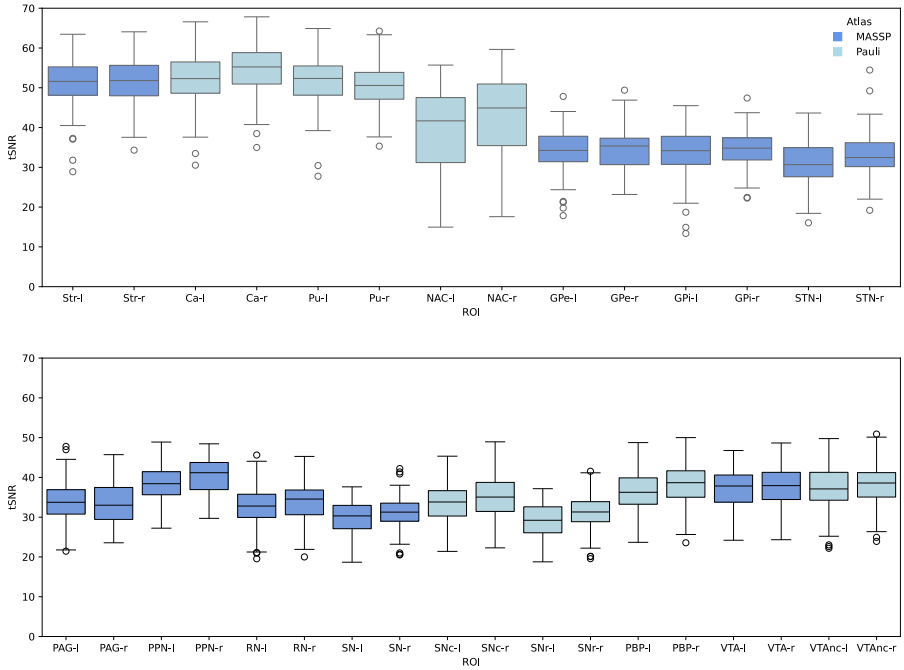

Figure C.1. Temporal signal-to-noise ratios (tSNR) for the masks used in the ROI-wise GLMs. The data plotted are the tSNR estimates across participants and runs of the reversal learning task fMRI session. Regions of the basal ganglia are plotted in the top row and midbrain region in the bottom row. Colour coding illustrates the origin of the masks, with dark blue indicating masks from MASSP (Bazin et al., 2020) and light blue masks derived from the probabilistic atlas of Pauli et al. (2018).

Bibliography

Abraham, A., Pedregosa, F., Eickenberg, M., Gervais, P., Mueller, A., Kossaifi, J., Gramfort, A., Thirion, B. & Varoquaux, G. (2014). Machine learning for neuroimaging with scikit-learn. *Frontiers in Neuroinformatics*, *8*(2), 1–10. https://doi.org/10.3389/fninf.2014.00014

Alkemade, A., Bazin, P. L., Balesar, R., Pine, K., Kirilina, E., Möller, H. E., Trampel, R., Kros, J. M., Keuken, M. C., Bleys, R. L. A. W., Swaab, D. F., Herrler, A., Weiskopf, N., & Forstmann, B. U. (2022). A unified 3D map of microscopic architecture and MRI of the human brain. *Science Advances, 8*(17), eabj7892. https://doi.org/10.1126/sciadv.abj7892

Alkemade, A., Keuken, M. C., & Forstmann, B. U. (2013). A perspective on terra incognita: Uncovering the neuroanatomy of the human subcortex. *Frontiers in Neuroanatomy, 7*, 40. https://doi.org/10.3389/fnana.2013.00040

Alkemade, A., Mulder, M. J., Groot, J. M., Isaacs, B. R., van Berendonk, N., Lute, N., Isherwood, S. J. S., Bazin, P.-L., & Forstmann, B. U. (2020). The Amsterdam Ultra-high field adult lifespan database (AHEAD): A freely available multimodal 7 Tesla submillimeter magnetic resonance imaging database. *NeuroImage, 221*, 117200. https://doi.org/10.1016/j.neuroimage.2020.117200.

Amunts, K., Mohlberg, H., Bludau, S., & Zilles, K. (2020). Julich-Brain: A 3D probabilistic atlas of the human brain's cytoarchitecture. *Science, 369*(6506), 988-992. https://doi.org/10.1126/science.abb4588

Andersson, J.L.R., & Sotiropoulos, S.N. (2016). An integrated approach to correction for off-resonance effects and subject movement in diffusion MR imaging. *Neuroimage,* 125, 1063-1078. 10.1016/j.neuroimage.2015.10.019

Andersson, J.L.R., Skare, S., & Ashburner, J. (2003). How to correct susceptibility distortions in spin-echo echo-planar images: application to diffusion tensor imaging. *Neuroimage*, 20, 870-888. 10.1016/S1053-8119(03)00336-7

Aransay, A., Rodríguez-López, C., García-Amado, M., Clascá, F., & Prensa, L. (2015). Long-range projection neurons of the mouse ventral tegmental area: a single-cell axon tracing analysis. *Frontiers in neuroanatomy*, *9*, 59. https://doi.org/10.3389/fnana.2015.00059

Armbruster, D. J., Ueltzhöffer, K., Basten, U., & Fiebach, C. J. (2012). Prefrontal cortical mechanisms underlying individual differences in cognitive flexibility and stability. *Journal of cognitive neuroscience, 24*(12), 2385-2399. https://doi.org/10.1162/jocn_a_00286

Arnsten, A. F., Wang, M., & Paspalas, C. D. (2015). Dopamine's Actions in Primate Prefrontal Cortex: Challenges for Treating Cognitive Disorders. *Pharmacological reviews*, *67*(3), 681–696. https://doi.org/10.1124/pr.115.010512

Auzias, G., Coulon, O., Brovelli, A. (2016). MarsAtlas: A cortical parcellation atlas for functional mapping. *Human Brain Mapping, 37*(4), 1573-1592. doi:10.1002/hbm.23121

Avants, B. B., Epstein, C. L., Grossman, M., & Gee, J. C. (2008). Symmetric diffeomorphic image registration with cross-correlation: evaluating automated labeling of elderly and neurodegenerative brain. *Medical image analysis*, *12*(1), 26–41. https://doi.org/10.1016/j.media.2007.06.004

Badre, D. (2012). Opening the gate to working memory. *Proceedings of the National Academy of Sciences*, *109*(49), 19878-19879.

Ballard, I. C., Murty, V. P., Carter, R. M., MacInnes, J. J., Huettel, S. A., & Adcock, R. A. (2011). Dorsolateral prefrontal cortex drives mesolimbic dopaminergic regions to initiate motivated behavior. *Journal of Neuroscience*, *31*(28), 10340–10346. http://doi.org/10.1523/JNEUROSCI.0895-11.2011

Bär, K. J., De la Cruz, F., Schumann, A., Koehler, S., Sauer, H., Critchley, H., & Wagner, G. (2016). Functional connectivity and network analysis of midbrain and brainstem nuclei. *NeuroImage*, *134*, 53–63. http://doi.org/10.1016/j.neuroimage.2016.03.071

Barnéoud, P., le Moal, M., & Neveu, P. J. (1990). Asymmetric distribution of brain monoamines in left- and right-handed mice. *Brain Research, 520*(1–2), 317–321. https://doi.org/10.1016/0006-8993(90)91721-R

Barry, R. L., Coaster, M., Rogers, B. P., Newton, A. T., Moore, J., Anderson, A. W., & Gore, J. C. (2013). On the origins of signal variance in fMRI of the human midbrain at high field. *PLoS One, 8*(4), e62708. https://doi.org/10.1371/journal.pone.0062708

Bautista, T., O'Muircheartaigh, J., Hajnal, J.V., & Tournier, J.-D. (2021). Removal of Gibbs ringing artefacts for 3D acquisitions using subvoxel shifts. *Proceedings of the International Society for Magnetic Resonance in Medicine*, *29*, 3535. https://archive.ismrm.org/2021/3535.html

Bayer, H. M., & Glimcher, P. W. (2005). Midbrain dopamine neurons encode a quantitative reward prediction error signal. *Neuron*, *47*(1), 129–141. https://doi.org/10.1016/j.neuron.2005.05.020

Bays, P. M., & Husain, M. (2008). Dynamic shifts of limited working memory resources in human vision. *Science*, *321*(5890), 851-854. https://doi.org/10.1126/science.1158023

Bazin, P.-L., Alkemade, A., Mulder, M. J., Henry, A. G., & Forstmann, B.U. (2020) Multi-contrast anatomical subcortical structures parcellation. *eLife*, 9, e59430. https://doi.org/10.7554/eLife.59430

Bazin, P.L.E.A. Forstmann, B.U. & Alkemade, Anneke (2022). Ahead Brain 152017 - 3D reconstructions. University of Amsterdam / Amsterdam University of Applied Sciences. Dataset. https://doi.org/10.21942/uva.14260064.v2

Bazin, P. L., Plessis, V., Fan, A. P., Villringer, A., & Gauthier, C. J. (2016). Vessel segmentation from quantitative susceptibility maps for local oxygenation venography. *Proceedings - International Symposium on Biomedical Imaging*, 1135–1138. https://doi.org/10.1109/ISBI.2016.7493466

Beckstead, R. M. (1979). An autoradiographic examination of corticocortical and subcortical projections of the mediodorsal-projection (prefrontal) cortex in the rat. *Journal of Comparative Neurology*, *184*(1), 43-62.

Bedwell, J. S., Horner, M. D., Yamanaka, K., Li, X., Myrick, H., Nahas, Z., & George, M. S. (2005). Functional neuroanatomy of subcomponent cognitive processes involved in verbal working memory. *International Journal of Neuroscience, 115*(7), 1017-1032. https://doi.org/10.1080/00207450590901530

Behzadi, Y., Restom, K., Liau, J., & Liu, T. T. (2007). A component-based noise correction method (CompCor) for BOLD and perfusion based fMRI. *NeuroImage, 37*(1), 90–101. https://doi.org/10.1016/j.neuroimage.2007.04.042

Beier, K. T., Steinberg, E. E., DeLoach, K. E., Xie, S., Miyamichi, K., Schwarz, L., Gao, X. J., Kremer, E. J., Malenka, R. C., & Luo, L. (2015). Circuit Architecture of VTA Dopamine Neurons Revealed by Systematic Input-Output Mapping. *Cell, 162*(3), 622-634. https://doi.org/10.1016/j.cell.2015.07.015.

Berger, B., Gaspar, P., & Verney, C. (1991). Dopaminergic innervation of the cerebral cortex: unexpected differences between rodents and primates. *Trends in neurosciences*, *14*(1), 21–27. https://doi.org/10.1016/0166-2236(91)90179-x

Berridge, K. C., & Kringelbach, M. L. (2013). Neuroscience of affect: Brain mechanisms of pleasure and displeasure. *Current Opinion in Neurobiology*, *23*(3), 294–303. http://doi.org/10.1016/j.conb.2013.01.017

Bevan, M. D. (2021). Motor control: Basal ganglia feedback circuit for action suppression. *Current Biology, 31*(4), R191-R193. https://doi.org/10.1016/j.cub.2020.11.067

Birn, R. M., Smith, M. A., Jones, T. B., & Bandettini, P. A. (2008). The respiration response function: The temporal dynamics of fMRI signal fluctuations related to changes in respiration. *NeuroImage, 40*(2), 644–654. https://doi.org/10.1016/j.neuroimage.2007.11.059

Björklund, A., & Dunnett, S. B. (2007). Dopamine neuron systems in the brain: an update. *Trends in neurosciences*, *30*(5), 194–202. https://doi.org/10.1016/j.tins.2007.03.006

Blaess, S., & Ang, S. (2015). Genetic control of midbrain dopaminergic neuron development., WIREs Dev Biol, 4: 113-134. doi:10.1002/wdev.169

Bledowski, C., Kaiser, J., & Rahm, B. (2010). Basic operations in working memory: contributions from functional imaging studies. *Behavioural brain research*, *214*(2), 172-179.

Boag, R. J., Stevenson, N., van Dooren, R., Trutti, A. C., Sjoerds, Z., & Forstmann, B. U. (2021). Cognitive control of working memory: A model-based approach. *Brain Sciences*, *11*(6), 721. https://doi.org/10.3390/brainsci11060721

Boag, R. J., Strickland, L., Heathcote, A., Neal, A., Palada, H., & Loft, S. (2023). Evidence accumulation modelling in the wild: understanding safety-critical decisions. *Trends in cognitive sciences*, *27*(2), 175–188. https://doi.org/10.1016/j.tics.2022.11.009

Bocanegra, B. R., & Hommel, B. (2014). When cognitive control is not adaptive. *Psychological Science, 25*(6), 1249–1255. https://doi.org/10.1177/0956797614528522

Bogacz, R. (2020). Dopamine role in learning and action inference. *eLife, 9*, e53262. https://doi.org/10.7554/eLife.53262

Bouarab, C., Polter, A. M., & Thompson, B. (2019). VTA GABA Neurons at the Interface of Stress and Reward. *Frontiers in neural circuits*, *13*, 78.

Braver, T. S. (2012). The variable nature of cognitive control: a dual mechanisms framework. *Trends in cognitive sciences*, *16*(2), 106-113. https://doi.org/10.1016/j.tics.2011.12.010

Braver, T. S., & Cohen, J. D. (2000). *On the control of control: The role of dopamine in regulating prefrontal function and working memory.* In S. Monsell & J. Drive (Eds.), Control of Cognitive Processes: Attention and Performance Xviii (pp. 712–737). https://doi.org/10.7551/mitpress/1481.001.0001

Brischoux, F., Chakraborty, S., Brierley, D. I., & Ungless, M. A. (2009). Phasic excitation of dopamine neurons in ventral VTA by noxious stimuli. *Proceedings of the National Academy of Sciences of the United States of America*, *106*(12), 4894–4899. https://doi.org/10.1073/pnas.0811507106

Brown, R. M., Crane, A. M., & Goldman, P. S. (1979). Regional distribution of monoamines in the cerebral cortex and subcortical structures of the rhesus monkey: concentrations and in vivo synthesis rates. *Brain research*, *168*(1), 133–150. https://doi.org/10.1016/0006-8993(79)90132-x

Brown, S. D., & Heathcote, A. (2008). The simplest complete model of choice response time: Linear ballistic accumulation. *Cognitive Psychology, 57*(3), 153-178. https://doi.org/10.1016/j.cogpsych.2007.12.002

Brozoski, T., Brown, R., Rosvold, H., & Goldman, P. (1979). Cognitive deficit caused by regional depletion of dopamine in prefrontal cortex of rhesus monkey. *Science, 205*(4409), 929–932. https://doi.org/10.1126/science.112679

Büchel, C., Peters, J., Banaschewski, T., Bokde, A. L. W., Bromberg, U., Conrod, P. J., … Ziesch, V. (2017). Blunted ventral striatal responses to anticipated rewards foreshadow problematic drug use in novelty-seeking adolescents. *Nature Communications*. http://doi.org/10.1038/ncomms14140

Bunney, B. S., & Aghajanian, G. K. (1976). The precise localization of nigral afferents in the rat as determined by a retrograde tracing technique. *Brain Research, 117*(3), 423-435. https://doi.org/10.1016/0006-8993(76)90751-4.

Caan, M., Bazin, P.-L., Fracasso, A., Marques, J., Dumoulin, S., & van der Zwaag, W. (2018). MP2RAGEME: T1, T2 and QSM mapping in one sequence at 7 Tesla. *Human Brain Mapping, 40*(6), 1786–1798. https://doi.org/10.1002/hbm.24490

Cabezas, M., Oliver, A., Lladó, X., Freixenet, J., & Bach Cuadra, M. (2011). A review of atlas-based segmentation for magnetic resonance brain images. *Computer Methods and Programs in Biomedicine*, *104*(3), e158–e177. http://doi.org/10.1016/j.cmpb.2011.07.015

Cabib, S., D'Amato, F. R., Neveu, P. J., Deleplanque, B., Le Moal, M., & Puglish-Allegra, S. (1995). Paw preference and brain dopamine asymmetries. *Neuroscience, 64*(2), 427–432. https://doi.org/10.1016/0306-4522(94)00401-P

Cai, J., & Tong, Q. (2022). Anatomy and Function of Ventral Tegmental Area Glutamate Neurons. *Frontiers in neural circuits*, *16*, 867053. https://doi.org/10.3389/fncir.2022.867053

Calamante, F. (2019). The Seven Deadly Sins of Measuring Brain Structural Connectivity Using Diffusion MRI Streamlines Fibre-Tracking. *Diagnostics, 9*, 115. https://doi.org/10.3390/diagnostics9030115

Cavalcanti, J. R. L. P., Pontes, A. L. B., Fiuza, F. P., Silva, K. D. A., Guzen, F. P., Lucena, E. E. S., … Cavalcante, J. S. (2016). Nuclear organization of the substantia nigra, ventral tegmental area and retrorubral field of the common marmoset (Callithrix jacchus): A cytoarchitectonic and TH-immunohistochemistry study. *Journal of Chemical Neuroanatomy*, *77*, 100–109. http://doi.org/10.1016/j.jchemneu.2016.05.010

Cavanagh, J. F. (2015). Cortical delta activity reflects reward prediction error and related behavioral adjustments, but at different times. *NeuroImage*, *110*, 205-216. https://doi.org/10.1016/j.neuroimage.2015.02.007

Cavanagh, J. F., & Frank, M. J. (2014). Frontal theta as a mechanism for cognitive control. *Trends in cognitive sciences*, *18*(8), 414-421. https://doi.org/10.1016/j.tics.2014.04.012

Chakravarty, M. M., Bertrand, G., Hodge, C. P., Sadikot, A. F., & Collins, D. L. (2006). The creation of a brain atlas for image guided neurosurgery using serial histological data. *NeuroImage, 30*(2), 359–376. https://doi.org/10.1016/j.neuroimage.2005.09.041

Caldwell, J. (2009). Action Potential Initiation and Conduction in Axons. In *Encyclopedia of Neuroscience* (pp. 23–29). https://doi.org/10.1016/B978-008045046-9.01642-9

Chang, C., Crottaz-Herbette, S., & Menon, V. (2007). Temporal dynamics of basal ganglia response and connectivity during verbal working memory. *NeuroImage, 34*(3), 1253-1269. https://doi.org/10.1016/j.neuroimage.2006.08.056

Chang, C., Cunningham, J. P., & Glover, G. H. (2009). Influence of heart rate on the BOLD signal: The cardiac response function. *NeuroImage 44*(3), 857–869. https://doi.org/10.1016/j.neuroimage.2008.09.029

Chatham, C. H., & Badre, D. (2015). Multiple gates on working memory. *Current Opinion in Behavioral Sciences, 1*, 23-31. https://doi.org/10.1016/j.cobeha.2014.08.001

Chen, J. C., Hardy, P. A., Clauberg, M., Joshi, J. G., Parravano, J., Deck, J. H., Henkelman, R. M., Becker, L. E., & Kucharczyk, W. (1989). T2 values in the human brain: comparison with quantitative assays of iron and ferritin. *Radiology, 173*(2), 521–526. https://doi.org/10.1148/radiology.173.2.2798884

Chen, X., Hackett, P. D., DeMarco, A. C., Feng, C., Stair, S., Haroon, E., Ditzen, B., Pagnoni, G., & Rilling, J. K. (2016). Effects of oxytocin and vasopressin on the neural response to unreciprocated cooperation within brain regions involved in stress and anxiety in men and women. *Brain Imaging and Behavior*, *10*(2), 581–593. http://doi.org/10.1007/s11682-015-9411-7

Chen, X., Qu, L., Xie, Y., Ahmad, S., & Yap, P.-T. (2023). A paired dataset of T1- and T2-weighted MRI at 3 Tesla and 7 Tesla. Scientific Data, 10, 489. https://doi.org/10.1038/s41597-023-02400-y

Cohen, J. D., Braver, T. S., & Brown, J. W. (2002). Computational perspectives on dopamine function in prefrontal cortex. *Current Opinion in Neurobiology*, *12*(2), 223–229. https://doi.org/10.1016/s0959-4388(02)00314-8

Cohen, J. Y., Haesler, S., Vong, L., Lowell, B. B., & Uchida, N. (2012). Neuron-type-specific signals for reward and punishment in the ventral tegmental area. *Nature*, *482*(7383), 85–88. https://doi.org/10.1038/nature10754

Cohen, M. X. (2014). A neural microcircuit for cognitive conflict detection and signaling. *Trends in neurosciences*, *37*(9), 480-490. https://doi.org/10.1016/j.tins.2014.06.004

Cohen, M. X., & Donner, T. H. (2013). Midfrontal conflict-related theta-band power reflects neural oscillations that predict behavior. *Journal of Neurophysiology*, *110*(12), 2752-2763. https://doi.org/10.1152/jn.00479.2013

Collins, A. G., & Frank, M. J. (2012). How much of reinforcement learning is working memory, not reinforcement learning? A behavioral, computational, and neurogenetic analysis. *European Journal of Neuroscience*, *35*(7), 1024-1035.

Collins, D. L., Neelin, P., Peters, T. M., & Evans, A. C. (1995). Automatic 3-D model-based neuroanatomical segmentation. *Human Brain Mapping, 3*(3), 190-208. https://doi.org/10.1002/hbm.460030304

Colzato, L. S., Pratt, J., & Hommel, B. (2010). Dopaminergic control of attentional flexibility: Inhibition of return is associated with the dopamine transporter gene (DAT1). *Frontiers in Human Neuroscience*, *4*, 1–6. http://doi.org/10.3389/fnhum.2010.00053

Colzato, L. S., Slagter, H. a., de Rover, M., & Hommel, B. (2011). Dopamine and the management of attentional resources: Genetic markers of striatal D2 dopamine predict individual differences in the Attentional Blink. *Journal of Cognitive Neuroscience*, *23*(11), 3576–3585. http://doi.org/10.1162/jocn_a_00049

Colzato, L. S., van den Wildenberg, W. P. M., & Hommel, B. (2013). The genetic impact (C957T-DRD2) on inhibitory control is magnified by aging. *Neuropsychologia*, *51*(7), 1377–1381. https://doi.org/10.1016/j.neuropsychologia.2013.01.014

Colzato, L. S., van der Wel, P., Sellaro, R., & Hommel, B. (2016). A single bout of meditation biases cognitive control but not attentional focusing: Evidence from the global-local task. *Consciousness and Cognition*, *39*, 1–7. http://doi.org/10.1016/j.concog.2015.11.003

Cools, R. (2006). Dopaminergic modulation of cognitive function-implications for l-DOPA treatment in Parkinson's disease. *Neuroscience & Biobehavioral Reviews, 30*(1), 1-23. https://doi.org/10.1016/j.neubiorev.2005.03.024

Cools, R. (2008). Role of dopamine in the motivational and cognitive control of behavior. *The Neuroscientist, 14*(4), 381–395. https://doi.org/10.1177/1073858408317009

Cools, R. (2019). Chemistry of the Adaptive Mind: Lessons from Dopamine. *Neuron*, *104*(1), 113-131.

Cools, R., & D'Esposito, M. (2011). Inverted-U-shaped dopamine actions on human working memory and cognitive control. *Biological Psychiatry, 69*(12), https://doi.org/10.1016/j.biopsych.2011.03.028e113-e125.

Cools, R., Clark, L., & Robbins, T. W. (2004). Differential responses in human striatum and prefrontal cortex to changes in object and rule relevance. *The Journal of neuroscience: the official journal of the Society for Neuroscience*, *24*(5), 1129–1135. https://doi.org/10.1523/JNEUROSCI.4312-03.2004

Cools, R., Sheridan, M., Jacobs, E., & D'Esposito, M. (2007). Impulsive personality predicts dopamine-dependent changes in frontostriatal activity during component processes of working memory. *Journal of Neuroscience*, *27*(20), 5506-5514.

Cooper, J. C., Dunne, S., Furey, T., & O'Doherty, J. P. (2012). Human dorsal striatum encodes prediction errors during observational learning of instrumental actions. *Journal of Cognitive Neuroscience, 24*(1), 106–118. https://doi.org/10.1162/jocn_a_00114

Cordero-Grande, L., Christiaens, D., Hutter, J., Price, A.N., & Hajnal, J.V. (2019). Complex diffusion-weighted image estimation via matrix recovery under general noise models. *NeuroImage*, 391-404. 10.1016/j.neuroimage.2019.06.039

Corlett, P. R., Mollick, J. A., & Kober, H. (2022). Meta-analysis of human prediction error for incentives, perception, cognition, and action. *Neuropsychopharmacology, 47*(7)*,* 1339–1349. https://doi.org/10.1038/s41386-021-01264-3

Cowan, N. (1988). Evolving conceptions of memory storage, selective attention, and their mutual constraints within the human information-processing system. *Psychological bulletin*, *104*(2), 163. https://doi.org/10.1037/0033-2909.104.2.163

Cowan, N. (2001). The magical number 4 in short-term memory: A reconsideration of mental storage capacity. *Behavioral and brain sciences*, *24*(1), 87-114. https://doi.org/10.1017/S0140525X01003922

Cox, R. W., & Hyde, J. S. (1997). Software tools for analysis and visualization of fMRI data. *NMR in Biomedicine, 10* (4-5), 171–78. https://doi.org/10.1002/(SICI)1099-1492(199706/08)10:4/5<171::AID-NBM453>3.0.CO;2-L

D'Esposito, M., & Postle, B. R. (2015). The cognitive neuroscience of working memory. *Annual review of psychology*, *66*, 115-142.

D'Esposito, M., Postle, B. R., Ballard, D., & Lease, J. (1999). Maintenance versus manipulation of information held in working memory: an event-related fMRI study. *Brain and cognition*, *41*(1), 66-86.

D'Ardenne, K., McClure, S. M., Nystrom, L. E., & Cohen, J. D. (2008). BOLD reflecting dopaminergic signals in the human ventral tegmental area. *Scientific Reports, 319*, 1264 - 1267. http://doi.org/10.1126/science.1229223

da Silva, J., Tecuapetla, F., Paixão, V., & Costa, R.M. (2018). Dopamine neuron activity before action initiation gates and invigorates future movements. *Nature*, 554, 244–248. https://doi.org/10.1038/nature25457

Dahlin, E., Neely, A. S., Larsson, A., Bäckman, L., & Nyberg, L. (2008). Transfer of learning after updating training mediated by the striatum. *Science*, *320*(5882), 1510-1512. https://doi.org/10.1126/science.1155466

Dahlström, A., & Fuxe, K. (1964). Evidence for the existence of monoamine-containing neurons in the central nervous system. 1. Demonstration of monoamines in the cell bodies of brain stem neurons. *Acta Physiologica Scandinavica,* 62, Suppl. 282, 1-55.

Damier, P., Hirsch, E. C., Agid, Y., & Graybiel, A. M. (1999). The substantia nigra of the human brain: II. Patterns of loss of dopamine-containing neurons in Parkinson's disease. *Brain, 122*(8), 1437–1448. https://doi.org/10.1093/brain/122.8.1437

Daneman, M., & Carpenter, P. A. (1980). Individual differences in working memory and reading. *Journal of Memory and Language*, *19*(4), 450. https://doi.org/10.1016/S0022-5371(80)90312-6

de Hollander, G., Forstmann, B. U., & Brown, S. D. (2016). Different ways of linking behavioral and neural data via computational cognitive models. *Biological Psychiatry: Cognitive Neuroscience and Neuroimaging*, *1*(2), 101-109. https://doi.org/10.1016/j.bpsc.2015.11.004

de Hollander, G., Keuken, M. C., & Forstmann, B. U. (2015). The subcortical cocktail problem; mixed signals from the subthalamic nucleus and substantia nigra. *PloS One, 10*(3), e0120572. https://doi.org/10.1371/journal.pone.0120572

de Hollander, G., Keuken, M. C., van der Zwaag, W., Forstmann, B. U., & Trampel, R. (2017). Comparing functional MRI protocols for small, iron-rich basal ganglia nuclei such as the subthalamic nucleus at 7 T and 3 T. *Human brain mapping*, *38*(6), 3226–3248. https://doi.org/10.1002/hbm.23586

Desikan, R. S., Ségonne, F., Fischl, B., Quinn, B. T., Dickerson, B. C., Blacker, D., Buckner, R. L., Dale, A. M., Maguire, R. P., Hyman, B. T., Albert, M. S., & Killiany, R. J. (2006). An automated labeling system for subdividing the human cerebral cortex on MRI scans into gyral-based regions of interest. *Neuroimage, 31*(3), 968-980.

Ding, S. L., Royall, J. J., Sunkin, S. M., Ng, L., Facer, B. A. C., Lesnar, P., Guillozet-Bongaarts, A., McMurray, B., Szafer, A., Dolbeare, T. A., Stevens, A., Tirrell, L., Benner, T., Caldejon, S., Dalley, R. A., Dee, N., Lau, C., Nyhus, J., Reding, M., Riley, Z. L., … Lein, E. S. (2016). Comprehensive cellular-resolution atlas of the adult human brain. *Journal of Comparative Neurology*, *524*(16), 3127–3481. http://doi.org/10.1002/cne.24080

Ditterich, J. (2010). A comparison between mechanisms of multi-alternative perceptual decision making: ability to explain human behavior, predictions for neurophysiology, and relationship with decision theory. *Frontiers in neuroscience*, *4*, 184. https://doi.org/10.3389/fnins.2010.00184

Donkin, C., Nosofsky, R. M., Gold, J. M., & Shiffrin, R. M. (2013). Discrete-slots models of visual working-memory response times. *Psychological Review*, *120*(4), 873–902. https://doi.org/10.1037/a0034247

Dreessen de Gervai, P., Sboto-Frankenstein, U. N., Bolster, R. B., Thind, S., Gruwel, M. L. H., Smith, S. D., & Tomanek, B. (2014). Tractography of Meyer's loop asymmetries. *Epilepsy Research, 108*, 872–882. https://doi.org/10.1016/j.eplepsyres.2014.03.006

Dreisbach, G. (2012). Mechanisms of cognitive control: The functional role of task rules. *Current Directions in Psychological Science, 21*(4), 227-231. https://doi.org/10.1177/0963721412449830

Dreisbach, G., & Fröber, K. (2019). On How to Be Flexible (or Not): Modulation of the Stability-Flexibility Balance. *Current Directions in Psychological Science*, *28*(1), 3-9. https://doi.org/10.1177/0963721418800030

Dreisbach, G., Müller, J., Goschke, T., Strobel, A., Schulze, K., Lesch, K. P., & Brocke, B. (2005). Dopamine and cognitive control: the influence of spontaneous eyeblink rate and dopamine gene polymorphisms on perseveration and distractibility. *Behavioral neuroscience*, *119*(2), 483. https://doi.org/10.1037/0735-7044.119.2.483

Duarte, I. C., Onia Afonso, S., Jorge, H., Cayolla, R., Ferreira, C., & Castelo-Branco, M. (2017). Tribal love: the neural correlates of passionate engagement in football fans. *Social Cognitive and Affective Neuroscience*, 1–11. http://doi.org/10.1093/scan/nsx003

Durstewitz, D. & Seamans, J.K. (2008). The dual-state theory of prefrontal cortex dopamine function with relevance to catechol-O-methyltransferase genotypes and schizophrenia. *Biological Psychiatry, 64,* 739-749. https://doi.org/10.1016/j.biopsych.2008.05.015

Düzel, E., Bunzeck, N., Guitart-Masip, M., & Düzel, S. (2010). NOvelty-related Motivation of Anticipation and exploration by Dopamine (NOMAD): Implications for healthy aging. *Neuroscience and Biobehavioral Reviews*, *34*(5), 660–669. http://doi.org/10.1016/j.neubiorev.2009.08.006

Eapen, M., & Gore, J. C. (2009). Identifying the functional architecture of the human ventral tegmental area and the substantia nigra using high resolution magnetic resonance imaging. *Neuroscience Vanderbilt Reviews*, *1*, 32–38.

Eapen, M., Zald, D. H., Gatenby, J. C., Ding, Z., & Gore, J. C. (2011). Using high-resolution MR imaging at 7T to evaluate the anatomy of the midbrain dopaminergic system. *American Journal of Neuroradiology, 32*(4), 688–694. https://doi.org/10.3174/ajnr.A2355

Ecker, U. K., Lewandowsky, S., Oberauer, K., & Chee, A. E. (2010). The components of working memory updating: an experimental decomposition and individual differences. *Journal of Experimental Psychology: Learning, Memory, and Cognition*, *36*(1), 170. https://doi.org/10.1037/a0017891

Ecker, U. K., Oberauer, K., & Lewandowsky, S. (2014). Working memory updating involves item-specific removal. *Journal of Memory and Language*, *74*, 1-15. https://doi.org/10.1016/j.jml.2014.03.006

Edwards, N. J., Tejeda, H. A., Pignatelli, M., Zhang, S., McDevitt, R. A., Wu, J., Bass, C. E., Bettler, B., Morales, M., & Bonci, A. (2017). Circuit specificity in the inhibitory architecture of the VTA regulates cocaine-induced behavior. *Nature Neuroscience, 20*(3), 438–448. https://doi.org/10.1038/nn.4482

Eidels, A., Donkin, C., Brown, S. D., & Heathcote, A. (2010). Converging measures of workload capacity. *Psychonomic bulletin & review*, *17*(6), 763-771. https://doi.org/10.3758/PBR.17.6.763

Engels-Domínguez, N., Koops, E. A., Prokopiou, P. C., Van Egroo, M., Schneider, C., Riphagen, J. M., Singhal, T., & Jacobs, H. I. L. (2023). State-of-the-art imaging of neuromodulatory subcortical systems in aging and Alzheimer's disease: Challenges and opportunities. *Neuroscience & Biobehavioral Reviews, 144*, 104998. https://doi.org/10.1016/j.neubiorev.2022.104998

Enomoto, K., Matsumoto, N., Nakai, S., Satoh, T., Sato, T. K., Ueda, Y., Inokawa, H., Haruno, M., & Kimura, M. (2011). Dopamine neurons learn to encode the long-term value of multiple future rewards. *Proceedings of the National Academy of Sciences of the United States of America*, *108*(37), 15462–15467. https://doi.org/10.1073/pnas.1014457108

Esteban, O., Markiewicz, C. J., Blair, R. W., Moodie, C. A., Isik, A. I., Erramuzpe, A., Kent, J. D., Goncalves, M., DuPre, E., Snyder, M., Oya, H., Ghosh, S. S., Wright, J., Durnez, J., Poldrack, R. A., & Gorgolewski. K. J. (2019). fMRIPrep: a robust preprocessing pipeline for functional MRI. *Nature Methods, 16*(1), 111-116. https://doi.org/10.1038/s41592-018-0235-4

Esteban, O., Markiewicz, C. J., Goncalves, M., Provins, C., Salo, T., Kent, J. D., DuPre, E., Ciric, R., Pinsard, B., Blair, R. W., Poldrack, R. A., & Gorgolewski, K. J. (2018). fMRIPrep. Software. Zenodo. https://doi.org/10.5281/zenodo.852659

Evans, A. C., Collins, D. L., Mills, S. R., Brown, E. D., Kelly, R. L., & Peters, T. M. (1994). 3D statistical neuroanatomical models from 305 MRI volumes. In *Proceedings of the IEEE-Nuclear Science Symposium and Medical Imaging Conference*.

Evans, A. C., Janke, A. L., Collins, D. L., & Baillet, S. (2012). Brain templates and atlases. *NeuroImage*, *62*(2), 911–922. https://doi.org/10.1016/j.neuroimage.2012.01.024

Everitt, B. J., & Robbins, T. W. (2005). Neural systems of reinforcement for drug addiction: from actions to habits to compulsion. *Nature Neuroscience, 8*, 1481–1489. https://doi.org/10.1038/nn1579

Ewert, S., Plettig, P., Li, N., Chakravarty, M. M., Collins, D. L., Herrington, T. M., … Horn, A. (2018). Toward defining deep brain stimulation targets in MNI space: A subcortical atlas based on multimodal MRI, histology and structural connectivity. *NeuroImage, 170*, 271–282. https://doi.org/10.1016/j.neuroimage.2017.05.015

Fallon, J. H., & Moore, R. Y. (1978a). Catecholamine innervation of the basal forebrain. IV. Topography of the dopamine projection to the basal forebrain and neostriatum. *The Journal of comparative neurology*, *180*(3), 545–580. https://doi.org/10.1002/cne.901800310

Fallon, J. H., & Moore, R. Y. (1978b). Catecholamine innervation of the basal forebrain. III. Olfactory bulb, anterior olfactory nuclei, olfactory tubercle and piriform cortex. *Journal of Comparative, 180*(3), 533–544. https://doi.org/10.1002/cne.901800309

Fallon, J. H., Koziell, D. A., & Moore, R. Y. (1978). Catecholamine innervation of the basal forebrain. II. Amygdala, suprarhinal cortex and entorhinal cortex. *Journal of Comparative Neurology, 180*(3), 509–532. https://doi.org/10.1002/cne.901800308

Farquharson, S., Tournier, J.-D., Calamante, F., Fabinyi, G., Schneider-Kolsky, M., Jackson, G. D., & Connelly, A. (2013). White matter fiber tractography: why we need to move beyond DTI. *Journal of Neurosurgery*, 118(6), 1367–1377. https://doi.org/10.3171/2013.2.JNS121294

Faure, A., Haberland, U., Condé, F., & El Massioui, N. (2005). Lesion to the nigrostriatal dopamine system disrupts stimulus-response habit formation. *The Journal of Neuroscience, 25*(11), 2771–2780. https://doi.org/10.1523/JNEUROSCI.3894-04.2005

Federative Committee on Anatomical Terminology. (ed.). (1998). *Terminologia Anatomica*. New York, NY: Thieme Stuttgart.

Feredoes, E., Heinen, K., Weiskopf, N., Ruff, C., & Driver, J. (2011). Causal evidence for frontal involvement in memory target maintenance by posterior brain areas during distracter interference of visual working memory. *Proceedings of the National Academy of Sciences*, *108*(42), 17510-17515. https://doi.org/10.1073/pnas.1106439108

Ferraro, F., Nigri, A., Bruzzone, M. G., Medina Carrion, J. P., Fedeli, D., Demichelis, G., Chiapparini, L., Ciullo, G., Gonzalez, A. A., Cecchini, A. P., Giani, L., Becker, B., & Leone, M. (2024). Involvement of the ipsilateral-to-the-pain anterior–superior hypothalamic subunit in chronic cluster headache. *The Journal of Headache and Pain, 25*(7). https://doi.org/10.1186/s10194-023-01711-0

Ferreira, J. G. P., Del-Fava, F., Hasue, R. H., & Shammah-Lagnado, S. J. (2008). Organization of ventral tegmental area projections to the ventral tegmental area-nigral complex in the rat. *Journal of Neuroscience, 153*(1), 196–213. https://doi.org/10.1016/j.neuroscience.2008.02.003

Folstein, J. R., & van Petten, C. (2008). Influence of cognitive control and mismatch on the N2 component of the ERP: a review. *Psychophysiology*, *45*(1), 152-170. https://doi.org/10.1111/j.1469-8986.2007.00602.x

Fonov, V. S., Evans, A. C., McKinstry, R. C., Almli, C. R., & Collins, D. L. (2009). Unbiased nonlinear average age-appropriate brain templates from birth to adulthood. *NeuroImage, 47* (Supplement 1), S102. https://doi.org/10.1016/S1053-8119(09)70884-5.

Fontanesi, L., Gluth, S., Rieskamp, J., & Forstmann, B. U. (2019). The role of dopaminergic nuclei in predicting and experiencing gains and losses: A 7T human fMRI study. *BioRxiv,* 732560. https://doi.org/10.1101/732560

Forstmann, B. U., & Wagenmakers, E.-J. (2015). *An Introduction to Model-Based Cognitive Neuroscience*. New York: Springer.

Forstmann, B. U., de Hollander, G., Van Maanen, L., Alkemade, A., & Keuken, M. C. (2017). Towards a mechanistic understanding of the human subcortex. *Nature Reviews Neuroscience*, *18*, 57–65. https://doi.org/10.1038/nrn.2016.163

Forstmann, B. U., Dutilh, G., Brown, S., Neumann, J., von Cramon, D. Y., Ridderinkhof, K. R., & Wagenmakers, E. J. (2008). Striatum and pre-SMA facilitate decision-making under time pressure. *Proceedings of the National Academy of Sciences of the United States of America*, *105*(45), 17538–17542. https://doi.org/10.1073/pnas.0805903105

Forstmann, B. U., Keuken, M. C., Jahfari, S., Bazin, P.-L., Neumann, J., Schaefer, A., Anwander, A., & Turner, R. (2012). Cortico-subthalamic white matter tract strength predicts interindividual efficacy in stopping a motor response. *NeuroImage, 60*, 370-375. https://doi.org/10.1016/j.neuroimage.2011.12.044

Forstmann, B. U., Wagenmakers, E. J., Eichele, T., Brown, S., & Serences, J. T. (2011). Reciprocal relations between cognitive neuroscience and formal cognitive models: opposites attract? *Trends in cognitive sciences*, *15*(6), 272-279. https://doi.org/10.1016/j.tics.2011.04.002

Forstmann, B.U., Keuken, M.C., Schafer, A., Bazin, P., Alkemade, A., Turner, R. (2014). Multi-modal ultra-high resolution structural 7-Tesla MRI data repository. *Scientific Data, 1*, 140050. https://doi.org/10.1038/sdata.2014.50

Frank, M. J., & O'Reilly, R. C. (2006). A mechanistic account of striatal dopamine function in human cognition: Psychopharmacological studies with cabergoline and haloperidol. *Behavioral Neuroscience, 120*(3), 497–517. https://doi.org/10.1037/0735-7044.120.3.497

Frank, M. J., Loughry, B., & O'Reilly, R. C. (2001). Interactions between frontal cortex and basal ganglia in working memory: a computational model. *Cognitive, Affective, & Behavioral Neuroscience*, *1*(2), 137–160. https://doi.org/10.3758/cabn.1.2.137

Frankle, W. G., Laruelle, M., & Haber, S. N. (2006). Prefrontal cortical projections to the midbrain in primates: evidence for a sparse connection. *Neuropsychopharmacology, 31*, 1627–1636.

Frässle, S., Aponte, E. A., Bollmann, S., Brodersen, K. H., Do, C. T., Harrison, O. K., Heinzle, J., Iglesias, S., Kasper, L., Lomakina, E. I., Mathys, C., Müller-Schrader, M., Pereira, I., Petzschner, F. H., Raman, S., Schöbi, D., Toussaint, B., Weber, L. A., Yao, Y., … Stephan, K. E. (2021). TAPAS: An open-source software package for translational neuromodeling and computational psychiatry. *Frontiers in Psychiatry, 12,* 857. https://doi.org/10.3389/fpsyt.2021.680811

Friston, K. J. (2009). Modalities, modes, and models in functional neuroimaging. *Science*, *326*(5951), 399-403. https://doi.org/10.1126/science.1174521

Fu, Y. H., Paxinos, G., Watson, C., & Halliday, G. M. (2016). The substantia nigra and ventral tegmental dopaminergic neurons from development to degeneration. *Journal of Chemical Neuroanatomy, 76*, 98–107. https://doi.org/10.1016/j.jchemneu.2016.02.001

Fu, Y. H., Yuan, Y., Halliday, G., Rusznák, Z., Watson, C., & Paxinos, G. (2012). A cytoarchitectonic and chemoarchitectonic analysis of the dopamine cell groups in the substantia nigra, ventral tegmental area, and retrorubral field in the mouse. *Brain Structure and Function*, *217*(2), 591–612. http://doi.org/10.1007/s00429-011-0349-2

Fudge, J. L., & Haber, S. N. (2000). The central nucleus of the amygdala projection to dopamine subpopulations in primates. *Neuroscience, 97*(3), 479-494. https://doi.org/10.1016/S0306-4522(00)00092-0.

Fürst, A. J., & Hitch, G. J. (2000). Separate roles for executive and phonological components of working memory in mental arithmetic. *Memory & cognition*, *28*(5), 774-782.

Garavan, H. (1998). Serial attention within working memory. *Memory & cognition*, *26*(2), 263-276. https://doi.org/10.3758/BF03201138

Garrison, J., Erdeniz, B., & Done, J. (2013). Prediction error in reinforcement learning: A meta-analysis of neuroimaging studies. *Neuroscience & Biobehavioral Reviews*, *37*(7), 1297-1310. https://doi.org/10.1016/j.neubiorev.2013.03.023

German, D. C., & Manaye, K. F. (1993). Midbrain dopaminergic neurons (nuclei A8, A9, and A10): Three-dimensional reconstruction in the rat. *Journal of Comparative Neurology*, *331*(3), 297–309. http://doi.org/10.1002/cne.903310302

German, D. C., Schlusselberg, D. S., & Woodward, D. J. (1983). Three-dimensional computer reconstruction of midbrain dopaminergic neuronal populations: from mouse to man. *Journal of Neural Transmission*, *57*(4), 243–254. http://doi.org/10.1007/BF01248996

Gershman, S. (2013). Computation with Dopaminergic Modulation. In Jaeger D., Jung R. (Eds.)*, Encyclopedia of Computational Neuroscience. New York: Springer.* https://doi.org/10.1007/978-1-4614-7320-6_631-3

Gillies, G. E., & McArthur, S. (2010a). Independent influences of sex steroids of systemic and central origin in a rat model of Parkinson's disease: A contribution to sex-specific neuroprotection by estrogens. *Hormones and Behavior, 57*, 23-34. https://doi.org/10.1016/j.yhbeh.2009.06.002

Gillies, G. E., & McArthur, S. (2010b). Estrogen actions in the brain and the basis for differential action in men and women: A case for sex-specific medicines. *Pharmacological Reviews, 62*(2), 155-198. https://doi.org/10.1124/pr.109.002071

Gillies, G. E., Murray, H. E., Dexter, D., & McArthur, S. (2004). Sex dimorphisms in the neuroprotective effects of estrogen in an animal model of Parkinson's disease. In *Pharmacology Biochemistry and Behavior, 78,* 513–522. https://doi.org/10.1016/j.pbb.2004.04.022

Gillies, G. E., Virdee, K., McArthur, S., & Dalley, J. W. (2014a). Sex-dependent diversity in ventral tegmental dopaminergic neurons and developmental programing: A molecular, cellular and behavioral analysis. *Journal of Neuroscience, 282,* 69–85. https://doi.org/10.1016/j.neuroscience.2014.05.033

Gillies, G. E., Pienaar, I. S., Vohra, S., & Qamhawi, Z. (2014b). Sex differences in Parkinson's disease. *Frontiers in Neuroendocrinology, 35*(3)*,* 370-384. https://doi.org/10.1016/j.yfrne.2014.02.002

Glajch, K. E., Kelver, D. A., Hegeman, D. J., Cui, Q., Xenias, H. S., Augustine, E. C., Hernandez, V. M., Verma, N., Huang, T. Y., Luo, M., Justice, N. J. & Chan, C. S. (2016). Npas1+ pallidal neurons target striatal projection neurons. *Journal of Neuroscience, 36*(20), 5472–5488. https://doi.org/10.1523/jneurosci.1720-15.2016

Glasser, M. F., Coalson, T. S., Robinson, E. C., et al. (2016). A multi-modal parcellation of human cerebral cortex. *Nature, 536*, 171–178. https://doi.org/10.1038/nature18933

Glover, G. H. (1999). Deconvolution of impulse response in event-related BOLD fMRI1. *NeuroImage, 9*(4), 416–429. https://doi.org/10.1006/nimg.1998.0419

Glover, G. H., Li, T. Q., & Ress, D. (2000). Image-based method for retrospective correction of physiological motion effects in fMRI: RETROICOR. *Magnetic Resonance in Medicine*, *44*(1), 162–167. https://doi.org/10.1002/1522-2594(200007)44:1%3C162::AID-MRM23%3E3.0.CO;2-E

Goense, J. B. M., & Logothetis, N. K. (2008). Neurophysiology of the BOLD fMRI Signal in Awake Monkeys. *Current Biology, 18*(9), 631-640. https://doi.org/10.1016/j.cub.2008.03.054

Goldman-Rakic, P. (1995). Cellular basis of working memory. *Neuron, 14*(3)*,* 477-485. https://doi.org/10.1016/0896-6273(95)90304-6

Good, C. D., Johnsrude, I. S., Ashburner, J., Henson, R. N. A., Friston, K. J., & Frackowiak, R. S. J. (2001). A voxel-based morphometric study of ageing in 465 normal adult human brains. *NeuroImage, 14*(1), 21–36. https://doi.org/10.1006/nimg.2001.0786

Gorgolewski, K. J., Esteban, O., Markiewicz, C. J., Ziegler, E., Ellis, D. G., Jarecka, D., Notter, M. P., Johnson, H., Burns, C., Manhães-Savio, A., Hamalainen, C., Yvernault, B., Salo, T., Goncalves, M., Jordan, K., Waskom, M., Wong, J., Modat, M., Loney, F., … Ghosh, S. (2018). Nipype. Software. Zenodo. https://doi.org/10.5281/zenodo.596855.

Gorgolewski, K., Burns, C. D., Madison, C., Clark, D., Halchenko, Y. O., Waskom, M. L., & Ghosh, S. (2011). Nipype: A flexible, lightweight and extensible neuroimaging data processing framework in Python. *Frontiers in Neuroinformatics, 5*, 13. https://doi.org/10.3389/fninf.2011.00013

Goschke, T., & Bolte, A. (2014). Emotional modulation of control dilemmas: the role of positive affect, reward, and dopamine in cognitive stability and flexibility. *Neuropsychologia*, *62*, 403–423. http://doi.org/10.1016/j.neuropsychologia.2014.07.015

Graham, M.S., Drobnjak, I., Jenkinson, M., & Zhang, H. (2017). Quantitative assessment of the susceptibility artefact and its interaction with motion in diffusion MRI. *PLoS One*, 12, 10.1371/journal.pone.0185647e0185647

Greve, D. N., & Fischl, B. (2009). Accurate and robust brain image alignment using boundary-based registration. *NeuroImage, 48*(1), 63–72. https://doi.org/10.1016/j.neuroimage.2009.06.060.

Gulbinaite, R., van Rijn, H., & Cohen, M. X. (2014). Fronto-parietal network oscillations reveal relationship between working memory capacity and cognitive control. *Frontiers in human neuroscience*, *8*, 761.

Haacke, E. M., Cheng, N. Y., House, M. J., Liu, Q., Neelavalli, J., Ogg, R. J., Khan, A., Ayaz, M., Kirsch, W., & Obenaus, A. (2005). Imaging iron stores in the brain using magnetic resonance imaging. *Magnetic resonance imaging*, *23*(1), 1–25. https://doi.org/10.1016/j.mri.2004.10.001

Haber, S. N. (2003). The primate basal ganglia: parallel and integrative networks. *Journal of Chemical Neuroanatomy, 26*(4), 317-330. https://doi.org/10.1016/j.jchemneu.2003.10.003.

Haber, S. N. (2014). The place of dopamine in the cortico-basal ganglia circuit. *Neuroscience*, *282*, 248–257. https://doi.org/10.1016/j.neuroscience.2014.10.008

Haber, S. N., & Fudge, J. L. (1997). The primate substantia nigra and VTA: Integrative circuitry and function. *Critical Reviews in Neurobiology*, *11*(4), 323–342. https://doi.org/10.1615/critrevneurobiol.v11.i4.40

Haber, S. N., Fudge, J. L., & McFarland, N. R. (2000). Striatonigrostriatal pathways in primates form an ascending spiral from the shell to the dorsolateral striatum. *The Journal of Neuroscience*, *20*(6), 2369–2382. https://doi.org/10.1523/JNEUROSCI.20-06-02369.2000

Haber, S. N., & Knutson, B. (2010). The reward circuit: linking primate anatomy and human imaging. *Neuropsychopharmacology*, *35*(1), 4–26. https://doi.org/10.1038/npp.2009.129

Haber, S.N., Lynd, E., Klein, C., & Groenewegen, H.J. (1990). Topographic Organization of the Ventral Striatal Efferent Projections in the Rhesus Monkey: An Anterograde Tracing Study. *The Journal of comparative neurology, 293*(2), 282–298. https://doi.org/10.1002/cne.902930210

Hadley, J. A., Nenert, R., Kraguljac, N. V., Bolding, M. S., White, D. M., Skidmore, F. M., Visscher, K. M., & Lahti, A. C. (2014). Ventral tegmental area/midbrain functional connectivity and response to antipsychotic medication in schizophrenia. *Neuropsychopharmacology*, *39*(4), 1020–30. http://doi.org/10.1038/npp.2013.305

Hagmann, P., Cammoun, L., Gigandet, X., Meuli, R., Honey, C., Wedeen, V. & Sporns, O. (2008). Mapping the Structural Core of Human Cerebral Cortex. *PLoS Biology, 6*(7), e159. https://doi.org/10.1371/journal.pbio.0060159

Hall, H., Reyes, S., Landeck, N., Bye, C., Leanza, G., Double, K., Thompson, L., Halliday, G., & Kirik, D. (2014). Hippocampal Lewy pathology and cholinergic dysfunction are associated with dementia in Parkinson's disease. *Brain*, *137*(9), 2493–2508. http://doi.org/10.1093/brain/awu193

Halliday, G. M., & Törk, I. (1986). Comparative anatomy of the ventromedial mesencephalic tegmentum in the rat, cat, monkey and human. The Journal of Comparative Neurology, 252(4), 423–445. https://doi.org/10.1002/cne.902520402

Halliday, G., Reyes, S., & Double, K. (2012). Substantia Nigra, Ventral Tegmental Area, and Retrorubral Fields. In J. K. Mai & G. Paxinos (Eds.), *The Human Nervous System* (Third Edition) (pp. 439-455). Academic Press. ISBN 9780123742360. https://doi.org/10.1016/B978-0-12-374236-0.10013-6

Han, L., Savalia, N. K., Chan, M. Y., Agres, P. F., Nair, A. S., & Wig, G. S. (2018). Functional parcellation of the cerebral cortex across the human adult lifespan. *Cerebral Cortex, 28*(12), 4403–4423. https://doi.org/10.1093/cercor/bhy218

Hare, T. A., O'Doherty, J., Camerer, C. F., Schultz, W., & Rangel, A. (2008). Dissociating the role of the orbitofrontal cortex and the striatum in the computation of goal values and prediction errors. *Journal of Neuroscience, 28*(22), 5623-5630. https://doi.org/10.1523/JNEUROSCI.1309-08.2008

Harmony, T. (2013). The functional significance of delta oscillations in cognitive processing. *Frontiers in integrative neuroscience*, *7*, 83.

Harrison, S. J., Bianchi, S., Heinzle, J., Stephan, K. E., Iglesias, S., & Kasper, L. (2021). A Hilbert-based method for processing respiratory timeseries. *NeuroImage, 230*, 117787. https://doi.org/10.1016/j.neuroimage.2021.117787

Harvey, A. K., Pattinson, K. T., Brooks, J. C., Mayhew, S. D., Jenkinson, M., & Wise, R. G. (2008). Brainstem functional magnetic resonance imaging: Disentangling signal from physiological noise. *Journal of Magnetic Resonance Imaging, 28*(6), 1337–1344. https://doi.org/10.1002/jmri.21623

Hasirci, A. S., Maldonado-Devincci, A. M., Beattie, M. C., O'Buckley, T. K., & Morrow, A. L. (2017). Cellular GABAergic Neuroactive Steroid (3alpha,5alpha)-3-Hydroxy-Pregnan-20-One (3alpha,5alpha-THP) immunostaining levels are increased in the ventral tegmental area of human alcohol use disorder patients: A postmortem study. *Alcoholism: Clinical and Experimental Research, 41*(2), 299-311. http://doi.org/10.1111/acer.13300

Hauser, T. U., Eldar, E., & Dolan, R. J. (2017a). Separate mesocortical and mesolimbic pathways encode effort and reward learning signals. *Proceedings of the National Academy of Sciences, 114*(35), E7395-E7404. https://doi.org/10.1073/pnas.1705643114

Hauser, T. U., Iannaccone, R., Dolan, R. J., Ball, J., Hättenschwiler, J., Drechsler, R., Rufer, M., Brandeis, D., Walitza, S., & Brem, S. (2017b). Increased fronto-striatal reward prediction errors moderate decision making in obsessive–compulsive disorder. *Psychological Medicine, 47*, 1246–1258. https://doi.org/10.1017/S0033291716003305

Hawkins, G. E., Mittner, M., Forstmann, B. U., & Heathcote, A. (2017). On the efficiency of neurally-informed cognitive models to identify latent cognitive states. *Journal of Mathematical Psychology*, *76*, 142–155. https://doi.org/10.1016/j.jmp.2016.06.007

Hazy, T. E., Frank, M. J., & O'Reilly, R. C. (2006). Banishing the homunculus: making working memory work. *Neuroscience, 139*(1), 105-118. https://doi.org/10.1016/j.neuroscience.2005.04.067

Hazy, T. E., Frank, M. J., & O'Reilly, R. C. (2007). Towards an executive without a homunculus: computational models of the prefrontal cortex/basal ganglia system. *Philosophical transactions of the Royal Society of London. Series B, Biological sciences*, *362*(1485), 1601–1613. https://doi.org/10.1098/rstb.2007.2055

He, Y., Madeo, G., Liang, Y., Zhang, C., Hempel, B., Liu, X., Mu, L., Liu, S., Bi, G. H., Galaj, E., Zhang, H. Y., Shen, H., McDevitt, R. A., Gardner, E. L., Liu, Q. S., & Xi, Z. X. (2022). A red nucleus–VTA glutamate pathway underlies exercise reward and the therapeutic effect of exercise on cocaine use. *Science Advances, 8*(35), eabo1440. https://doi.org/10.1126/sciadv.abo1440

Heathcote, A., Lin, Y. S., Reynolds, A., Strickland, L., Gretton, M., & Matzke, D. (2019). Dynamic models of choice. *Behavior Research*, 51, 961–985. https://doi.org/10.3758/s13428-018-1067-y

Heathcote, A., & Matzke, D. (2022). Winner Takes All! What Are Race Models, and Why and How Should Psychologists Use Them? *Current Directions in Psychological Science, 31*(5), 383-394. https://doi.org/10.1177/09637214221095852

Hegarty, S. V., Sullivan, A. M., & O'Keeffe, G. W. (2013). Midbrain dopaminergic neurons: A review of the molecular circuitry that regulates their development. *Developmental Biology*, *379*(2), 123–138. https://doi.org/10.1016/j.ydbio.2013.04.014

Hnasko, T. S., Hjelmstad, G. O., Fields, H. L., & Edwards, R. H. (2012). Ventral Tegmental Area Glutamate Neurons: Electrophysiological Properties and Projections. *Journal of Neuroscience, 32*(43), 15076-15085. https://doi.org/10.1523/JNEUROSCI.3128-12.2012

Holly, E. N., & Miczek, K. A. (2016). Ventral tegmental area dopamine revisited: Effects of acute and repeated stress. *Psychopharmacology*, *233*(2), 163–186. http://doi.org/10.1007/s00213-015-4151-3.

Hommel, B. (2015). Chapter Two - Between Persistence and Flexibility: The Yin and Yang of Action Control. In A. J. Elliot (Ed.), *Advances in Motivation Science, Volume 2* (pp. 33-67). Elsevier. ISSN 2215-0919, ISBN 9780128022702. https://doi.org/10.1016/bs.adms.2015.04.003

Hopkins, D. A., & Niessen, L. W. (1976). Substantia nigra projections to the reticular formation, superior colliculus and central gray in the rat, cat and monkey. *Neuroscience Letters*, 2(5), 253-259. ISSN 0304-3940. https://doi.org/10.1016/0304-3940(76)90156-7.

Howe, M. W., & Dombeck, D. A. (2016). Rapid signalling in distinct dopaminergic axons during locomotion and reward. *Nature, 535*(7613), 505–510. https://doi.org/10.1038/nature18942

Huang, X.-F., & Paxinos, G. (1995). *Atlas of the Human Brainstem* (1st ed.). Elsevier Science. ISBN: 0125476159

Hui, M., & Beier, K. T. (2022). Defining the interconnectivity of the medial prefrontal cortex and ventral midbrain. *Frontiers in Molecular Neuroscience*, 15. https://doi.org/10.3389/fnmol.2022.971349

Huntenburg, J., Steele, C., & Bazin, P.-L. (2018). Nighres: processing tools for high-resolution neuroimaging. *GigaScience*, *7*(7). https://doi.org/10.1093/gigascience/giy082

Hurd, Y. L., Suzuki, M., & Sedvall, G. C. (2001). D1 and D2 dopamine receptor mRNA expression in whole hemisphere sections of the human brain. *Journal of Chemical Neuroanatomy*, *22*(1–2), 127–137. https://doi.org/10.1016/S0891-0618(01)00122-3

Huys, Q. J., Maia, T. V., & Frank, M. J. (2016). Computational psychiatry as a bridge from neuroscience to clinical applications. *Nature neuroscience*, *19*(3), 404-413. https://doi.org/10.1038/nn.4238

Ikemoto, S. (2007). Dopamine reward circuitry: two projection systems from the ventral midbrain to the nucleus accumbens-olfactory tubercle complex. *Brain Research Reviews, 6*(9), 2166–2171. https://doi.org/10.1021/nl061786n

Isaacs, B., Mulder, M., Groot, J., van Berendonk, N., Lute, N., Bazin, P.-L., Forstmann, B.U., & Alkemade, A. (2020). 3 versus 7 Tesla Magnetic Resonance Imaging for parcellations of subcortical brain structures. *PLoS ONE, 15*(11),1–21. https://doi.org/10.1101/2020.07.02.184275

Isherwood, S. J. S., Bazin, P. L., Miletić, S., Stevenson, N. R., Trutti, A. C., Tse, D. H. Y., Heathcote, A., Matzke, D., Innes, R.J. Habli, S., Sokolowski, D.R., Alkemade, A. Håberg, A.K., & Forstmann, B. U. (2023). Investigating intra-individual networks of response inhibition and interference resolution using 7T MRI. *NeuroImage, 271*, 119988. https://doi.org/10.1016/j.neuroimage.2023.119988

Jackson, S., Horst, N., Axelsson, S., Horiguchi, N., Cockcroft, G., Robbins, T., & Roberts, A. (2018). Selective Role of the Putamen in Serial Reversal Learning in the Marmoset. *Cerebral Cortex (New York, NY)*, 29, 447 - 460. https://doi.org/10.1093/cercor/bhy276.

Jacob, S. N., & Nieder, A. (2014). Complementary roles for primate frontal and parietal cortex in guarding working memory from distractor stimuli. *Neuron, 83*(1), 226-237. https://doi.org/10.1016/j.neuron.2014.05.009

Janssen, R. J., Jylänki, P., Kessels, R. P. C., & van Gerven, M. A. J. (2015). Probabilistic model-based functional parcellation reveals a robust, fine-grained subdivision of the striatum. *NeuroImage, 119*, 398–405. http://doi.org/10.1016/j.neuroimage.2015.06.084

JASP Team (2023). JASP (Version 0.18) [Computer software].

Jeffreys, H., & Lindsay, R. B. (1939). *Theory of probability.* OuP Oxford.

Jenkinson, M., Bannister, P., Brady, M., & Smith, S. (2002). Improved optimization for the robust and accurate linear registration and motion correction of brain images. *NeuroImage, 17(*2), 825–41. https://doi.org/10.1006/nimg.2002.1132.

Jenkinson, M., Beckmann, C. F., Behrens, T. E., Woolrich, M. W., & Smith, S. M. (2012). FSL. *NeuroImage*, *62*(2), 782–790. https://doi.org/10.1016/j.neuroimage.2011.09.015

Jeurissen, B, Tournier, J-D, Dhollander, T, Connelly, A & Sijbers, J. (2014). Multi-tissue constrained spherical deconvolution for improved analysis of multi-shell diffusion MRI data. *NeuroImage*, 103, 411-426.

Jocham, G., Klein, T. A., & Ullsperger, M. (2011). Dopamine-mediated reinforcement learning signals in the striatum and ventromedial prefrontal cortex underlie value-based choices. *Journal of Neuroscience, 31*(5), 1606-1613. https://doi.org/10.1523/jneurosci.3904-10.2011

Jongkees, B. J. (2020). Baseline-dependent effect of dopamine's precursor L-tyrosine on working memory gating but not updating. *Cognitive, Affective, & Behavioral Neuroscience, 20*(3), 521-535. https://doi.org/10.3758/s13415-020-00783-8

Jongkees, B. J., Hommel, B., & Colzato, L. S. (2014). People are different: Tyrosine's modulating effect on cognitive control may depend on individual differences related to dopamine function. *Frontiers in Psychology, 5*, 1101. https://doi.org/10.3389/fpsyg.2014.01101

Joshua, M., Adler, A., & Bergman, H. (2009). The dynamics of dopamine in control of motor behavior. *Current Opinion in Neurobiology, 19*(6), 615-620. https://doi.org/10.1016/j.conb.2009.10.001

Kahn, I., & Shohamy, D. (2013). Intrinsic connectivity between the hippocampus, nucleus accumbens and ventral tegmental area in humans. *Hippocampus*, *23*(3), 187–192. https://doi.org/10.1002/hipo.22077

Kasper, L., Bollmann, S., Diaconescu, A. O., Hutton, C., Heinzle, J., Iglesias, S., Hauser, T. U., Sebold, M., Manjaly, Z. M., Pruessmann, K. P., & Stephan, K. E. (2017). The PhysIO toolbox for modeling physiological noise in fMRI data. *Journal of Neuroscience Methods, 276,* 56–72. https://doi.org/10.1016/j.jneumeth.2016.10.019

Kellner, E., Dhital, B., Kiselev, V.G., & Reisert, M. (2016). Gibbs-ringing artifact removal based on local subvoxel-shifts. *Magnetic Resonance in Medicine, 76*, 1574–1581. https://doi.org/10.1002/mrm.26054

Kessler, Y. (2018). N-2 repetition leads to a cost within working memory and a benefit outside it. *Annals of the New York Academy of Sciences*, *1424*(1), 268-277. https://doi.org/10.1111/nyas.13607

Kessler, Y., & Oberauer, K. (2014). Working memory updating latency reflects the cost of switching between maintenance and updating modes of operation. *Journal of Experimental Psychology: Learning, Memory, and Cognition*, *40*(3), 738-754. https://doi.org/10.1037/a0035545

Kessler, Y., & Rozanis, M. (2023). Task cues are quickly updated into working memory as part of their processing: The multiple-cue task-switching paradigm. *Psychonomic Bulletin & Review, 30*(3), 643-651. https://doi.org/10.3758/s13423-022-02186-x

Keuken, M. C., & Forstmann, B. U. (2015). A probabilistic atlas of the basal ganglia using 7 T MRI. *Data in brief*, *4*, 577–582. https://doi.org/10.1016/j.dib.2015.07.028

Keuken, M. C., Bazin, P.-L., Beekhuizen, S., Himmer, L., Kandola, A., Lafeber, J. J., Prochazkova, L., Trutti, A., Schaefer, A., Turner, R., & Forstmann, B. U. (2017). Effects of aging on T1, T2*, and QSM MRI values in the subcortex. *Brain Structure & Function, 222*, 2487-2505. https://doi.org/10.1007/s00429-016-1352-4

Keuken, M. C., Bazin, P., Crown, L., Hootsmans, J., Laufer, A., Müller-Axt, C., Van Der Putten, E. J., Schäfer, Turner, R., & Forstmann, B.U. (2014). Quantifying inter-individual anatomical variability in the subcortex using 7 T structural MRI. *Neuroimage, 94*, 40–46. https://doi.org/10.1016/j.neuroimage.2014.03.032

Keuken, M.C., Bazin, P.-L., Schäfer, A., Neumann, J., Turner, R., Forstmann, B.U. (2013). Ultra-high 7T MRI of structural age-related changes of the subthalamic nucleus. *Journal of Neuroscience, 33*(11), 4896–4900. https://doi.org/10.1523/JNEUROSCI.3241-12.2013.

Keuken, M. C., Liebrand, L. C., Bazin, P.-L., Alkemade, A., van Berendonk, N., Groot, J. M., Isherwood, S. J. S., Kemp, S., Lute, N., Mulder, M. J., Trutti, A. C., Caan, M. W. A., & Forstmann, B. U. (2022). A high-resolution multi-shell 3T diffusion magnetic resonance imaging dataset as part of the Amsterdam Ultra-high field adult lifespan database (AHEAD). *Data in Brief, 42*, 108086. https://doi.org/10.1016/j.dib.2022.108086

Keuken, M. C., Van Maanen, L., Bogacz, R., Schäfer, A., Neumann, J., Turner, R., & Forstmann, B. U. (2015). The subthalamic nucleus during decision-making with multiple alternatives. *Human Brain Mapping*. https://doi.org/10.1002/hbm.22896

Krebs, R. M., Heipertz, D., Schuetze, H., & Duzel, E. (2011). Novelty increases the mesolimbic functional connectivity of the substantia nigra/ventral tegmental area (SN/VTA) during reward anticipation: Evidence from high-resolution fMRI. *NeuroImage*, 58. http://doi.org/10.1016/j.neuroimage.2011.06.038

Krebs, R. M., Schott, B. H., & Düzel, E. (2009). Personality Traits Are Differentially Associated with Patterns of Reward and Novelty Processing in the Human Substantia Nigra/Ventral Tegmental Area. *Biological Psychiatry*, *65*(2), 103–110. http://doi.org/10.1016/j.biopsych.2008.08.019

Kwon, H. G., & Jang, S. H. (2014). Differences in neural connectivity between the substantia nigra and ventral tegmental area in the human brain. *Frontiers in Human Neuroscience, 8*. https://doi.org/10.3389/fnhum.2014.00041

Kyllonen, P. C., & Christal, R. E. (1990). Reasoning ability is (little more than) working-memory capacity?! *Intelligence*, *14*(4), 389-433. https://doi.org/10.1016/S0160-2896(05)80012-1

Lammel, S., Hetzel, A., Häckel, O., Jones, I., Liss, B., & Roeper, J. (2008). Unique Properties of Mesoprefrontal Neurons within a Dual Mesocorticolimbic Dopamine System. *Neuron*, *57*(5), 760–773. http://doi.org/10.1016/j.neuron.2008.01.022

Lammel, S., Ion, D. I., Roeper, J., & Malenka, R. C. (2011). Projection-Specific Modulation of Dopamine Neuron Synapses by Aversive and Rewarding Stimuli. *Neuron, 70*(5), 855–862. https://doi.org/10.1016/j.neuron.2011.03.025

Lammel, S., Lim, B. K., & Malenka, R. C. (2014). Reward and aversion in a heterogeneous midbrain dopamine system. *Neuropharmacology*, *76 Pt B*(0 0), 351–359. https://doi.org/10.1016/j.neuropharm.2013.03.019

Lammel, S., Lim, B. K., Ran, C., Huang, K. W., Betley, M. J., Tye, K. M., Deisseroth, K., & Malenka, R. C. (2012). Input-specific control of reward and aversion in the ventral tegmental area. *Nature, 491*(7423), 212–217. https://doi.org/10.1038/nature11527

Lanczos, C. (1964). Evaluation of noisy data. *Journal of the Society for Industrial and Applied Mathematics Series B Numerical Analysis, 1*(1), 76–85. https://doi.org/10.1137/0701007

Le Moal, M., Stinus, L., & Galey, D. (1976). Radiofrequency lesion of the ventral mesencephalic tegmentum: Neurological and behavioral considerations. *Experimental Neurology, 51*(2), 377–390. https://doi.org/10.1016/0014-4886(76)90024-8

Leber, A. B., Turk-Browne, N. B., & Chun, M. M. (2008). Neural predictors of moment-to-moment fluctuations in cognitive flexibility. *Proceedings of the National Academy of Sciences, 105*(36), 13592–13597. https://doi.org/10.1073/pnas.0805423105

Leemburg, S., Canonica, T., & Luft, A. (2018). Motor skill learning and reward consumption differentially affect VTA activation. *Scientific Reports, 8*(1), 687. https://doi.org/10.1038/s41598-017-18716-w

Lefebvre, G., Lebreton, M., Meyniel, F., Bourgeois-Gironde, S., & Palminteri, S. (2017). Behavioural and neural characterisation of optimistic reinforcement learning. *Nature Human Behaviour, 1*, 0067. https://doi.org/10.1038/s41562-017-0067

Lein, E. S., Hawrylycz, M. J., Ao, N., Ayres, M., Bensinger, A., Bernard, A., ... Jones, A. R. (2007). Genome-wide atlas of gene expression in the adult mouse brain. *Nature, 445*(7124), 168–176. DOI: 10.1038/nature05453

Lenglet, C., Abosch, A., Yacoub, E., de Martino, F., Sapiro, G., & Harel, N. (2012). Comprehensive in vivo mapping of the human basal ganglia and thalamic connectome in individuals using 7T MRI. *PLoS ONE*, *7*(1). http://doi.org/10.1371/journal.pone.0029153

Lewis-Peacock, J. A., Kessler, Y., & Oberauer, K. (2018). The removal of information from working memory. *Annals of the New York Academy of Sciences*, *1424*(1), 33-44. https://doi.org/10.1111/nyas.13714

Lewis, S. J., Dove, A., Robbins, T. W., Barker, R. A., & Owen, A. M. (2004). Striatal contributions to working memory: a functional magnetic resonance imaging study in humans. *European Journal of Neuroscience*, *19*(3), 755-760. https://doi.org/10.1111/j.1460-9568.2004.03108.x

Lewis, D. A., Melchitzky, D. S., Sesack, S. R., Whitehead, R. E., Auh, S., & Sampson, A. (2001). Dopamine transporter immunoreactivity in monkey cerebral cortex: regional, laminar, and ultrastructural localization. *The Journal Of Comparative Neurology*, *432*(1), 119–136. https://doi.org/10.1002/cne.1092

Lidow, M. S., Goldman-Rakic, P. S., Gallager, D. W., & Rakic, P. (1991). Distribution of dopaminergic receptors in the primate cerebral cortex: Quantitative autoradiographic analysis using [^{3}H]raclopride, [^{3}H]spiperone and [^{3}H]SCH23390. *Neuroscience*, *40*(3), 657–671. https://doi.org/10.1016/0306-4522(91)90003-7

Limbrick-Oldfield, E. H., Leech, R., Wise, R. J. S., & Ungless, M. A. (2019). Financial gain- and loss-related BOLD signals in the human ventral tegmental area and substantia nigra pars compacta. *European Journal of Neuroscience*, 49, 1196–1209. https://doi.org/10.1111/ejn.14288

Lloyd, B., de Voogd, L. D., Mäki-Marttunen, V., & Nieuwenhuis, S. (2023). Pupil size reflects activation of subcortical ascending arousal system nuclei during rest. *eLife, 12*, e84822. https://doi.org/10.7554/eLife.84822

Logie, R. H., Gilhooly, K. J., & Wynn, V. (1994). Counting on working memory in arithmetic problem solving. *Memory & cognition*, *22*(4), 395-410.

Love, B. C. (2016). Cognitive models as bridge between brain and behavior. *Trends in cognitive sciences*, *20*(4), 247-248. https://doi.org/10.1016/j.tics.2016.02.006

Ly, A., Marsman, M., Wagenmakers, E.-J. (2018). Analytic Posteriors for Pearson's Correlation Coefficient. *Statistica Neerlandica, 72*(1), 4-13. https://doi.org/10.1111/stan.12111

Ly, A., Verhagen, A. J. & Wagenmakers, E.-J. (2016). Harold Jeffreys's Default Bayes Factor Hypothesis Tests: Explanation, Extension, and Application in Psychology. *Journal of Mathematical Psychology, 72*, 19-32. https://doi.org/10.1016/j.jmp.2015.06.004

Ma, W. J., Husain, M., & Bays, P. M. (2014). Changing concepts of working memory. *Nature neuroscience*, *17*(3), 347. https://doi.org/10.1038/nn.3655

MacInnes, J. J., Dickerson, K. C., Chen, N., Adcock, R. A. (2016). Cognitive neurostimulation: Learning to volitionally sustain ventral tegmental area activation. *Neuron*, *89*(6), 1331–1342. http://doi.org/10.1016/j.neuron.2016.02.002

Mai, J. K., Majtanik, M., & Paxinos, G. (2016). *Atlas of the Human Brain* (4th ed.). Elsevier Inc.

Maizey, L., Evans, C. J., Muhlert, N., Verbruggen, F., Chambers, C. D., & Allen, C. P. (2020). Cortical and subcortical functional specificity associated with response inhibition. *NeuroImage*, 220, 117110. https://doi.org/10.1016/j.neuroimage.2020.117110

Mallet, N., Micklem, B. R., Henny, P., Brown, M. T., Williams, C., Bolam, J. P., Nakamura, K. C., & Magill, P. J. (2012). Dichotomous organization of the external globus pallidus. *Neuron, 74*(6), 1075–1086. https://doi.org/10.1016/j.neuron.2012.04.027

Mallet, N., Schmidt, R., Leventhal, D., Chen, F., Amer, N., Boraud, T., & Berke, J. D. (2016). Arkypallidal cells send a stop signal to striatum. *Neuron, 89*(2), 308–316. https://doi.org/10.1016/j.neuron.2015.12.017

Marques, J. P., Kober, T., Krueger, G., van der Zwaag, W., van de Moortele, P. F., & Gruetter, R. (2010). MP2RAGE, a self bias-field corrected sequence for improved segmentation and T1-mapping at high field. *NeuroImage, 49*(2), 1271–1281. https://doi.org/10.1016/j.neuroimage.2009.10.002

Marshuetz, C. (2005). Order information in working memory: an integrative review of evidence from brain and behavior. *Psychological bulletin*, *131*(3), 323. https://doi.org/10.1037/0033-2909.131.3.323

Marvel, C. L., Morgan, O. P., & Kronemer, S. I. (2019). How the motor system integrates with working memory. *Neuroscience & Biobehavioral Reviews, 102*, 184-194. https://doi.org/10.1016/j.neubiorev.2019.04.017

Mathy, F., & Feldman, J. (2012). What's magic about magic numbers? Chunking and data compression in short-term memory. *Cognition*, *122*(3), 346-362. https://doi.org/10.1016/j.cognition.2011.11.003

Matsuda, W., Furuta, T., Nakamura, K. C., Hioki, H., Fujiyama, F., Arai, R., & Kaneko, T. (2009). Single Nigrostriatal Dopaminergic Neurons Form Widely Spread and Highly Dense Axonal Arborizations in the Neostriatum. *Journal of Neuroscience*, *29*(2), 444–453. http://doi.org/10.1523/JNEUROSCI.4029-08.2009

Matsumoto, M., & Hikosaka, O. (2009). Two types of dopamine neuron distinctly convey positive and negative motivational signals. *Nature*, 459, 837–841. https://doi.org/10.1038/nature08028

Mazziotta, J., Toga, A., Evans, A., Fox, P., Lancaster, J., Zilles, K., ... & Pike, B. (2001). A probabilistic atlas and reference system for the human brain: International Consortium for Brain Mapping (ICBM). *Philosophical Transactions of the Royal Society of London. Series B: Biological Sciences, 356*(1412), 1293-1322. https://doi.org/10.1098/rstb.2001.0915

McDougle, S. D., & Collins, A. G. (2020). Modeling the influence of working memory, reinforcement, and action uncertainty on reaction time and choice during instrumental learning. *Psychonomic bulletin & review*, 1-20.

McNab, F., & Klingberg, T. (2008). Prefrontal cortex and basal ganglia control access to working memory. *Nature neuroscience*, *11*(1), 103-107.

McRitchie, D. A., Hardman, C. D., & Halliday, G. M. (1996). Cytoarchitectural distribution of calcium binding proteins in midbrain dopaminergic regions of rats and humans. *Journal of Comparative Neurology*, *364*(1), 121–150. https://doi.org/10.1002/(SICI)1096-9861(19960101)364:1<121::AID-CNE11>3.0.CO;2-1

Medeiros, H. H. A., Santana, M. A. D., Leite, M. D., Aquino, L. A. P., de Barros, M. A. S., Galvão, N. T., … Nascimento, E. S. (2016). The cytoarchitectonic and TH-immunohistochemical characterization of the dopamine cell groups in the substantia nigra, ventral tegmental area and retrorubral field in a bat (Artibeus planirostris). *Neuroscience Research*, *112*, 37–46. https://doi.org/10.1016/j.neures.2016.06.005

Mehta, M. A., Owen, A. M., Sahakian, B. J., Mavaddat, N., Pickard, J. D., & Robbins, T. W. (2000). Methylphenidate enhances working memory by modulating discrete frontal and parietal lobe regions in the human brain. *The Journal of Neuroscience, 20*(6), 1-6. https://doi.org/10.1523/jneurosci.20-06-j0004.2000

Mekern, V. N., Sjoerds, Z., & Hommel, B. (2019). How metacontrol biases and adaptivity impact performance in cognitive search tasks. *Cognition, 182*, 251-259. ISSN 0010-0277. https://doi.org/10.1016/j.cognition.2018.10.001.

Metere, R., Kober, T., Möller, H. E., & Schäfer, A. (2017). Simultaneous quantitative MRI mapping of T1, T2* and magnetic susceptibility with multi-echo MP2RAGE. *PLoS ONE, 12*(1), e0169265–28. http://doi.org/10.1371/journal.pone.0169265

Meyer, C., Moffat, B. A., Kuszpit, K., Bland, P. L., Chenevert, T. L., Rehemtulla, A., & Ross, B. D. (2006). A Methodology for Registration of a Histological Slide and in vivo MRI Volume based on Optimizing Mutual Information. *Molecular Imaging, 5*(1), 16–23. https://doi.org/10.2310/7290.2006.00002

Mier, D., Kirsch, P., & Meyer-Lindenberg, A. (2010). Neural substrates of pleiotropic action of genetic variation in COMT: a meta-analysis. *Molecular Psychiatry, 15*(9), 918–27. https://doi.org/10.1038/mp.2009.36

Miletić, S. (2023). *Modelling structure and function of the human subcortex*. [Thesis, fully internal, Universiteit van Amsterdam].

Miletić, S., Bazin, P. L., Weiskopf, N., van der Zwaag, W., Forstmann, B. U., Trampel, R. (2020). fMRI protocol optimization for simultaneously studying small subcortical and cortical areas at 7T. *NeuroImage, 219*, 116992. https://doi.org/10.1016/j.neuroimage.2020.116992

Miletić, S., Bazin, P.-L., Isherwood, S. J. S., Keuken, M. C., Alkemade, A., & Forstmann, B. U. (2022b). Charting human subcortical maturation across the adult lifespan with in vivo 7 T MRI. *NeuroImage, 245*, 118872. https://doi.org/10.1016/j.neuroimage.2022.118872

Miletić, S., Boag, R. J., Trutti, A. C., Stevenson, N., Forstmann, B. U., & Heathcote, A. (2021). A new model of decision processing in instrumental learning tasks. *eLife, 10*. https://doi.org/10.7554/eLife.63055

Miletić, S., Keuken, M. C., Mulder, M. J., Trampel, R., de Hollander, G., & Forstmann, B. U. (2022a). 7T functional MRI finds no evidence for distinct functional subregions in the subthalamic nucleus during a speeded decision-making task. *Cortex, 155*, 162-188. https://doi.org/10.1016/j.cortex.2022.06.014

Miller, E. K., & Cohen, J. D. (2001). An integrative theory of prefrontal cortex function. *Annual review of neuroscience*, *24*(1), 167-202. https://doi.org/10.1146/annurev.neuro.24.1.167

Mirenowicz, J., & Schultz, W. (1994). Importance of unpredictability for reward responses in primate dopamine neurons. *Journal of Neurophysiology,* 72, 1024–27. https://doi.org/10.1152/jn.1994.72.2.1024

Montague, P. R., Dayan, P., & Sejnowski, T. J. (1996). A framework for mesencephalic dopamine systems based on predictive Hebbian learning. *Journal of neuroscience, 16(*5), 1936-1947. https://doi.org/10.1523/JNEUROSCI.16-05-01936.1996

Montague, P. R., Hyman, S. E., & Cohen, J. D. (2004). Computational roles for dopamine in behavioural control. *Nature*, *431*(7010), 760–767. http://doi.org/10.1038/nature03015

Morales, M., & Margolis, E. (2017). Ventral tegmental area: cellular heterogeneity, connectivity and behaviour. *Nature Reviews Neuroscience, 18*, 73–85. https://doi.org/10.1038/nrn.2016.165

Morris, L., Kundu, P., Dowell, N., Mechelmans, D., Favre, P., Irvine, M., Robbins, T., Daw, N., Bullmore, E., Harrison, N., & Voon, V. (2016). Fronto-striatal organization: Defining functional and microstructural substrates of behavioural flexibility. *Cortex; a Journal Devoted to the Study of the Nervous System and Behavior*, 74, 118 - 133. https://doi.org/10.1016/j.cortex.2015.11.004.

Moustafa, A. A., Sherman, S. J., & Frank, M. J. (2008). A dopaminergic basis for working memory, learning and attentional shifting in Parkinsonism. *Neuropsychologia, 46*(13), 3144-3156. https://doi.org/10.1016/j.neuropsychologia.2008.07.011

Murty, V. P., Sambataro, F., Radulescu, E., Altamura, M., Iudicello, J., Zoltick, B., Weinberger, D. R., Goldberg, T. E., & Mattay, V. S. (2011). Selective updating of working memory content modulates meso-cortico-striatal activity. *NeuroImage*, 57(3), 1264-1272. https://doi.org/10.1016/j.neuroimage.2011.05.006

Murty, V. P., Shermohammed, M., Smith, D. V., Carter, R. M., Huettel, S. A., & Adcock, R. A. (2014). Resting state networks distinguish human ventral tegmental area from substantia nigra. *NeuroImage, 100,* 580–589. https://doi.org/10.1016/j.neuroimage.2014.06.047

Musslick, S., Jang, S. J., Shvartsman, M., Shenhav, A. & Cohen, J. D. (2018). Constraints associated with cognitive control and the stability-flexibility dilemma. In *Proc. 40th Annual Meeting of the Cognitive Science Society*. Cognitive Science Society: Madison, WI. 804-809.

Nair-Roberts, R. G., Chatelain-Badie, S. D., Benson, E., White-Cooper, H., Bolam, J. P., & Ungless, M. A. (2008). Stereological estimates of dopaminergic, GABAergic and glutamatergic neurons in the ventral tegmental area, substantia nigra and retrorubral field in the rat. *Neuroscience*, *152*(4), 1024–1031. https://doi.org/10.1016/j.neuroscience.2008.01.046

Nambu, A., Tokuno, H., & Takada, M. (2002). Functional significance of the cortico–subthalamo–pallidal 'hyperdirect' pathway. *Neuroscience Research*, *43*(2), 111-117. https://doi.org/10.1016/S0168-0102(02)00027-5

Nassar, M. R., Helmers, J. C., & Frank, M. J. (2018). Chunking as a rational strategy for lossy data compression in visual working memory. *Psychological review*, *125*(4), 486.

Navon, D. (1984). Resources—A theoretical soup stone? *Psychological review*, *91*(2), 216.

Nichols, T., & Hayasaka, S. (2003). Controlling the familywise error rate in functional neuroimaging: a comparative review. *Statistical methods in medical research*, *12*(5), 419–446. https://doi.org/10.1191/0962280203sm341ra

Nir-Cohen, G., Egner, T., & Kessler, Y. (2023). The neural correlates of updating and gating in procedural working memory. *Journal of Cognitive Neuroscience, 35*(6), 919–940. https://doi.org/10.1162/jocn_a_01988

Nir-Cohen, G., Kessler, Y., & Egner, T. (2019). Distinct neural substrates for opening and closing the gate from perception to working memory. *BioRxiv*, 853630.

Nir-Cohen, G., Kessler, Y., & Egner, T. (2020). Neural substrates of working memory updating. *Journal of Cognitive Neuroscience, 32*(12), 2285–2302. https://doi.org/10.1162/jocn_a_01625

Nomoto, K., Schultz, W., Watanabe, T., & Sakagami, M. (2010). Temporally Extended Dopamine Responses to Perceptually Demanding Reward-Predictive Stimuli. *Journal of Neuroscience*, 30(32), 10692–10702. https://doi.org/10.1523/JNEUROSCI.4828-09.2010

Norman, K. A., & O'Reilly, R. C. (2003). Modeling hippocampal and neocortical contributions to recognition memory: a complementary-learning-systems approach. *Psychological review*, *110*(4), 611.

O'Doherty, J. P., Cockburn, J., & Pauli, W. M. (2017). Learning, reward, and decision making. *Annual Review of Psychology, 68*(1), 73-100. https://doi.org/10.1146/annurev-psych-010416-044216

O'Doherty, J. P., Dayan, P., Friston, K., Critchley, H., & Dolan, R. J. (2003). Temporal difference models and reward-related learning in the human brain. *Neuron*, *38*(2), 329–337. https://doi.org/10.1016/s0896-6273(03)00169-7

O'Reilly, R. C. (2006). Biologically based computational models of high-level cognition. *Science, 314*(5796), 91-94. https://doi.org/10.1126/science.1127242

O'Reilly, R. C., & Norman, K. A. (2002). Hippocampal and neocortical contributions to memory: Advances in the complementary learning systems framework. *Trends in cognitive sciences*, *6*(12), 505-510. https://doi.org/10.1016/s1364-6613(02)02005-3

O'Reilly, R. C., & Frank, M. J. (2006). Making working memory work: a computational model of learning in the prefrontal cortex and basal ganglia. *Neural Computation, 18*, 283–328. https://doi.org/10.1162/089976606775093909

Oades, R. D., & Halliday, G. M. (1987). Ventral tegmental (A10) system: neurobiology. 1. Anatomy and connectivity. *Brain Research Reviews*, *12*(2), 117–165. http://doi.org/10.1016/0165-0173(87)90011-7

Oberauer, K. (2002). Access to information in working memory: exploring the focus of attention. *Journal of Experimental Psychology: Learning, Memory, and Cognition*, *28*(3), 411-421. https://doi.org/10.1037/0278-7393.28.3.411

Oberauer, K. (2009). Design for a working memory. In B. H. Ross (Ed.), *The psychology of learning and motivation* (pp. 45–100). Elsevier Academic Press. https://doi.org/10.1016/S0079-7421(09)51002-X

Olszewski, J., & Baxter, D. (1954). *Cytoarchitecture of the Human Brain Stem.* Basel: S. Karger.

Oren, S., Tittgemeyer, M., Rigoux, L., Schlamann, M., Schonberg, T., & Kuzmanovic, B. (2022). Neural encoding of food and monetary reward delivery. *NeuroImage*. https://doi.org/10.1016/j.neuroimage.2022.119335

Ott, T., & Nieder, A. (2019). Dopamine and cognitive control in prefrontal cortex. *Trends in Cognitive Sciences, 23*(3), 213–234. https://doi.org/10.1016/j.tics.2018.12.006

Owen, A. M. (1997). The functional organization of working memory processes within human lateral frontal cortex: the contribution of functional neuroimaging. *European Journal of Neuroscience*, *9*(7), 1329-1339.

Owen, A. M., McMillan, K. M., Laird, A. R., & Bullmore, E. (2005). N-back working memory paradigm: A meta-analysis of normative functional neuroimaging studies. *Human brain mapping*, *25*(1), 46-59.

Palestro, J. J., Bahg, G., Sederberg, P. B., Lu, Z. L., Steyvers, M., & Turner, B. M. (2018). A tutorial on joint models of neural and behavioral measures of cognition. *Journal of Mathematical Psychology*, *84*, 20-48. https://doi.org/10.1016/j.jmp.2018.03.003

Parent, A., & Hazrati, L. N. L.-N. (1995). Functional anatomy of the basal ganglia. *Brain Research Reviews*, *20*, 91–127. https://doi.org/10.1002/mds.10138

Park, M., Leahey, E., & Funk, R. J. (2023). Papers and patents are becoming less disruptive over time. *Nature, 613*, 138-144. https://doi.org/10.1038/s41586-022-05543-x

Pauli, W., Larsen, T., Collette, S., Tyszka, J. M., Seymour, B., & O'Doherty, J. P. (2015). Distinct Contributions of Ventromedial and Dorsolateral Subregions of the Human Substantia Nigra to Appetitive and Aversive Learning. *Journal of Neuroscience*, *35*(42), 14220-14233. https://doi.org/10.1523/JNEUROSCI.2277-15.2015

Pauli, W., Nili, A., & Tyszka, J. (2018). A high-resolution probabilistic in vivo atlas of human subcortical brain nuclei. *Scientific Data, 5*, 180063. https://doi.org/10.1038/sdata.2018.63

Paxinos, G. & Huang, X. (1995). *Atlas of the Human Brain Stem.* (1995 ed.). San Diego: Academic Press.

Paxinos, G., & Watson, C. (2007). *The rat brain in stereotaxic coordinates* (6th ed.). London: Academic Press. [ISBN: 9780123741219, 0123741211]

Paxinos, G., Huang, X.-F., Sengul, G., & Watson, C. (2011). Organization of brainstem nuclei. In Mai, J. K. & Paxinos, G. (Eds.). *The Human Nervous System.* (pp. 82-140). Elsevier.

Pearson, B., Raškevičius, J., Bays, P. M., Pertzov, Y., & Husain, M. (2014). Working memory retrieval as a decision process. *Journal of vision*, *14*(2), 2-2.

Perrotti, L. I., Bolanos, C. A., Choi, K., Russo, S. J., Edwards, S., Ulery, P. G., Wallace, D. L., Self, D. W., Nestler, E. J., & Barrot, M. (2005). FosB accumulates in a GABAergic cell population in the posterior tail of the ventral tegmental area after psychostimulant treatment, *21*, 2817–2824. https://doi.org/10.1111/j.1460-9568.2005.04110.x

Peters, J., Bromberg, U., Schneider, S., Brassen, S., Menz, M., Banaschewski, T., Conrod, P. J., Flor, H., Gallinat, J., Garavan, H., Heinz, A., Itterman, B., Lathrop, M., Martinot, J.-L., Paus, T., Poline, J.-B., Robbins, T. W., Rietschel, M., & Smolka, M. ... & IMAGEN Consortium. (2011). Lower ventral striatal activation during reward anticipation in adolescent smokers. *American Journal of Psychiatry*. http://doi.org/10.1176/appi.ajp.2010.10071024

Petri, S., Krampfl, K., Dengler, R., Bufler, J., Weindl, A., & Arzberger, T. (2002). Human GABA A receptors on dopaminergic neurons in the pars compacta of the substantia nigra. *The Journal of Comparative Neurology*, *452*(4), 360–6. http://doi.org/10.1002/cne.10379

Phillipson, O. T. (1979). The cytoarchitecture of the interfascicular nucleus and ventral tegmental area of tsai in the rat. *Journal of Comparative Neurology*, *187*(1), 85–98. http://doi.org/10.1002/cne.901870106

Pignatelli, M., & Bonci, A. (2018). Spiraling Connectivity of NAc-VTA Circuitry. *Neuron*, *97*(2), 261–262. https://doi.org/10.1016/j.neuron.2017.12.046

Pijnenburg, R., Scholtens, L. H., Ardesch, D. J., de Lange, S. C., Wei, Y., & van den Heuvel, M. P. (2021). Myelo- and cytoarchitectonic microstructural and functional human cortical atlases

reconstructed in common MRI space. *NeuroImage, 239*, 118274. https://doi.org/10.1016/j.neuroimage.2021.118274

Pioli, E. Y., Meissner, W., Sohr, R., Gross, C. E., Bezard, E., & Bioulac, B. H. (2008). Differential behavioral effects of partial bilateral lesions of ventral tegmental area or substantia nigra pars compacta in rats. *Neuroscience*, *153*(4), 1213–1224. http://doi.org/10.1016/j.neuroscience.2008.01.084

Poirier, L. J., Giguére, M., & Marchand, R. (1983). Comparative morphology of the substantia nigra and ventral tegmental area in the monkey, cat and rat. *Brain Research Bulletin*, *11*(3), 371–397. http://doi.org/10.1016/0361-9230(83)90173-9

Poldrack, R. (2006). Region of interest analysis for fMRI. *Social Cognitive and Affective Neuroscience*, *2*(1), 67-70. https://dx.doi.org/10.1093/scan/nsm006

Poldrack, R. A., & Yarkoni, T. (2016). From Brain Maps to Cognitive Ontologies: Informatics and the Search for Mental Structure. *Annual review of psychology*, *67*, 587–612. https://doi.org/10.1146/annurev-psych-122414-033729

Ponzi, A. (2008, September). Dynamical model of action reinforcement by gated working memory. In Advances in Cognitive Neurodynamics ICCN 2007: Proceedings of the International Conference on Cognitive Neurodynamics. ICCN 2007 Proceedings (pp. 463-467). Dordrecht: Springer Netherlands.

Power, J. D., Mitra, A., Laumann, T. O., Snyder, A. Z., Schlaggar, B. L., & Petersen, S. E. (2014). Methods to detect, characterize, and remove motion artifact in resting state fMRI. *NeuroImage, 84*, (Supplement C), 320–41. https://doi.org/10.1016/j.neuroimage.2013.08.048

Preuschoff, K., Quartz, S. R., & Bossaerts, P. (2008). Human insula activation reflects risk prediction errors as well as risk. *The Journal of Neuroscience*, *28*(11), 2745–2752. https://doi.org/10.1523/JNEUROSCI.4286-07.2008

Rac-Lubashevsky, R., & Kessler, Y. (2016a). Dissociating working memory updating and automatic updating: The reference-back paradigm. *Journal of Experimental Psychology: Learning, Memory, and Cognition*, *42*(6), 951–969. https://doi.org/10.1037/xlm0000219

Rac-Lubashevsky, R., & Kessler, Y. (2016b). Decomposing the n-back task: An individual differences study using the reference-back paradigm. *Neuropsychologia, 90*, 190-199. https://doi.org/10.1016/j.neuropsychologia.2016.07.013

Rac-Lubashevsky, R., & Kessler, Y. (2018). Oscillatory correlates of control over working memory gating and updating: an EEG study using the reference-back paradigm. *Journal of Cognitive Neuroscience, 30*(12), 1870-1882. https://doi.org/10.1162/jocn_a_01326

Rac-Lubashevsky, R., & Kessler, Y. (2019). Revisiting the relationship between the P3b and working memory updating. *Biological psychology*, *148*, 107769. https://doi.org/10.1016/j.biopsycho.2019.107769

Rac-Lubashevsky, R., Slagter, H. A., & Kessler, Y. (2017). Tracking real-time changes in working memory updating and gating with the event-based eye-blink rate. *Scientific reports*, *7*(1), 2547. https://doi.org/10.1038/s41598-017-02942-3

Ranaldi, R. (2014). Dopamine and reward seeking: The role of ventral tegmental area. *Reviews in the Neurosciences*, *25*(5), 621–630. http://doi.org/10.1515/revneuro-2014-0019

Ratcliff, R. (1978). A theory of memory retrieval. *Psychological review*, *85*(2), 59. https://doi.org/10.1037/0033-295X.85.2.59

Ratcliff, R., & Smith, P. L. (2004). A Comparison of Sequential Sampling Models for Two-Choice Reaction Time. *Psychological Review, 111*(2), 333–367. https://doi.org/10.1037/0033-295X.111.2.333

Richter, A., Reinhard, F., Kraemer, B., & Gruber, O. (2020). A high-resolution fMRI approach to characterize functionally distinct neural pathways within dopaminergic midbrain and nucleus

accumbens during reward and salience processing. *European Neuropsychopharmacology*, 36, 137-150. https://doi.org/10.1016/j.euroneuro.2020.05.005

Ricker, T. J., Vergauwe, E., & Cowan, N. (2016). Decay theory of immediate memory: From Brown (1958) to today (2014). *The Quarterly Journal of Experimental Psychology*, *69*(10), 1969-1995. https://doi.org/10.1080/17470218.2014.914546

Rohe, T., Weber, B., & Fliessbach, K. (2012). Dissociation of BOLD responses to reward prediction errors and reward receipt by a model comparison. *European Journal of Neuroscience, 36*(3), 2376-2382. https://doi.org/10.1111/j.1460-9568.2012.08125.x

Root, D. H., Wang, H.-L., Liu, B., Barker, D. J., Mód, L., Szocsics, P., Silva, A. C., Maglóczky, Z., & Morales, M. (2016). Glutamate neurons are intermixed with midbrain dopamine neurons in nonhuman primates and humans. *Scientific Reports*, *6*(1), 30615. https://doi.org/10.1038/srep30615

Roth, J. K., Serences, J. T., & Courtney, S. M. (2006). Neural system for controlling the contents of object working memory in humans. *Cerebral Cortex*, *16*(11), 1595-1603. https://doi.org/10.1093/cercor/bhj096

Rouder, J. N., Speckman, P. L., Sun, D., Morey, R. D., & Iverson, G. (2009). Bayesian t tests for accepting and rejecting the null hypothesis. *Psychonomic Bulletin & Review,* 16, 225-237. https://doi.org/10.3758/PBR.16.2.225

Salamone, J. D., & Correa, M. (2012). The Mysterious Motivational Functions of Mesolimbic Dopamine. *Neuron*, *76*(3), 470–485. http://doi.org/10.1016/j.neuron.2012.10.021

Satterthwaite, T. D., Elliott, M. A., Gerraty, R. T., Ruparel, K., Loughead, J., Calkins, M. E., Eickhoff, S. B., Hakonarson, H., Gur, R.C., Gur, R. E., & Wolf, D. H. (2013). An improved framework for confound regression and filtering for control of motion artifact in the preprocessing of resting-state functional connectivity data. *NeuroImage, 64*(1), 240–256. https://doi.org/10.1016/j.neuroimage.2012.08.052

Schall, J. D. (2019). Accumulators, Neurons, and Response Time. *Trends in neurosciences.* https://doi.org/10.1016/j.tins.2019.10.001

Schilling, K. G., Tax, C. M. W., Rheault, F., Landman, B. A., Anderson, A. W., Descoteaux, M., & Petit, L. (2022). Prevalence of white matter pathways coming into a single white matter voxel orientation: The bottleneck issue in tractography. *Human brain mapping*, *43*(4), 1196–1213. https://doi.org/10.1002/hbm.25697

Schridde, U., Khubchandani, M., Motelow, J. E., Sanganahalli, B. G., Hyder, F., & Blumenfeld, H. (2008). Negative BOLD with large increases in neuronal activity. *Cerebral cortex, 18*(8), 1814–1827. https://doi.org/10.1093/cercor/bhm208

Schultz W. (1998). Predictive reward signal of dopamine neurons. *Journal Of Neurophysiology*, *80*(1), 1–27. https://doi.org/10.1152/jn.1998.80.1.1

Schultz, W. (2007). Behavioral dopamine signals. *Trends in Neurosciences, 30*(5), 203–210. https://doi.org/10.1016/j.tins.2007.03.007

Schultz, W. (2013). Updating dopamine reward signals. *Current Opinion in Neurobiology, 23*(2), 229-238. https://doi.org/10.1016/j.conb.2012.11.012

Schultz, W. (2015). Neuronal reward and decision signals: From theories to data. *Physiological Reviews, 95*, 853–951. https://doi.org/10.1152/physrev.00023.2014

Schultz, W., Apicella, P., & Ljungberg, T. (1993). Responses of monkey dopamine neurons to reward and conditioned stimuli during successive steps of learning a delayed response task. *Journal of Neuroscience, 13*(3), 900–913. https://doi.org/10.1523/JNEUROSCI.13-03-00900.1993

Schultz, W., Dayan, P., & Montague, P. R. (1997). A neural substrate of prediction and reward. *Science, 275*(5306), 1593–1599. https://doi.org/10.1126/science.275.5306.1593

Schultz, W., Ruffieux, A., & Aebischer, P. (1983). The activity of pars compacta neurons of the monkey substantia nigra in relation to motor activation. Experimental Brain Research, 51, 377–387. https://doi.org/10.1007/ BF00237874

Sewell, D. K., Lilburn, S. D., & Smith, P. L. (2016). Object selection costs in visual working memory: A diffusion model analysis of the focus of attention. *Journal of experimental psychology: learning, memory, and cognition*, *42*(11), 1673.

Shenhav, A., Botvinick, M. M., & Cohen, J. D. (2013). The expected value of control: an integrative theory of anterior cingulate cortex function. *Neuron*, *79*(2), 217-240. https://doi.org/10.1016/j.neuron.2013.07.007

Sherbondy, A. J., Dougherty, R. F., Napel, S., & Wandell, B. A. (2008). Identifying the human optic radiation using diffusion imaging and fiber tractography. *Journal of Vision, 8*(10), 1–11. https://doi.org/10.1167/8.10.12

Smith, K. S., Berridge, K. C., & Aldridge, J. W. (2011). Disentangling pleasure from incentive salience and learning signals in brain reward circuitry. *Proceedings of the National Academy of Sciences of the United States of America*, *108*(27), E255-64. http://doi.org/10.1073/pnas.1101920108

Smith, R. E., Tournier, J.-D., Calamante, F. & Connelly, A. (2015). SIFT2: Enabling dense quantitative assessment of brain white matter connectivity using streamlines tractography. *NeuroImage*, 119, 338-351. https://doi.org/10.1016/j.neuroimage.2015.06.092

Smith, S. M. (2002). Fast robust automated brain extraction. *Human Brain Mapping, 17*, 143-155. https://doi.org/10.1002/hbm.10062

Smith, S. M., & Brady, J. M. (1997). SUSAN—A new approach to low level image processing. *International Journal of Computer Vision, 23*(1), 45–78. https://doi.org/10.1023/A:1007963824710

Smith, S. M., Jenkinson, M., Woolrich, M. W., Beckmann, C. F., Behrens, T. E., Johansen-Berg, H., Bannister, P. R., De Luca, M., Drobnjak, I., Flitney, D. E., Niazy, R. K., Saunders, J., Vickers, J., Zhang, Y., De Stefano, N., Brady, J. M., & Matthews, P. M. (2004). Advances in functional and structural MR image analysis and implementation as FSL. *NeuroImage*, 23, 208-219. https://doi.org/10.1016/j.neuroimage.2004.07.051

Snyder, J. M., Hagan, C. E., Bolon, B., & Keene, C. D. (2018). Nervous System. In *Comparative Anatomy and Histology (Second Edition): A Mouse, Rat, and Human Atlas* (pp. 403–444). https://doi.org/10.1016/B978-0-12-802900-8.00020-8

Stevenson, N., Innes, R., Boag, R. J., Miletic, S., Isherwood, S.J.S., Trutti, A.C., Heathcote, A., & Forstmann, B.U. (2024a). Joint modelling of latent cognitive mechanisms shared across decision-making domains. *Computational Brain & Behavior, 7*, 1-22. https://doi.org/10.1007/s42113-023-00192-3

Stevenson, N., Donzallaz, M. C., Innes, R. J., Forstmann, B., Matzke, D., & Heathcote, A. (2024b). EMC2: An R Package for cognitive models of choice. *PsyArXiv*. https://doi.org/10.31234/osf.io/2e4dq

Sun, T., & Walsh, C. A. (2006). Molecular approaches to brain asymmetry and handedness. *Nature Reviews Neuroscience*, *7*(8), 655–662. https://doi.org/10.1038/nrn1930

Surmeier, D. J., Ding, J., Day, M., Wang, Z., & Shen, W. (2007). D1 and D2 dopamine-receptor modulation of striatal glutamatergic signaling in striatal medium spiny neurons. *Trends in Neurosciences*, 30(5), 234–241. https://doi.org/10.1016/j.tins.2007.03.008

Sutton, R. S., & Barto, A. G. (1998). *Reinforcement learning: An introduction.* (Vol. 135, pp. 223-260). Cambridge: MIT press.

Sutton, R. S., & Barto, A. G. (2018). *Reinforcement learning: An introduction.* Cambridge: MIT press.

Swanson, L. W. (1982). The projections of the ventral tegmental area and adjacent regions: A combined fluorescent retrograde tracer and immunofluorescence study in the rat. *Brain Research Bulletin*, *9*(1–6), 321–353. http://doi.org/10.1016/0361-9230(82)90145-9

Taber, E. (1961). The cytoarchitecture of the brain stem of the cat. I. Brain stem nuclei of cat. *Journal of Comparative Neurology*, *116*(1), 27–69. http://doi.org/10.1002/cne.901160104

Takahashi, H., Kato, M., Takano, H., Arakawa, R., Okumura, M., Otsuka, T., Kodaka, F., Hayashi, M., Okubo, Y., Ito, H., & Suhara, T. (2008). Differential contributions of prefrontal and hippocampal dopamine D(1) and D(2) receptors in human cognitive functions. *Journal of Neuroscience, 28*(46), 12032–12038. https://doi.org/10.1523/JNEUROSCI.3446-08.2008

Takahashi, H., Koeda, M., Oda, K., Matsuda, T., Matsushima, E., Matsuura, M., Asai, K., & Okubo, Y. (2004). An fMRI study of differential neural response to affective pictures in schizophrenia. *NeuroImage*, *22*(3), 1247–1254. http://doi.org/10.1016/j.neuroimage.2004.03.028

Takahashi, Y. K., Stalnaker, T. A., Mueller, L. E., Harootonian, S. K., Langdon, A. J., & Schoenbaum, G. (2023). Dopaminergic prediction errors in the ventral tegmental area reflect a multithreaded predictive model. *Nature Neuroscience*, 26, 830–839. https://doi.org/10.1038/s41593-023-01310-x

Tan, H. Y., Chen, Q., Goldberg, T. E., Mattay, V. S., Meyer-Lindenberg, A., Weinberger, D. R., & Callicott, J. H. (2007). Catechol-O-methyltransferase Val158Met modulation of prefrontal–parietal–striatal brain systems during arithmetic and temporal transformations in working memory. *Journal of Neuroscience*, *27*(49), 13393-13401. https://doi.org/10.1523/JNEUROSCI.4041-07.2007

Tang, Y., Sun, W., Toga, A. W., Ringman, J. M., & Shi, Y. (2018). A probabilistic atlas of human brainstem pathways based on connectome imaging data. *NeuroImage, 169*, 227-239. https://doi.org/10.1016/j.neuroimage.2017.12.042.

Thalmann, M., Souza, A. S., & Oberauer, K. (2019). How does chunking help working memory? *Journal of Experimental Psychology: Learning, Memory, and Cognition*, *45*(1), 37-55. https://doi.org/10.1037/xlm0000578

Tian, J., Huang, R., Cohen, J. Y., Osakada, F., Kobak, D., Machens, C. K., Callaway, E. M., Uchida, N., & Watabe-Uchida, M. (2016). Distributed and mixed information in monosynaptic inputs to dopamine neurons. *Neuron, 91*(6), 1374-1389. https://doi.org/10.1016/j.neuron.2016.08.018.

Tittgemeyer, M., Rigoux, L., & Knösche, T. R. (2018). Cortical parcellation based on structural connectivity: A case for generative models. *NeuroImage*, *173*(June 2016), 592–603. http://doi.org/10.1016/j.neuroimage.2018.01.077

Tobler, P. N., O'Doherty, J. P., Dolan, R. J., & Schultz, W. (2006). Human neural learning depends on reward prediction errors in the blocking paradigm. *Journal of neurophysiology, 95*(1), 301–310. https://doi.org/10.1152/jn.00762.2005

Tomasi, D., & Volkow, N. D. (2014). Functional connectivity of substantia nigra and ventral tegmental area: Maturation during adolescence and effects of ADHD. *Cerebral Cortex*, *24*(4), 935–944. http://doi.org/10.1093/cercor/bhs382

Tournier, J.-D. (2019). Diffusion MRI in the brain – Theory and concepts. *Progress in Nuclear Magnetic Resonance Spectroscopy, 112–113, 1-16*. https://doi.org/10.1016/j.pnmrs.2019.03.001

Tournier, J.-D., Calamante, F. & Connelly, A. (2010). Improved probabilistic streamlines tractography by 2nd order integration over fibre orientation distributions. *Proceedings of the International Society for Magnetic Resonance in Medicine,* 167.

Tournier, J.-D.; Calamante, F., Gadian, D.G. & Connelly, A. (2004). Direct estimation of the fiber orientation density function from diffusion-weighted MRI data using spherical deconvolution. *NeuroImage, 23,* 1176-1185. https://doi.org/10.1016/j.neuroimage.2004.07.037

Tournier, J.-D., Mori, S., & Leemans, A. (2011). Diffusion tensor imaging and beyond. *Magnetic Resonance in Medicine, 65*, 1532–1556. https://doi.org/10.1002/mrm.22924

Tournier, J.-D., Smith, R. E., Raffelt, D., Tabbara, R., Dhollander, T., Pietsch, M., Christiaens, D., Jeurissen, B., Yeh, C. H., & Connelly, A. (2019). MRtrix3: A fast, flexible and open software framework for medical image processing and visualisation. *NeuroImage*, 202, 116137. https://doi.org/10.1016/j.neuroimage.2019.116137

Trutti, A. C., Fontanesi, L., Mulder, M. J., Bazin, P.-L., Hommel, B., & Forstmann, B. U. (2021). A probabilistic atlas of the human ventral tegmental area (VTA) based on 7 Tesla MRI data. *Brain Structure and Function, 226*(4), 1155–1167. https://doi.org/10.1007/s00429-021-02231-w

Trutti, A. C., Mulder, M. J., Hommel, B., & Forstmann, B. U. (2019). Functional neuroanatomical review of the ventral tegmental area. *NeuroImage, 191*, 258–268. https://doi.org/10.1016/j.neuroimage.2019.01.062

Trutti, A. C., Verschooren, S., Forstmann, B. U., & Boag, R. J. (2021). Understanding subprocesses of working memory through the lens of model-based cognitive neuroscience. *Current Opinion in Behavioral Sciences, 38*, 57-65. https://doi.org/10.1016/j.cobeha.2020.10.002.

Tsai, C. (1925). The optic tracts and centers of the opossum. Didelphis virginiana. *Journal of Comparative Neurology*, *39*(2), 173–216. http://doi.org/10.1002/cne.900390202

Turner, B. M., Forstmann, B. U., Wagenmakers, E. J., Brown, S. D., Sederberg, P. B., & Steyvers, M. (2013). A Bayesian framework for simultaneously modeling neural and behavioral data. *NeuroImage, 72*, 193-206. https://doi.org/10.1016/j.neuroimage.2013.01.048

Turner, B. M., Palestro, J. J., Miletić, S., & Forstmann, B. U. (2019). Advances in techniques for imposing reciprocity in brain-behavior relations. *Neuroscience & Biobehavioral Reviews*. https://doi.org/10.1016/j.neubiorev.2019.04.018

Turner, B. M., Rodriguez, C. A., Norcia, T. M., McClure, S. M., & Steyvers, M. (2016). Why more is better: Simultaneous modeling of EEG, fMRI, and behavioral data. *NeuroImage*, *128*, 96-115. https://doi.org/10.1016/j.neuroimage.2015.12.030

Turner, B. M., Sederberg, P. B., Brown, S. D., & Steyvers, M. (2013a). A method for efficiently sampling from distributions with correlated dimensions. *Psychological Methods, 18*(3), 368–384. https://doi.org/10.1037/a0032222

Tustison, N. J., Avants, B. B., Cook, P. A., Zheng, Y., Egan, A., Yushkevich, P. A., & Gee, J. C. (2010). N4ITK: Improved N3 bias correction. *IEEE Transactions on Medical Imaging, 29*(6), 1310–20. https://doi.org/10.1109/TMI.2010.2046908.

Ungerstedt, U. (1971). Stereotaxic Mapping of the Monoamine Pathways in the Rat Brain. *Acta Physiologica Scandinavica*, *82*(367 S), 1–48. http://doi.org/10.1111/j.1365-201X.1971.tb10998.x

Utter, A. A., & Basso, M. A. (2008). The basal ganglia: An overview of circuits and function. *Neuroscience and Biobehavioral Reviews*, *32*(3), 333–342. http://doi.org/10.1016/j.neubiorev.2006.11.003

Vaillancourt, D. E., Prodoehl, J., Abraham, I., Corcos, D. M., Zhou, X. J., Cornelia, C. L., & Little, D. M. (2009). High-resolution diffusion tensor imaging in the substantia nigra of de novo Parkinson disease. *Neurology*, *72*(16), 1378–1384. https://doi.org/10.1212/01.wnl.0000340982.01727.6e

Vallentin, D., Bongard, S., & Nieder, A. (2012). Numerical rule coding in the prefrontal, premotor, and posterior parietal cortices of macaques. *Journal of Neuroscience, 32*(19), 6621-6630. https://doi.org/10.1523/JNEUROSCI.5071-11.2012

van der Velden, L., Vinck, M., Werkman, T. R., & Wadman, W. J. (2017). Tuning of neuronal interactions in the lateral Ventral Tegmental Area by dopamine sensitivity. *Neuroscience*, 10, 1–8. https://doi.org/10.1016/j.neuroscience.2017.10.009

van der Zwaag, W., Schäfer, A., Marques, J. P., Turner, R., & Trampel, R. (2016). Recent applications of UHF-MRI in the study of human brain function and structure: a review. *NMR in biomedicine*, *29*(9), 1274–1288. https://doi.org/10.1002/nbm.3275

van Dijck, J. P., Abrahamse, E. L., Majerus, S., & Fias, W. (2013). Spatial attention interacts with serial-order retrieval from verbal working memory. *Psychological Science*, *24*(9), 1854-1859. https://doi.org/10.1177/0956797613479610

van Domburg, P., & ten Donkelaar, H. (1991). The human substantia nigra and ventral tegmental area: a neuroanatomical study with notes on ageing and ageing disease. *Advances in Anatomy, Embryology and Cell Biology, 121,* 1-132. http://doi.org/10.1007/978-3-642-75846-1

van Schouwenburg, M. R., den Ouden, H. E., & Cools, R. (2010). The human basal ganglia modulate frontal-posterior connectivity during attention shifting. *Journal of Neuroscience*, *30*(29), 9910-9918. https://doi.org/10.1523/JNEUROSCI.1111-10.2010

van Schouwenburg, M. R., Onnink, A. M. H., ter Huurne, N., Kan, C. C., Zwiers, M. P., Hoogman, M., Franke, B., Buitelaar, J. K., & Cools, R. (2014). Cognitive flexibility depends on white matter microstructure of the basal ganglia. *Neuropsychologia,* 53, 171-177. https://doi.org/10.1016/j.neuropsychologia.2013.11.015

van Zessen, R., Phillips, J. L., Budygin, E. A., & Stuber, G. D. (2012). Activation of VTA GABA neurons disrupts reward consumption. *Neuron*, *73*(6), 1184-1194. https://doi.org/10.1016/j.neuron.2012.02.016

Veenvliet, J.V., Smidt, M.P. (2014). Molecular mechanisms of dopaminergic subset specification: fundamental aspects and clinical perspectives. *Cellular and Molecular Life Sciences,* 71, 4703–4727. https://doi.org/article/10.1007%2Fs00018-014-1681-5

Veraart, J., Fieremans, E., & Novikov, D. S. (2016a). Diffusion MRI noise mapping using random matrix theory. *Magnetic resonance in medicine*, *76*(5), 1582–1593. https://doi.org/10.1002/mrm.26059

Veraart, J., Novikov, D.S., Christiaens, D., Adesaron, B., Sijbers, J. & Fieremans, E. (2016b). Denoising of diffusion MRI using random matrix theory. *NeuroImage*, *142*, 394-406. https://doi.org/10.1016/j.neuroimage.2016.08.016

Verschooren, S., Kessler, Y., & Egner, T. (2021). Evidence for a single mechanism gating perceptual and long-term memory information into working memory. *Cognition, 212*, 104668. https://doi.org/10.1016/j.cognition.2021.104668

Verschooren, S., Pourtois, G., & Egner, T. (2020). More efficient shielding for internal than external attention? Evidence from asymmetrical switch costs. *Journal of Experimental Psychology: Human Perception and Performance, 46*(9), 912–925. https://doi.org/10.1037/xhp0000758

Vicq d'Azyr, F. (1786). *Traité d'anatomie et de physiologie, avec des planches coloriées représentant au naturel les divers organes de l'homme et des animaux*. Didot, Paris. https://doi.org/10.11588/diglit.13811#0209

Viereckel, T., Dumas, S., Smith-Anttila, C. J. A., Vlcek, B., Bimpisidis, Z., Lagerström, M. C., … Wallén-Mackenzie, A. (2016). Midbrain Gene Screening Identifies a New Mesoaccumbal Glutamatergic Pathway and a Marker for Dopamine Cells Neuroprotected in Parkinson's Disease. *Scientific Reports, 6*, 1–16. https://doi.org/10.1038/srep35203

Wade, A. R. (2002). The negative BOLD signal unmasked. *Neuron, 36*(6), 993–995. https://doi.org/10.1016/S0896-6273(02)01138-8

Watabe-Uchida, M., Eshel, N., & Uchida, N. (2017). Neural Circuitry of Reward Prediction Error. *Annual Review of Neuroscience*, 40(1), 373-394.

Watabe-Uchida, M., Zhu, L., Ogawa, S. K., Vamanrao, A., & Uchida, N. (2012). Whole-brain mapping of direct inputs to midbrain dopamine neurons. *Neuron*, *74*(5), 858–873. https://doi.org/10.1016/j.neuron.2012.03.017

Weilbächer, R. A., & Gluth, S. (2017). The interplay of hippocampus and ventromedial prefrontal cortex in memory-based decision making. *Brain sciences*, *7*(1), 4. https://doi.org/10.3390/brainsci7010004

Weiskopf, N., Mohammadi, S., Lutti, A., & Callaghan, M. F. (2015). Advances in MRI-based computational neuroanatomy. *Current Opinion in Neurology*, *28*(4), 313–322. http://doi.org/10.1097/WCO.0000000000000222

Williams, M. S., & Goldman-Rakic, P. S. (1998). Widespread origin of the primate mesofrontal dopamine system. *Cerebral Cortex, 8*(4), 321–345. https://doi.org/10.1093/cercor/8.4.321

Williams, M. A., Li, C., Kash, T. L., Matthews, R. T., & Winder, D. G. (2014). Excitatory drive onto dopaminergic neurons in the rostral linear nucleus is enhanced by norepinephrine in an α-1 adrenergic receptor-dependent manner. *Neuropharmacology*, *86*, 116–124. http://doi.org/10.1016/j.neuropharm.2014.07.001

Wise R. A. (2004). Dopamine, learning and motivation. *Nature reviews Neuroscience*, *5*(6), 483–494. https://doi.org/10.1038/nrn1406

Wise, R. A. (2009). Roles for nigrostriatal — not just mesocorticolimbic — dopamine in reward and addiction. *Trends in Neurosciences*, *32*(10), 517–524. https://doi.org/10.1016/j.tins.2009.06.004

Wood, J., & Ahmari, S. E. (2015). A Framework for Understanding the Emerging Role of Corticolimbic-Ventral Striatal Networks in OCD-Associated Repetitive Behaviors. *Frontiers in systems neuroscience*, *9*, 171. https://doi.org/10.3389/fnsys.2015.00171

Woolrich, M. W., Ripley, B. D., Brady, M., & Smith, S. M. (2001). Temporal autocorrelation in univariate linear modeling of FMRI data. *NeuroImage, 14*(6), 1370–1386. https://doi.org/10.1006/nimg.2001.0931

World Health Organization. (2022). *Parkinson disease: A public health approach*. Technical brief. Geneva. https://www.who.int/publications/i/item/9789240050983

Xiao, Y., Fonov, V., Chakravarty, M. M., Beriault, S., Al Subaie, F., Sadikot, A., Pike, G. B., Bertrand, G., & Collins, D. L. (2017). A dataset of multi-contrast population-averaged brain MRI atlases of a Parkinson's disease cohort. *Data in brief*, *12*, 370–379. https://doi.org/10.1016/j.dib.2017.04.013

Yang, H., de Jong, J. W., Tak, Y. E., Peck, J., Bateup, H. S., & Lammel, S. (2018). Nucleus Accumbens Subnuclei Regulate Motivated Behavior via Direct Inhibition and Disinhibition of VTA Dopamine Subpopulations. *Neuron, 97*(2), 434–449. https://doi.org/10.1016/j.neuron.2017.12.022

Yao, Z., van Velthoven, C. T. J., Kunst, M., Zhang, M., McMillen, D., Lee, C., Jung, W., Goldy, J., Abdelhak, A., Baker, P., Barkan, E., Bertagnolli, D., Campos, J., Carey, D., Casper, T., Chakka, A. B., Chakrabarty, R., Chavan, S., Chen, M., Clark, M., … Zeng, H. (2023). A high-resolution transcriptomic and spatial atlas of cell types in the whole mouse brain. *Nature, 624*, 317–332. https://doi.org/10.1038/s41586-023-06812-z

Yekutieli, D., & Benjamini, Y. (1999). Resampling-based false discovery rate controlling multiple test procedures for correlated test statistics. *Journal of Statistical Planning and Inference, 82*(1-2), 171–196. https://doi.org/10.1016/S0378-3758(99)00041-5

Yoo, J. H., Zell, V., Gutierrez-Reed, N., Wu, J., Ressler, R., Shenasa, M. A., Johnson, A. B., Fife, K. H., Faget, L., & Hnasko, T. S. (2016). Ventral tegmental area glutamate neurons co-release GABA and promote positive reinforcement. *Nature Communications, 7*, 1–13. https://doi.org/10.1038/ncomms13697

Yu, Y., FitzGerald, T. H., & Friston, K. J. (2013). Working memory and anticipatory set modulate midbrain and putamen activity. *Journal of Neuroscience*, *33*(35), 14040-14047. https://doi.org/10.1523/JNEUROSCI.1176-13.2013

Zapparoli, L., Devoto, F., Giannini, G., Zonca, S., Gallo, F., & Paulesu, E. (2022). Neural structural abnormalities behind altered brain activation in obesity: Evidence from meta-analyses of

brain activation and morphometric data. *NeuroImage: Clinical, 36*, 103179. https://doi.org/10.1016/j.nicl.2022.103179

Zhang, C., Stock, A.-K., Mückschel, M., Hommel, B., & Beste, C. (2023). Aperiodic neural activity reflects metacontrol. *Cerebral Cortex, 33*(12), 7941–7951. https://doi.org/10.1093/cercor/bhad089

Zhang, T. A., Placzek, A. N., & Dani, J. A. (2010). In vitro identification and electrophysiological characterization of dopamine neurons in the ventral tegmental area. *Neuropharmacology*, *59*(6), 431–436. http://doi.org/10.1016/j.neuropharm.2010.06.004

Zhang, W., & Luck, S. J. (2008). Discrete fixed-resolution representations in visual working memory. *Nature*, *453*(7192), 233-235. https://doi.org/10.1038/nature06860

Zhang, Y., Brady, M., & Smith, S. (2001). Segmentation of brain MR images through a hidden Markov random field model and the expectation-maximization algorithm. *IEEE Transactions on Medical Imaging, 20*(1), 45–57. https://doi.org/10.1109/42.906424

Zhang, Y., Larcher, K. M.-H., Misic, B., & Dagher, A. (2017). Anatomical and functional organization of the human substantia nigra and its connections. *eLife, 6*, 1–23. https://doi.org/10.7554/eLife.26653

Zou, K. H., Warfield, S. K., Bharatha, A., Tempany, C. M. C., Kaus, M. R., Haker, S. J., Wells III, W. M., Jolesz, F. A., & Kikinis, R. (2004). Statistical Validation of Image Segmentation Quality Based on a Spatial Overlap Index. *Academic Radiology*, *11*(2), 178–189. https://doi.org/10.1016/S1076-6332(03)00671-8

Data and code availability

The code utilised in the research work presented in this thesis was made accessible to the public. Additionally, the corresponding data was uploaded to a public repository whenever possible.

Chapter 2

The code used to construct the interactive Figure 2.1. can be found at:
https://github.com/ACTrutti/VTA_component_nuclei/blob/gh-pages/index.html

Chapter 3

The probabilistic VTA atlas described in this chapter is accessible in the Open Science Framework: https://osf.io/9pzj3/

The structural 7T data used for delineations is part of the Amsterdam Ultra-high field adult lifespan database (AHEAD) and can be accessed via figshare:
https://uvaauas.figshare.com/articles/dataset/The_Amsterdam_Ultra-high_field_adult_lifespan_database_AHEAD_A_freely_available_multimodal_7_Tesla_submillimeter_magnetic_resonance_imaging_database/10007840/1

Code for data processing and analysis is available on github:
https://github.com/ACTrutti/VTA-atlas

Chapter 4

The analysis code can be found at:
https://github.com/ACTrutti/midbrain_tractography_MRtrix3

The high-resolution multi-shell 3T diffusion MRI data is part of the AHEAD dataset and can be accessed together with the preprocessing code through figshare:
https://uvaauas.figshare.com/projects/A_high-resolution_multi-shell_3T_diffusion_magnetic_resonance_imaging_dataset_as_part_of_the_Amsterdam_Ultra-high_field_adult_lifespan_database_AHEAD_/125377

Chapter 6

The preprocessing and analysis code can be found at:
https://github.com/ACTrutti/WM-updating-subcortex

The analysed data is part of a larger collection that will be published in a public repository when the entire dataset is ready for publication.

Chapter 7

This chapter is still being analysed and has no public repository yet. The analysed data is part of a larger collection that will be published in a public repository when the entire dataset is ready for publication**.**

Author contributions

Below, you can find a description of the contributions made by each chapter, which is organized according to the Contributor Roles Taxonomy (CRediT) system.

Chapter 2

This paper is published as:

Trutti, A. C., Mulder, M. J., Hommel, B., & Forstmann, B. U. (2019). Functional neuroanatomical review of the ventral tegmental area. *NeuroImage, 191*, 258–268. https://doi.org/10.1016/j.neuroimage.2019.01.062

Author contributions:
Anne C. Trutti: Conceptualization, Methodology, Investigation, Writing – Original draft preparation, Writing – Review & editing, Visualization, **Martijn J. Mulder** : Conceptualization, Methodology, Supervision, Writing – Review & editing, **Bernhard Hommel**: Conceptualization, Investigation, Resources, Funding acquisition, Writing – Review & editing **Birte U. Forstmann**: Conceptualization, Investigation, Resources, Funding acquisition, Writing – Review & editing.

Acknowledgements:
This research was supported by grants from the European Research Council to B.U.F. (ERC-2012-Stg-313481) and to B.H. (ERC-2015-AdG- 694722), and a Vidi grant from the Netherlands Organization for Scientific Research to B.U.F. (452-11-008).

Chapter 3

This paper is published as:

Trutti, A. C., Fontanesi, L., Mulder, M. J., Bazin, P.-L., Hommel, B., & Forstmann, B. U. (2021). A probabilistic atlas of the human ventral tegmental area (VTA) based on 7 Tesla MRI data. *Brain Structure and Function, 226*(4), 1155–1167. https://doi.org/10.1007/s00429-021-02231-w

Author contributions:
Anne C. Trutti: Conceptualization, Formal analysis, Methodology, Investigation, Writing – Original draft preparation, Writing – Review & editing, Visualization, **Laura Fontanesi**: Conceptualization, Data curation, Methodology, Investigation,

Writing – Review & editing, **Martijn J. Mulder** : Conceptualization, Methodology, Supervision, Writing – Review & editing, **Bernhard Hommel**: Conceptualization, Investigation, Resources, Funding acquisition, Writing – Review & editing, **Birte U. Forstmann**: Conceptualization, Investigation, Resources, Project administration, Funding acquisition, Writing – Review & editing.

Acknowledgements:
This research was supported by grants from the European Research Council to B.U.F. (ERC-2012-Stg-313481) and B.H. (ERC-2015-AdG- 694722), and a Vidi grant from the Netherlands Organization for Scientific Research to B.U.F. (452-11-008).

Chapter 4

This paper is in preparation for publication.

Author contributions:
Anne C. Trutti: Conceptualization, Software, Data curation, Formal analysis, Methodology, Investigation, Writing – Original draft preparation, Writing – Review & editing, Visualization, **Zsuzsika Sjoerds**: Conceptualization, Methodology, Supervision, Writing – Review & editing, **Sarah Kemp**: Software, Data curation, Writing – Review & editing, **Max C. Keuken**: Software, Data curation, **Pierre-Louis Bazin**: Conceptualization, Investigation, Software, Data curation, Methodology, Supervision Writing – Review & editing, **Birte U. Forstmann**: Resources, Project administration, Funding acquisition, Writing – Review & editing.

Acknowledgements:
This work was supported by grants from the European Research Council to B.U.F. (ERC Consolidator -8674750; ERC PoC), and a Vici grant from the Netherlands Organization for Scientific Research to B.U.F. (016.Vici.185.052).

Chapter 5

This paper is published as:

Trutti, A. C., Verschooren, S., Forstmann, B. U., & Boag, R. J. (2021). Understanding subprocesses of working memory through the lens of model-based cognitive neuroscience. *Current Opinion in Behavioral Sciences, 38*, 57-65. https://doi.org/10.1016/j.cobeha.2020.10.002.

Author contributions:
Anne C. Trutti: Conceptualization, Investigation, Writing – Original draft preparation, Writing – Review & editing, **Sam Verschooren**: Writing – Review & editing, **Birte U. Forstmann**: Funding acquisition, Writing – Review & editing, **Russell J. Boag**: Conceptualization, Methodology, Supervision, Writing – Original draft preparation; Review & editing, Visualization

Acknowledgements:
We thank Dr Yoav Kessler for making several suggestions to improve an earlier version of this manuscript. This work was supported by a grant from the Netherlands Organisation for Scientific Research (NWO; grant number 016.Vici.185.052; BUF).

Chapter 6

This chapter is accepted for publication in a peer-reviewed open-access journal.

A preprint is available as:

Trutti, A.C., Sjoerds, Z., Boag, R.J., Walstra, S.L.Y., Miletić, S., Isherwood, S.J.S., Bazin, PL., Tse, D.H.Y., Habli, S., Håberg, A.K., Hommel, B., & Forstmann, B.U. (2024). Investigating working memory updating processes of the human subcortex using 7 Tesla fMRI. *eLife*. https://doi.org/10.7554/eLife.97874.1

Author contributions:
Anne C. Trutti: Conceptualization, Formal analysis, Methodology, Investigation, Writing – Original draft preparation, Writing – Review & editing, Visualization, **Zsuzsika Sjoerds**: Conceptualization, Methodology, Supervision, Writing – Review & editing, **Russell J. Boag**: Conceptualization, Formal analysis, Supervision, Writing – Original draft, Writing – Review & editing, **Solenn L. Y. Walstra**: Conceptualization, Methodology, Writing – Review & editing, **Steven Miletić**: Methodology, Software, Data curation, Formal analysis, Investigation, Writing – Review & editing, Visualization, **Pierre-Louis Bazin**: Investigation, Methodology, Software, Writing – Review & editing, **Scott J. S. Isherwood**: Data curation, Investigation, Methodology, **Bernhard Hommel**: Conceptualization, Investigation, Resources, Funding acquisition, Writing – Review & editing**, Sarah Habli**: Investigation, **Desmond H. Y. Tse**: Methodology, Investigation, Software, **Pål Erik Goa**: Resources, Project administration, **Asta K. Håberg**: Resources, Funding acquisition, Project administration, Writing – Review & editing, **Birte U.**

Forstmann: Conceptualization, Investigation, Resources, Project administration, Funding acquisition, Writing – Review & editing.

Acknowledgements:
We would like to express our gratitude to Pål Erik Goa for supporting this study by facilitating data acquisition. We also thank Niek Stevenson, Roel van Dooren, and Bryant Jongkees for their valuable contributions to the preceding work and for stimulating discussions on the reference-back paradigm. This work was supported by grants from the European Research Council to B. U. F. (8674750) and B. H. (ERC-2015-AdG- 694722), and a Vici grant from the Netherlands Organization for Scientific Research to B. U. F. (016.Vici.185.052).

Chapter 7

This chapter is in preparation for publication.

Author contributions:
Anne C. Trutti: Conceptualization, Formal analysis, Methodology, Investigation, Writing – Original draft preparation, Writing – Review & editing, Visualization, **Steven Miletić**: Methodology, Software, Data curation, Formal analysis, Investigation, Writing – Review & editing, Visualization, **Zsuzsika Sjoerds**: Conceptualization, Methodology, Supervision, Writing – Review & editing, **Scott J. S. Isherwood**: Data curation, Investigation, Methodology, **Solenn Walstra**: Methodology, Writing – Review & editing, **Pierre-Louis Bazin**: Investigation, Methodology, Software, **Bernhard Hommel**: Conceptualization, Investigation, Resources, Funding acquisition, Writing – Review & editing**, Sarah Habli**: Investigation, **Desmond H. Y. Tse**: Methodology, Investigation, Software, **Asta K. Håberg**: Resources, Funding acquisition, Project administration, Writing – Review & editing, **Birte U. Forstmann**: Conceptualization, Investigation, Resources, Project administration, Funding acquisition, Writing – Review & editing.

Acknowledgements:
We would like to express our gratitude to Pål Erik Goa for facilitating data acquisition and supporting this study. This work was supported by grants from the European Research Council to B. U. F. (8674750) and B. H. (ERC-2015-AdG—694722) and a Vici grant from the Netherlands Organization for Scientific Research to B. U. F. (016.Vici.185.052).

Full Publication List

Trutti, A.C., Miletić, S., Sjoerds, Z., Isherwood, S.J.S., Bazin, PL., Tse, D.H.Y., Habli, S., Goa, P.E., Håberg, A.K., Hommel, B., & Forstmann, B.U. (2024). Exploring working memory updating processes of the human subcortex using 7 Tesla fMRI. *eLife*. https://doi.org/10.7554/eLife.97874.1

Boag, R. J., Miletić, S., **Trutti, A. C.**, & Forstmann, B. U. (2024). Toward a Model-Based Cognitive Neuroscience of Working Memory Subprocesses. In B. U. Forstmann & B. M. Turner (Eds.), *An Introduction to Model-Based Cognitive Neuroscience* (pp. 265-302). Springer Nature Switzerland AG. https://doi.org/10.1007/978-3-031-45271-0

Stevenson, N., Innes, R., Boag, R. J., Miletic, S., Isherwood, S.J.S., **Trutti, A.C.,** Heathcote, A., & Forstmann, B.U. (2024). Joint modelling of latent cognitive mechanisms shared across decision-making domains. *Computational Brain & Behavior, 7*, 1–22. https://doi.org/10.1007/s42113-023-00192-3

Skandalakis, G. P., Neudorfer, C., Payne, C. A., Bond, E., Tavakkoli, A. D., Barrios-Martinez, J., **Trutti, A. C.**, Koutsarnakis, C., Coenen, V. A., Komaitis, S., Hadjipanayis, C. G., Stranjalis, G., Yeh, F.-C., Banihashemi, L., Hong, J., Simmons, N. E., Lozano, A. M., Kogan, M., Horn, A., Evans, L. T., & Kalyvas, A. (2024). Establishing structural connectivity through microdissections of disparate midbrain stimulation-related neural circuits. *Brain*. https://doi.org/10.1093/brain/awae173

Isherwood, S.J.S, Bazin, PL., Miletić, S., Stevenson, N.R**., Trutti, A.C.**, Tse, D.H.Y., Heathcote, A., Matzke, D., … & Forstmann, B.U. (2023). Investigating Intra-Individual Networks of Response Inhibition and Interference Resolution using 7T MRI**.** *NeuroImage, 271*, 119988. https://doi.org/10.1016/j.neuroimage.2023.119988

Alkemade, A., Mulder, M., **Trutti, A.C.**, & Forstmann, B. (2022). Manual Delineation approaches for direct imaging of the subcortex. *Brain, Structure and Function, 227*, 219–297. https://doi.org/10.1007/s00429-021-02400-x

Keuken, M.C., Liebrand, L.C., Bazin, P.-L., Alkemade, A., Berendonk, N., Groot, J.M., Isherwood, S.J.S., Kemp, S., … **Trutti**, **A.C.,** Caan, M.W.A., & Forstmann, B.U. (2022). A high-resolution multi-shell 3T diffusion magnetic resonance imaging dataset as part of the Amsterdam Ultra-high field adult

lifespan database (AHEAD). *Data in Brief*, 42. https://doi.org/10.1016/j.dib.2022.108086

Trutti, A.C., Fontanesi, L., Mulder, M.J., Bazin, P.-L., Hommel, B.H., & Forstmann, B.U. (2021). A probabilistic atlas of the ventral tegmental area using 7 T MRI. *Brain, Structure and Function*. 10.1007/s00429-021-02231-w

Trutti, A.C., Verschooren, S., Forstmann, B. U., & Boag, R. J. (2021). Understanding subprocesses of working memory through the lens of model-based cognitive neuroscience. *Current Opinion in Behavioral Sciences, 38*, 57–65. https://doi.org/10.1016/j.cobeha.2020.10.002

Miletić, S., Boag, R. J., **Trutti, A. C.**, Forstmann, B. U., & Heathcote, A. (2021). A new model of decision processing in instrumental learning tasks. *eLife,* 1–32. https://doi.org/10.7554/eLife.63055

Boag, R. J., Stevenson, N., Van Dooren, R., **Trutti, A.C.**, Sjoerds, Z., & Forstmann, B. U. (2021). Cognitive control of working memory: A model-based approach. *Brain Sciences, 11*(6), 21–25. https://doi.org/10.3390/brainsci11060721

Trutti, A.C., Mulder, M.J., Hommel, B.H., & Forstmann, B. (2019). Functional neuroanatomical review of the ventral tegmental area. *NeuroImage, 191*, 258-268. https://doi.org/10.1016/j.neuroimage.2019.01.062

Trutti, A.C., Sjoerds, Z., & Hommel, B.H. (2019). Attentional blink and putative non-invasive dopamine markers: two experiments to consolidate possible associations. *Cognitive, Affective, and Behavioral Neuroscience, 19*, 1444–1457. https://doi.org/10.3758/s13415-019-00717-z

Isaacs, B., **Trutti, A.C.**, Pelzer, E., Tittgemeyer, M., Temel, Y., Forstmann, B.U., & Keuken, M.C. (2019). Cortico-basal white matter alterations occurring in Parkinson's disease. PLOSONE, *14*(8): e0214343. https://doi.org/10.1371/journal.pone.0214343

Keuken, M. C., Bazin, P.-L., Beekhuizen, S., Himmer, L., Kandola, A., Lafeber, J. J., Prochazkova, L., **Trutti, A.**, Schaefer, A., Turner, R., & Forstmann, B. U. (2017). Effects of aging on T1, T2*, and QSM MRI values in the subcortex. *Brain Structure & Function, 222*, 2487-2505. https://doi.org/10.1007/S00429-016-1352-4

de Hollander, G., Labruna, L., Sellaro, R., **Trutti, A.**, Colzato, L., Ratcliff, R., Ivry, R., & Forstmann, B. U. (2016). Transcranial direct current stimulation does

not influence the speed-accuracy tradeoff in perceptual decision-making: Evidence from three independent replication studies. *Journal of Cognitive Neuroscience, 7*, 1-12. https://doi.org/10.1162/jocn_a_00967